A DROSOPHILA MODEL OF CELLULAR AND MOLECULAR MECHANISMS OF FRAGILE X SYNDROME

By

Luyuan Pan

Dissertation

Submitted to the Faculty of the Graduate School of Vanderbilt University

In partial fulfillment of the requirements for the degree of

Doctor of Philosophy

In

Biological Science

December, 2007

Nashville, Tennessee

Approved

Professor Lilianna Solnica-Krezel

Professor Kendal S. Broadie

Professor Bruce Appel

Professor David Miller

Professor Bih-Hwa Shieh

ACKNOWLEDGEMENTS

It has been six years since I began my graduate study. Many people have given me great care and counsel in my research, my life, or both. I cannot even totally express my appreciation in these two simple pages, but I would like to try.

First, I want to thank my degree mentor, Dr. Kendal Broadie. Thank you for opening the door of *Drosophila* neuroscience for me, and indicating the road I should take to become an independent scientist. I appreciate your guidance, support, and enthusiasm over these years. As a successful scientist, erudite and diligent, you are also an excellent model in my future scientific endeavors.

Next, I sincerely thank my thesis committee, Dr. Lilianna Solnica-Krezel, Dr. Bruce Appel, Dr. David Miller, and Dr. Bih-Hwa Shieh. I appreciate your ever-present involvement, advice, suggestions on my research. I would like to extend special thanks to Lila for her abounding support and direction as my committee chair.

My work would not have been possible without the involvement of so many knowledgeable and friendly colleagues. Dr. Yong Q. Zhang, one of the most senior researchers, who pioneered the *Drosophila* FXS model, gave me patient and thorough instruction when I was just a beginner in the field. Dr. Heinrich Matthies and Dr. Jeffrey Rohrbough helped me to improve my approach to genetics and imaging techniques. Mr. Elvin Woodruff is not only an electron

microscopy expert, but also a warm-hearted friend in life. I received indispensable support from Dr. Cheryl Gatto and Dr. Charles Tessier, who helped me a lot both on my research and my career plan. And, Mr. Lane Coffee offered enthusiastic help in critically reading portions of my thesis and suggesting presentation improvements. All of you make the FXS research group in the Broadie Lab collaborative, inviting, and open. I also want to thank all other former and current members of the Broadie Lab. Ms. Emma Rushton helped with my fly-crossing schemes, and Dr. Nick Trotta and Dr. Yanping Yan helped with advice on imaging quantification techniques. Also, I want to thank Ms. Ping Liang, Ms. Nicole Bibus Christianson, and Ms. Qingxia Chen for their hard work and technical support that made my research progress more smoothly.

Next, I want to extend my most gracious and special thanks to my parents. Thank you for your edification and enlightenment in all aspects of my life. You have taught me the most important things in life by your own example. I appreciate the endless support and encouragement you have given me over the years. I hope, by trying my best, I can make you proud.

Finally, I thank all of my good friends, who have given me incalculable help along the way in both my research and my life. Thanks Alma for helping me to improve my Photoshop skill. I want to specially thank my co-workers in two volunteer organizations in China, LOH and Baixi. Your tireless efforts make the world warmer, and make the people suffering hardship happier. Your insistence

has encouraged me and convinced me that there are some things in this world, which are difficult but beautiful, worth our time, effort, and life, maybe just like science. I hope I can share this, one of the most memorable and happiest moments in my life, with you.

TABLE OF CONTENTS

List of Figures and Tables

Table Page

LIST OF ABBREVIATIONS

µM	micrometer
AMPA	α-amino-3-hydroxy-5-methyl- 4-isoxazole propionic acid
Arc	activity-regulated cytoskeleton associated protein
CamKII	calcium/calmodulin-dependent protein kinase II
CNS	central nervous system
CYFIP	cytoplasmic FMR1 interacting protein
DA	dendritic arborization
DC	dorsal cluster
dFMR1	*Drosophila FMR1*
dFMRP	*Drosophila* FMRP
Dicer	double-stranded RNA-specific RNaseIII
DLG	Discs Large
DmGluRA	*Drosophila* metabotropic glutamate receptor A
EJC	Excitatory junctional current
EM	electron microscopy
FMR1	*Fragile X Mental Retardation 1*
FMRP	Fragile X Mental Retardation Protein
FXR1	*Fragile X Related 1*

FXR2	*Fragile X Related 2*
FXS	Fragile X Syndrome
GFP	green fluorescent protein
GluR	glutamate receptor
hnRNP	heterogeneous nuclear ribonucleoprotein
HRP	Horseradish Peroxidase
iGluR	ionotropic glutamate receptor
IQ	Intelligence Quotient
KH	pre-mRNA binding heterogeneous nuclear ribonucleoprotein K
KO	knock-out
LNv	Lateral Neurons
LTD	Long-term depression
LTP	Long-term Potentiation
MAP1B	microtubule associated protein 1B
MARCM	Mosaic Analysis with a Repressible Cell Marker
MB	Mushroom Body
mGluR	metabotropic glutamate receptor
MOE	muscle over-expression
MR	Mental Retardation
mRNA	messenger RNA
mRNP	messenger ribonucleoprotein

NES	nuclear export signal
NLS	nuclear localization signal
NMJ	neuromuscular junction
MOE	neuronal over-expression
OE	over-expression
PBS	phosphate buffered saline
PNS	peripheral nervous system
PSD95	postsynaptic density protein 95
RGG	arginine-glycine-glycine
RISC	RNA-induced silencing complex
RNA	ribonucleatic acid
RNAi	RNA interference
SEM	Standard Error of Mean
SV	synaptic vesicles
UTR	untranslated region
WT	wild type
XLMR	X-linked mental retardation

CHAPTER I

INTRODUCTION

Mental Retardation (MR) is defined as a cognitive disability characterized by an overall intelligence quotient (IQ) lower than 70, which is associated with functional deficits in adaptive skills, including communication, self-care, ability to live independently, social and interpersonal skills, use of public services, decision making, functional academic skills, work, leisure, and health and safety, with onset before the age of 18 years (Ropers and Hamel, 2005; Chelly et al., 2006). MR affects 1-3% of general population, and therefore MR is one of the problems with the highest healthcare expenditure (Chelly et al., 2006). According to the classification by the World Health Organization, MR is subdivided into 5 categories by IQ; Profound (IQ<20), Severe (20<IQ<35), Moderate (35<IQ<50), Mild (50<IQ<70), and borderline (70<IQ<80) (Ropers and Hamel, 2005).

Causes of MR can be environmental, chromosomal, or monogenic. According to clinical observation and statistical data, there are significantly more male MR patients than females. The male to female ratio is about 1.4:1 in moderate to severe MR (IQ<50), while in mild MR the ratio is around 1.9:1 (Leonard and Wen, 2002; Ropers, 2006). This sex bias has suggested that X-linked gene defects are important causes of MR. Up to 2006, 61 X-linked genes

were identified in MR disorders (Ropers and Hamel, 2005). X-linked mental retardation (XLMR) can be subdivided into syndromic forms and non-syndromic forms, according to whether other physical abnormalities are found in addition to mental retardation (Ropers and Hamel, 2005). There are about 140 syndromic XLMR diseases described. Fragile X Syndrome (FXS) is the most common cause of inherited mental retardation (Ropers and Hamel, 2005).

Fragile X Syndrome

Fragile X Syndrome (FXS) is the most common form of inherited mental retardation and the most common known genetic cause of autistic disorders. The disease occurs about one in 4000 males and one in 8000 females (Turner et al., 1996; Reddy, 2005; Visootsak et al., 2005).

Patients with FXS display several identifiable physical, behavioral and cognitive abnormalities. Physical symptoms include tall stature, large testes, long narrow face, prominent forehead, prominent mandible and large ears, and hyperextensibility of joints (Terracciano et al., 2005; Visootsak et al., 2005). These symptoms are more significant in male patients than in females, and tend to be more and more marked with age (Terracciano et al., 2005). Male FXS patients also display hyperactivity, attention deficits, social avoidance, anxiety in novel situations, sleep disorders, obsessive compulsive behaviors, stereotypic behaviors like hand flapping, and autistic features. Seizures are also present in

childhood but disappear with adolescence. Symptoms in female patients tend to be more subtle, which include shyness, poor eye contact, and attention deficits (Terracciano et al., 2005; Visootsak et al., 2005). Mild to severe mental retardation is the major symptom of FXS. The IQ of FXS patients is in the range of 20 to 70, with 40 as the average (Terracciano et al., 2005). Delays in language development are common in males, and both male and female patients display weakness on quantitative skills and short-term memory of visually represented abstract stimuli (Visootsak et al., 2005). In addition, 33% of FXS children have autism (Rogers et al., 2001).

While mental retardation is the major symptom of FXS, the overall brain structure of patients is normal. There are only slight and debatable structural changes described, including diminished white-gray ratio, enlarged caudate nucleus and hippocampus, and a decreased cerebellar vermis with enlarged fourth ventricle (Terracciano et al., 2005). The only significant neuronal morphological anomalism described in human patients has been abnormal dendritic spines of pyramidal cells in layer III and V of parietooccipital neocortex (Hinton et al., 1991; Irwin et al., 2001). Compared with the mushroom-shaped normal mature dendritic spines, FXS patients display longer, thinner, and more tortuous dendritic spines. Spine density was also found increased in FXS patients (Irwin et al., 2000).

The first literature report of FXS occurred in 1943 (O'Donnell and Warren,

2002; Visootsak et al., 2005). Martin and Bell described a large family with MR history, which displayed a strong sex bias with many more affected males than females. They concluded this mental retardation is caused by a X-chromosome linked recessive factor. In 1977, Sutherland found a fragile site on the distal long arm of X chromosome in FXS cells when cell culture media lacking folic acid was used (Sutherland, 1977). This phenotype is the basis of the current disease name. This fragile site was mapped to the position Xq27.3 (Proops and Webb, 1981). In 1991, the gene causing the disease was identified (Verkerk et al., 1991).

Fragile X Mental Retardation 1 (FMR1) **Gene**

Fragile X syndrome is a single gene disorder, which is caused by loss of functional gene product of the *Fragile X Mental Retardation 1* (*FMR1*) gene (Verkerk et al., 1991). *FMR1* has 17 exons representing 40 kb total genomic length. The transcript can be spliced in alternate ways. Full length mRNA is about 4kb and translated to a 69kDa protein, the Fragile X Mental Retardation Protein (FMRP) (Pieretti et al., 1991). *FMR1* belongs to a highly conserved gene family, which includes two human autosomal paralogs, *Fragile X Related 1* (*FXR1*) and *Fragile X Related 2* (*FXR2*). Paralog genes were also identified in animals from *Drosophila* to zebrafish, to mouse (Ashley et al., 1993a; Siomi et al., 1995; Zhang et al., 1995; Wan et al., 2000).

In the 5’ untranslated region (UTR) of *FMR1*, a CGG trinucleotide repeat

exists with variable length (Fu et al., 1991; Verkerk et al., 1991). In the general population, the copy number of the CGG repeat is 6 to 50 with 30 as average, which is stably transmitted across generations. The situation with 60 to 200 CGG copies has been called the FXS premutation, which is unstable and tends to expand through generations from female carriers to their offspring (Fu et al., 1991; Malter et al., 1997). The premutation carriers have been thought not to be affected. However, in recent years, a disease called Fragile X-associated tremor/ataxia syndrome was found in some aged male premutation carriers (Hagerman et al., 2001), and 20% of female carriers showed ovarian dysfunction (Allingham-Hawkins et al., 1999; Hagerman and Hagerman, 2002). When the repeat number grows larger than 200, the situation is called the FXS full mutation. In this condition, the CGG repeats and upstream CpG islands are hypermethylated (Heitz et al., 1991), leading to silence the transcription of the downstream *FMR1* gene and causing the disease (Figure 1.1A) (Zalfa and Bagni, 2004). Using a methylation inhibitor to treat full mutation cells can rescue part of the FMRP expression (Chiurazzi et al., 1998). FXS can also arise because of missense mutations or deletions of encoding regions within the *FMR1* gene (Gedeon et al., 1992; Wohrle et al., 1992; De Boulle et al., 1993). These results indicate that loss of the functional expression product of *FMR1*, FMRP, is the sole known cause of Fragile X syndrome.

Figure1.1 *FMR1* gene structure, Hypermethylation, and FMRP structure.

A. The *FMR1* gene has 17 exons over 40 kb of genomic length. A CGG repeat region presents in the 5'-untranslated region (UTR) of *FMR1*. In the normal situation, the CGG copy number is less than 50, and *FMR1* is transcribed and translated at normal levels. When CGG copy number is from 55 to 200, which is called the premutation situation, there is a higher *FMR1* mRNA level in cells, but the protein level is lower than normal. Premutation is an unstable situation, and expand to longer repeats when transmitted from female carriers to their offspring. When the CGG repeat is longer than 200 copies, the upstream regulatory region is hypermethylated, consequently silencing the transcription of downstream *FMR1* gene. This is called the full mutation, which is the reason of most cases of Fragile X Mental Retardation.

B. Human FMRP is a 69 kDa protein composed of 632 amino acids. FMRP contains 8 known functional domains, including one NLS (nuclear localization signal), one NES (nuclear export signal), two KH domains (pre-mRNA binding heterogeneous nuclear ribonucleoprotein K homology domains), one RGG (arginine-glycine-glycine) box, two coiled-coil domains, and one N-terminal motif implicated in both protein and mRNA binding.

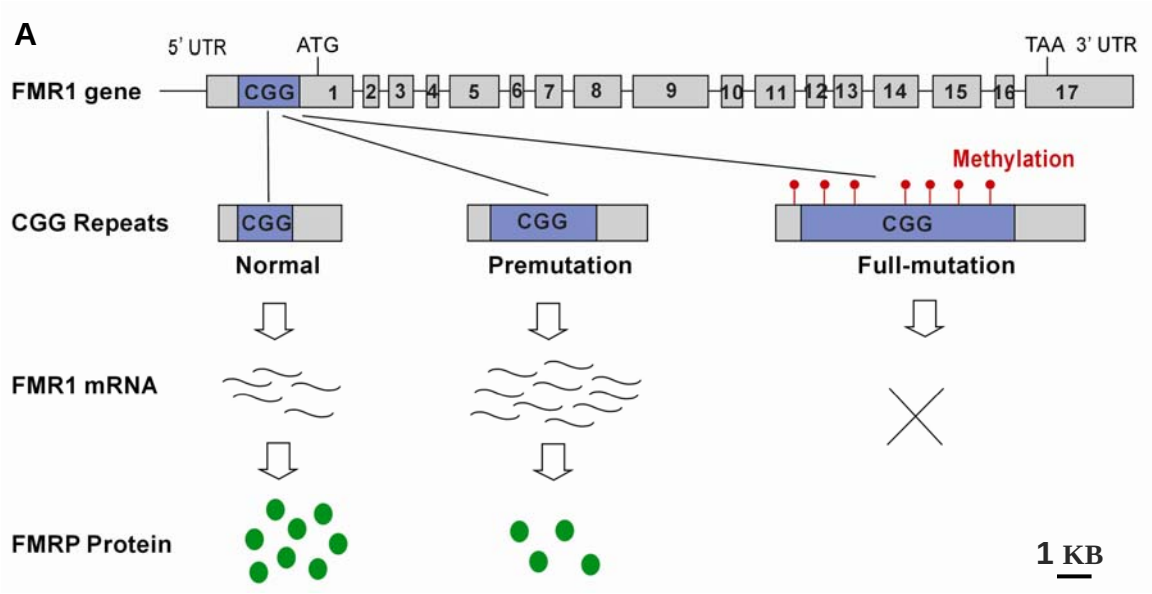
A
5' UTR
ATG
TAA 3' UTR
FMR1 gene
CGG
1
2
3
4
5
6
7
8
9
10
11
12
13
14
15
16
17
Methylation
CGG Repeats
CGG
CGG
CGG
Normal
Premutation
Full-mutation
FMR1 mRNA
FMRP Protein
1 KB

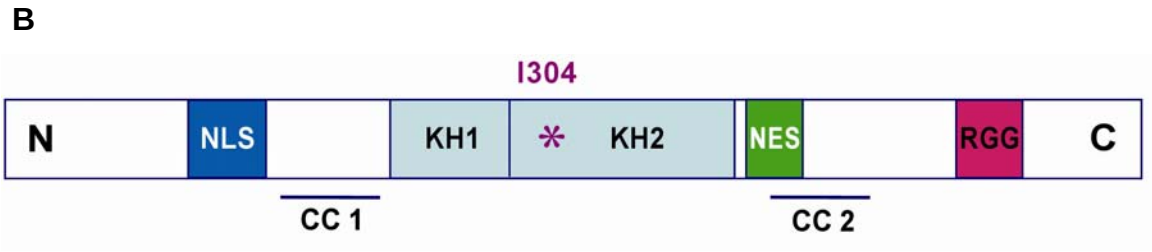
B
I304
N
NLS
KH1
KH2
NES
RGG
C
CC 1
CC 2

Fragile X Mental Retardation Protein (FMRP)

Human FMRP is composed of 632 amino acids and is expressed in most tissues, albeit with particular enrichment in the nervous system and testes (Hinds et al., 1993; Verheij et al., 1993). FMRP contains 8 known functional domains, including one NLS (nuclear localization signal), one NES (nuclear export signal), two KH domains (pre-mRNA binding heterogeneous nuclear ribonucleoprotein K homology domains), one RGG (arginine-glycine-glycine) box, two coiled-coil domains, and one N-terminal motif (Adinolfi et al., 1999a; Adinolfi et al., 2003; Zalfa and Bagni, 2004) (Figure 1.1B).

The KH domain is an evolutionarily conserved motif from bacteria to human, which frequently presents in the heterogeneous nuclear ribonucleoprotein (hnRNP) family (Siomi et al., 1993). KH domains preferentially bind mRNA, although a specific sequence binding target has not yet been identified (Adinolfi et al., 1999b). Two KH domains present back to back in the middle region of FMRP. A missense point mutation (I304) has been identified in one FXS patient, who had normal copy number of CGG repeats but displayed very severe FXS symptoms. This point mutation shifted one isoleucine in the second KH domain to asparagine, and consequently altered the RNA-binding activity of FMRP and the assembly of the 80S ribosomal complex (De Boulle et al., 1993). This point mutation provided the community with the idea that the KH domains are essential to FMRP's function.

RGG box is a cluster of Arg-Gly-Gly repeats, which is also known as an RNA binding motif (Ghisolfi et al., 1992; Kiledjian and Dreyfuss, 1992). In the studies of

FMRP function, the RGG box was found specifically associated with an mRNA secondary structure G-quartet (Darnell et al., 2001; Schaeffer et al., 2001). Several identified or potential mRNA targets of FMRP contain G quartet structures (Darnell et al., 2001). The N-terminus of FMRP is not homologous to any known functional motif. However, it has also been shown to have a binding affinity to mRNA, and also is important for protein-protein interactive features of FMRP. This region is called the NDF fold (N-terminal domain of FMRP) (Adinolfi et al., 1999a; Ramos et al., 2006). Two coiled coil domains are also likely involved in protein-protein interactions. FMRP rarely exists in isolation, but mostly associates with large messenger ribonucleoprotein (mRNP) particles and binds polyribosomes (Siomi et al., 1996).

FMRP has been suggested to have an affinity for about 4% of total brain mRNA. Based on immunoprecipitation pull-down, microarray analysis of mouse brain identified 432 mRNA binding with FMRP (Brown et al., 2001). FMRP is known to negatively regulate the translational level of several mRNA targets (Brown et al., 1998; Laggerbauer et al., 2001; Sung et al., 2003). Most of these targets are important for neuronal structure and function, including microtubule associated protein 1B (MAP1B)/Futsch (Zhang et al., 2001; Lu et al., 2004), α-subunit of calcium/calmodulin-dependent protein kinase II (α-CamKII) (Zalfa et al., 2003), GTPase Rac1 (Lee et al., 2003), myelin basic protein (Brown et al., 1998), activity-regulated cytoskeleton associated protein (Arc)/Arg3.1 (Zalfa et al., 2003), and postsynaptic density protein 95 (PSD95/DLG) (Todd et al., 2003a; Muddashetty et al., 2007). In addition, FMRP can bind its own mRNA and inhibit

translation of itself (Ashley et al., 1993b; Sung et al., 2000).

The mechanisms of FMRP regulating mRNA translation are still unclear. It has been found, however, that FMRP interacts with Argonaute 1 (AGO1) (Caudy et al., 2002), Argonaute 2 (AGO2) (Caudy et al., 2002; Ishizuka et al., 2002), the RNA-induced silencing complex (RISC) (Caudy et al., 2002; Ishizuka et al., 2002), and double-stranded RNA-specific RNaseIII (Dicer) (Jin et al., 2004), which are all important components in microRNA and RNA interference (RNAi) pathways. These findings suggest FMRP may play a role in the regulation of mRNA stability, or regulate target translation though the microRNA pathway. Moreover, the small dendritic non-translatable RNA BC1 was found directly associated with both FMRP and FMRP target mRNA. Blocking BC1 reportedly inhibits regulation of FMRP to its targets, which suggests FMRP may recruit specific mRNA targets with the help of BC1 (Zalfa et al., 2003). FMRP is best described as a translation repressor, since most known FMRP direct targets were translated in a higher level in absence of FMRP (Laggerbauer et al., 2001; Li et al., 2001). And in postsynaptic terminals, neurotransmission activity-induced local protein synthesis is FMRP-dependent (Miyashiro et al., 2003; Todd et al., 2003a; Weiler et al., 2004).

The NLS and NES domains suggest that FMRP shuttles between the nucleus and cytoplasm (Eberhart et al., 1996; Adinolfi et al., 1999a). Although essentially all FMRP is found localized in cytoplasm, a small quantity has been reported in the nucleus (Feng et al., 1997). Furthermore, FMRP has been found associated with some nuclear proteins or shuttle proteins, for example, Nucleolin

(Ceman et al., 1999), 82-FIP (82 KDa FMRP interacting protein) (Bardoni et al., 2003b), and NUFIP (nuclear FMRP interacting protein) (Bardoni et al., 1999; Bardoni et al., 2003a), which suggest FMRP may bind its target in nucleus and take part in mRNA transport from the nucleus. In the nervous system, almost all FMRP is found in neuronal soma cytosol, while both FMRP and FMR1 mRNA have been detected in neuronal processes and synaptic terminals (Weiler et al., 1997; Antar et al., 2004; Antar et al., 2005; Antar et al., 2006). In dendrites, FMRP is a component of mRNA transport granules, whose movement is neuronal activity induced (Antar et al., 2004; Antar et al., 2005). Moreover, local translation of some cargo mRNAs has been found to be reduced in *fmr1* null dendrites (Miyashiro et al., 2003).

Putting all of these features together, FMRP is considered a RNA-binding protein, which may play a role in RNA transport, RNA stability, and translational regulation. The most strongly supported theory is that FMRP is a translational repressor.

Animal Models of FXS

The human *FMR1* gene was identified in 1991 (Verkerk et al., 1991). It has two autosomal homologues in the human genome, and highly conserved homologues in mouse, chick, zebrafish and fruit fly (Laval et al., 1992; Siomi et al., 1995; Zhang et al., 1995; Wan et al., 2000; van 't Padje et al., 2005). The first knockout (KO) mouse was generated in 1994 by inserting a neomycin resistance cassette into exon 5 of mouse *FMR1* gene (Bakker, 1994). Little or no functional

FMRP protein is expressed in this KO mouse model, which therefore mimics the FXS full mutation situation of human patients. The *FMR1* KO mouse displays some similar phenotypes with human symptoms, including enlarged testes in males (Bakker, 1994; Kooy et al., 1996), increased locomotor activity (Bakker, 1994; Mineur et al., 2002), and increased audiogenic seizures susceptibility (Musumeci et al., 2000; Chen and Toth, 2001). Like human patients, the *FMR1* KO mouse has grossly normal brain structure, while denser, longer, and tortuous dendritic spines are also observed in the visual cortex of the KO mouse (Comery et al., 1997; Irwin et al., 2002). According to corticosterone level test, acute stress response is misregulated in *FMR1* KO mice (Markham et al., 2006). In addition, KO mice displayed significant reduce on social interaction, which is comparable with autistic features in human patients (Mineur et al., 2006). In the Morris water maze test, *FMR1* KO mouse displayed a mild impairment, indicative of a mild deficit in spatial learning (Bakker, 1994; Kooy et al., 1996; D'Hooge et al., 1997; Dobkin et al., 2000). The FMR1 KO mouse is deficient in leverpress escape/avoidance task test, which also suggests a learning defect (Brennan et al., 2006) (Table1.1).

The *Drosophila FMR1* homologue (*dFMR1*, also known as *dFXR*, *Drosophila* Fragile X related) was characterized in 2000 (Wan et al., 2000). Whereas three *FMR1* related genes (*FMR1, FXR1, FXR2*) are present in vertebrate genomes, *Drosophila* contains a single gene, which is similarly related with all three human counterparts. Since no homologue has been found in C.elegans or yeast, *Drosophila FMR1* might be a prototype of this gene family (Wan et al., 2000).

Table 1.1 Phenotype Comparison of FXS patients and animal models

	Human	Mouse	*Drosophila*
Cognitive	MR	Learning deficits	short-term memory deficits
Behavioral	Hyperactivity	Hyperactivity	Hyperactivity
	Sleep Disorder	ND	Circadian Arrhythmia
	Autistic features	Autistic features	ND
Testes	Macroorchidism	Macroorchidism	Macroorchidism
Neuronal Structure	Dendritic Pruning Defects	Dendritic Pruning Defects	Overgrowth & Overbranching
Synapse	Excess Spines	Excess Spines	Excess Boutons
Function	ND	Increased LTD Decreased LTP	Altered Plasticity

MR, Mental Retardation; ND, Not determined; LTD, Long-term depression; LTP, Long-term Potentiation; EJC, Excitatory junctional current. Table is modified and updated from Zhang&Broadie, Trends in Genetics, 2005

dFMR1 is located on the *Drosophila* third chromosome cytological position and encodes a 681 amino acid protein, dFMRP (*Drosophila* fragile X mental retardation protein), which shares all functional domains with human FMRP (Figure1.2A) (Wan et al., 2000; Zhang et al., 2001). The first *Drosophila* FXS model was established in the Broadie Lab in 2001 by deleting regulatory and part of coding regions of *dFMR1* gene (Zhang et al., 2001). Several other *dfmr1* null alleles have been reported in more recent years (Dockendorff et al., 2002; Lee et al., 2003). Similar to mammalian FMRP, dFMRP is highly enriched in nervous system and testes (Wan et al., 2000; Zhang et al., 2001; Zhang et al., 2004). Also similar to human FXS patients, *dfmr1* mutant flies are viable, but display several behavioral defects, including locomotory problems (Zhang et al., 2001; Xu et al., 2004), eclosion failure (Inoue et al., 2002; Morales et al., 2002), circadian rhythmic defects (Dockendorff et al., 2002; Inoue et al., 2002; Morales et al., 2002), and defective learning and memory (Dockendorff et al., 2002). *dfmr1* male flies also display enlarged testes, spermatogenesis and sterility defects (Zhang et al., 2004), while females display oogenesis defects (Costa et al., 2005). Overgrowth and overbranching neuronal processes were found in both central and peripheral nervous systems of *dfmr1* mutant flies (Zhang et al., 2001; Lee et al., 2003; Pan et al., 2004) (Table1.1, and see below for detailed description).

Defects of Neuronal Structure in *fmr1* mutants

As discussed above, loss of FMRP is associated with abnormal postsynaptic dendritic spines in Fragile X Syndrome (FXS) patients and in the mouse knockout

model, which are denser and morphologically altered compared to normal (Hinton et al., 1991; Irwin et al., 2001; Irwin et al., 2002). While similar dendritic spine abnormalities occur in other neurological diseases, including Down's Syndrome and Alzheimer's Disease (Purpura, 1974; Fiala et al., 2002), increased spine density appears to be a unique feature of FXS (Kooy, 2003). In the mouse FXS model, layer V pyramidal neurons in the visual cortex display longer, thinner, and tortuous spines rather than the normal short, mushroom-shaped mature spines (Irwin et al., 2002). The largest difference between normal and mutant dendritic spines has been found in the one week postnatal stage; and in mice older than 4 weeks, these defects may be lost (Nimchinsky et al., 2001). During this period, spines normally display very active changes in length, density, and motility, which may reflect a developmental pruning stage dependent on FMRP. FXS mice also exhibit this apparent pruning defect in dendrites of spiny stellate cells in the inner barrel wall of layer IV somatosensory cortex, maintaining a septa-oriented morphology characteristic of an early development stage (Galvez et al., 2003). Such defects in dendritic spine pruning and maturation indicate that FMRP may regulate experience-dependent synaptogenesis.

Our lab previously established a *Drosophila* FXS model to test the hypothesis that FMRP regulates synaptic differentiation, utilizing the well-characterized fly neuromuscular junction (NMJ) (Zhang et al., 2001). We showed that the level of dFMRP regulates both structural complexity and synaptic transmission strength; *dfmr1* null mutants display overgrowth and overbranching, whereas dFMRP overexpression caused the opposite phenotypes of undergrowth

Figure1.2 *Drosophila* FXS Model

A. *Drosophila* Fragile X Mental Retardation Protein (dFMRP) shares all the functional domains with human FMRP (hFMRP). aa, amino acid. Modified from Gao, FB, Neuron, 2002.

B. In *dfmr1* null flies, NMJ displayed more synaptic boutons and more branches than wild type, while dFMRP overexpression (OE) displayed opposite phenotypes. The scale bar equals 10 μm.

C. At NMJ, evoked excitatory junctional current (EJC) was increased in *dfmr1* null mutants, but no change in overexpression (OE).

B&C are taken from Zhang, YQ et al., Cell, 2001.

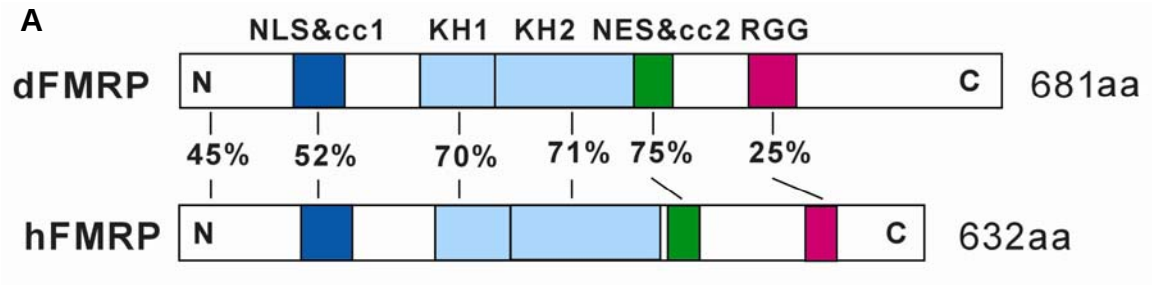
A
NLS&cc1
KH1
KH2
NES&cc2
RGG
dFMRP
N
C
681aa
45%
52%
70%
71%
75%
25%
hFMRP
N
C
632aa

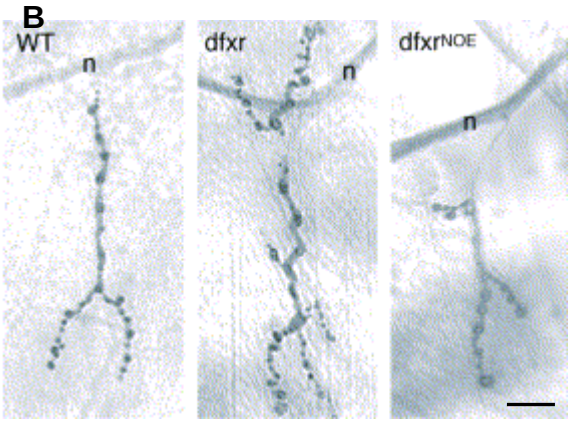
B
WT
n
dfxr
n
dfxrNOE
n

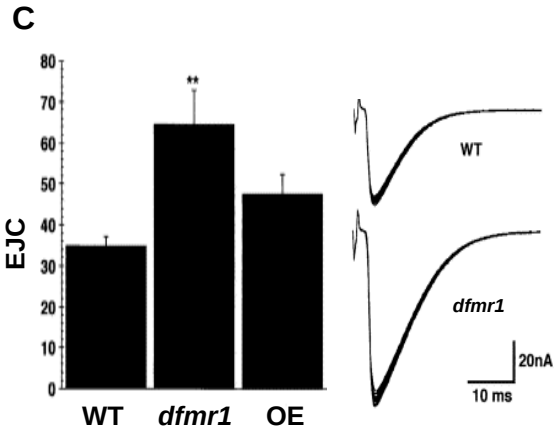
C
EJC
80
70
60
50
40
30
20
10
0
**
WT
dfmr1
OE
WT
dfmr1
20nA
10 ms

and underbranching. Loss of dFMRP caused increase of bouton. Number and branch number at NMJ terminal (Zhang et al., 2001). Similar results were reported in another peripheral nervous system model, dendritic arborization (DA) neurons, which are a subtype of *Drosophila* peripheral sensory neurons (Lee et al., 2003). In DA neurons, *dfmr1* mutants display increased higher-order sensory dendritic branching, whereas dFMRP overexpression inhibited dendritic branching and reduced the complexity of sensory processes. In my Ph.D thesis work, I examined *dfmr1* mutant neuronal structure in the Mushroom Body (MB), the learning and memory center in *Drosophila* brain. *dfmr1* null MB neurons display more complex neuronal structure, including overgrowth and overbranching in dendrites and axon, more excess processes from cell bodies, and abnormal synapse formation. In contrast, dFMRP overexpression simplified neuronal structure, causing undergrowth and underbranching. Another *Drosophila* FXS lab also reported that the Mushroom Body β-lobe displayed an over-extending phenotype, which caused the β-lobe axon crossing the midline between two Mushroom bodies. Taken together, these results suggest that dFMRP acts a negative regulator in both central and peripheral nervous systems to control the differentiation of neuronal architecture (Pan et al., 2004).

Defects of Neuronal Plasticity in *fmr1* mutants

FMRP is believed to be a translation regulator, and it suppresses its own translation in a negative feedback loop (Weiler et al., 1997; Sung et al., 2003). Both FMRP and *FMR1* mRNA were found localized in neuronal processes and

synaptic terminals (Weiler et al., 1997; Antar et al., 2004). These facts raise the speculation that FMRP regulates local protein synthesis at synaptic terminals, which is an important process in synaptic development and/or plasticity.

In *fmr1* knockout mice, hippocampal long-term depression (LTD), dependent on activation of the group I class 5 metabotropic glutamate receptor (mGluR) , is selectively enhanced (Huber et al., 2002; Koekkoek et al., 2005), while hippocampal long-term potentiation (LTP) is normal (Godfraind et al., 1996). This LTD increase is caused by aberrant GluR1 AMPA (α-amino-3-hydroxy-5-methyl-4-isoxazole propionic acid) glutamate receptor expression (Bear et al., 2004; Nosyreva and Huber, 2006) and local protein synthesis dependent. Treating *fmr1* KO mice with the mGluR5 antagonist MPEP, which blocks mGluR5 activity, can rescue two major FXS phenotypes, reduced habituation in open field tests and increased sensitivity to audiogenic seizures (Yan et al., 2005). Moreover, cerebral cortex LTP is reduced concomitant with reduced GluR1 expression in *fmr1* mutant mouse (Li et al., 2002; Larson et al., 2005; Zhao et al., 2005).

At the *Drosophila* NMJ, which is a glutamatergic synapse, evoked excitatory junctional current (EJC) is significantly increased in *dfmr1* null mutants. In addition, quantal analysis showed that both the amplitude and frequency of spontaneous transmission are increased at the *dfmr1* NMJ (Zhang et al., 2001). Ultrastructure analysis of *dfmr1* mutants showed enlarged synaptic boutons, and abnormal synaptic vesicle accumulation in presynaptic boutons (Pan et al., 2004). These data suggest a neuronal transmission deficit in *dfmr1* mutants.

Molecular Mechanism of FXS

Loss of functional FMRP is the only known cause of Fragile X Syndrome, so the major efforts to understand molecular mechanism of FXS were to explore the function of FMRP. As an RNA binding protein, FMRP is believed to be a translational regulator, which may function in both neuronal soma and synaptic terminals. Therefore, a key question is to determine the downstream targets and downstream pathways that FMRP may regulate.

The identification of the first direct target of FMRP, was when our lab first found that expression of Futsch, the *Drosophila* homologue of microtubule associated protein 1B (MAP1B), was down-regulated by dFMRP; and that *FUTSCH* mRNA can be immunoprecipitated by anti-FMRP antibody (Zhang et al., 2001). Moreover, *futsch; dfmr1* double mutations can rescue the synaptic structure and functional defects in *dfmr1* null. This result was confirmed in *fmr1* KO mice; MAP1B expression is enhanced in the hippocampus of *fmr1* mice and microtubule stability is increased in *fmr1* mutant culture neurons (Lu et al., 2004). In another research system of dFMRP, the *Drosophila* testes, our lab found that the conventional 9+2 structure of microtubules in sperm tail axoneme was changed in *dfmr1* mutants, with the two central pairs lost (Zhang et al., 2004). All these data suggest that FMRP may influence microtubule structure by regulating microtubule binding protein level.

Also in the *Drosophila* model, other identified targets of dFMRP include the small GTPase Rac1 (Lee et al., 2003), and actin-binding Profilin (Reeve et al., 2005), which are both important for actin dynamics and microfilament remodeling.

Both Rac1 and Profilin levels are increased in *dfmr1* mutants. FMRP and GTPase Rac1 can both regulate the branching pattern of dendritic arborization (DA) neurons (Lee et al., 2003). Loss of dFMRP causes overbranching in DA dendries, and over-expression dFMRP causes underbranching. *Rac1* mutants display opposite phenotypes to *dfmr1* mutants; and co-overexpression of these two proteins can reverse dendritic branching to wild type level. A Similar relationship was also found between FMRP and Profilin (*chickadee*). Both of them regulate neuronal process patterning in Lateral Neurons (LNv), but do so in opposite directions. *dProfilin; dfmr1* double mutants display normal pattern of LNv (Reeve et al., 2005). In addition, FMRP was also found interacted with CYFIP, a protein affecting axon growth and interacted with Rac1 pathway (Schenck et al., 2003). These results suggest FMRP may regulate actin dynamics and microfilament remodeling by regulating the levels of actin associated proteins.

Furthermore in *fmr1* KO mice, both MAP1B and activity-regulated cytoskeleton-associated protein (Arc) mRNA were found associated with FMRP and BC1 non-translatable RNA complex, and upregulated in *fmr1* mutants (Zalfa et al., 2003). The cooperation between FMRP and BC1 RNA is one of the most potential mechanisms of FMRP recognizing and regulating its targets. Taken together, FMRP regulates the expression of several cytoskeleton associated proteins, consequently affecting cytoskeleton stability or remodeling in neuronal processes and synapses. This is therefore one attractive mechanism by which FMRP may contribute to neuronal elaboration and function (Figure1.3A).

In *fmr1* KO mice, the enhanced hippocampus LTD was a particularly exciting

Figure 1.3 Molecular Mechanisms of FXS

A. Cytoskeleton mechanism: Cytoskeleton associated proteins, including MAP1B/Futsch, Arc, CamKII, GTPase Rac1, are directly regulated by FMRP in a negative translation mechanism, consequently influence microtubule stability or actin reorganization and synaptic structure and functions.

B. mGluR theory: In the normal situation, mGluR signal induced LTD is *in situ* protein synthesis dependent. Some newly expressed proteins are regulators of AMPA glutamate receptor membrane expression. FMRP may regulate the level of this process by inhibiting translation in a negative feedback loop. When FMRP is not available, some synthesis may not be initiated or protein synthesis is aberrantly constantly upregulated. Membrane-expressed AMPA receptor levels are abnormal, consequently resulting in increased LTD. Modified from Bagni and Greenough, 2005.

A

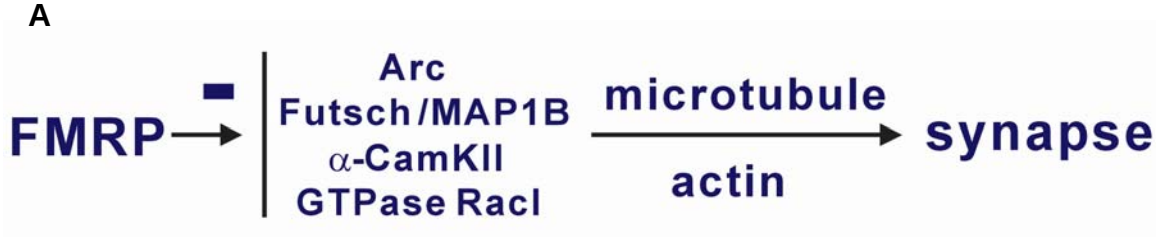
FMRP
Arc
Futsch/MAP1B
α-CamKII
GTPase Racl
microtubule
actin
synapse

B

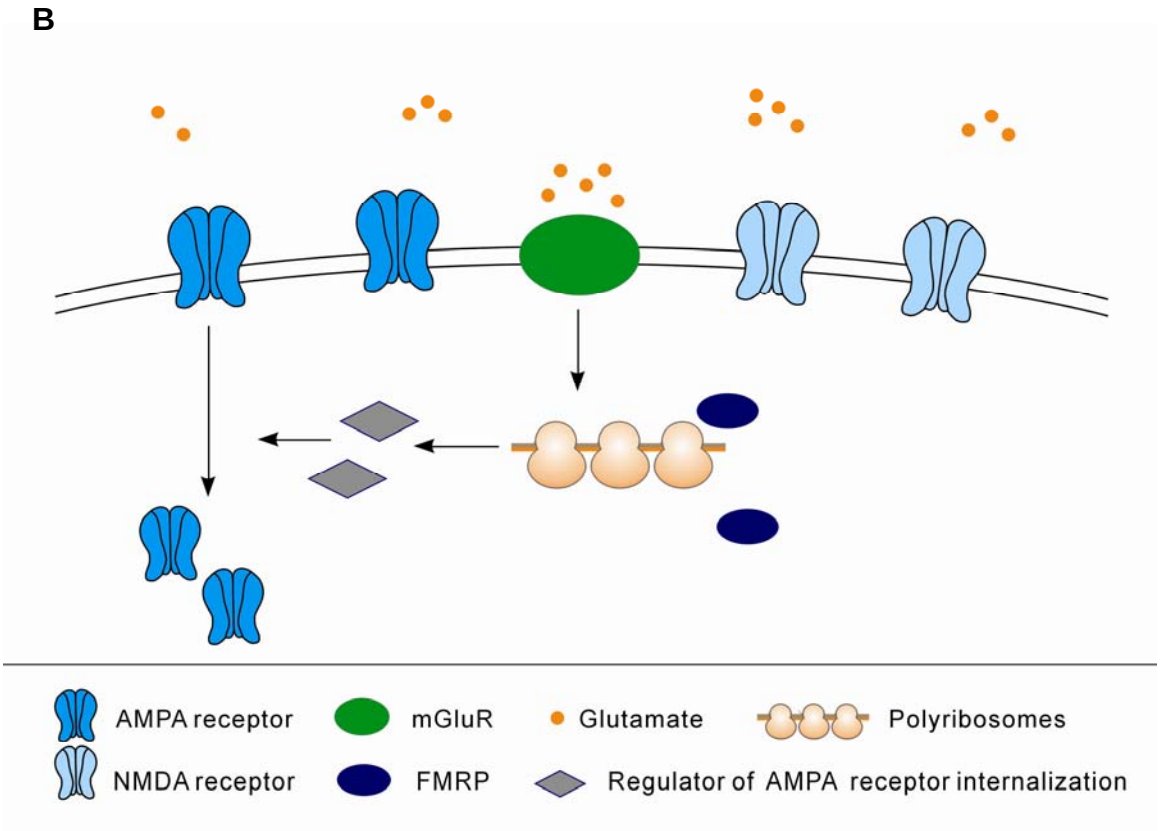
AMPA receptor
mGluR
Glutamate
Polyribosomes
NMDA receptor
FMRP
Regulator of AMPA receptor internalization

finding in the field. FMRP is a translation regulator, which presents in both pre- and postsynaptic terminals. Neurotransmitter-stimulated local protein synthesis is known to be essential for some types of synaptic plasticity (Schuman et al., 2006). In addition, FMRP is *in situ* translated at postsynaptic terminals (Weiler et al., 1997; Todd et al., 2003b), a process stimulated, like other local synaptic protein synthesis, by group I mGluR5 activation (Huber et al., 2000; Huber et al., 2001; Weiler et al., 2004; Pfeiffer and Huber, 2006). All of these facts raised the support for the conclusion that FMRP function is related to synaptic plasticity.

Both FMRP synaptic localization and expression are increased by glutamatergic activity, and this regulation is blocked by MPEP (mGluR5 antagonist) and increased by DHPG (mGluR5 agonist) (Weiler et al., 1997; Antar et al., 2004; Weiler et al., 2004; Hou et al., 2006). mGluR-dependent LTD is normally completely dependent on new translation, but in the absence of FMRP, mGluR5 activation does not trigger protein synthesis (Weiler et al., 2004; Aschrafi et al., 2005). Anisomycin, a translation inhibitor, can suppress mGluR5-induced LTD. However, this inhibitive response is lost and the DHPG-induced increase of synaptic proteins synthesis is reduced in *fmr1* KO mice (Hou et al., 2006; Nosyreva and Huber, 2006). One outcome of mGluR5 activation is to regulate trafficking of AMPA GluRs (Carroll et al., 1999; Snyder et al., 2001; Xiao et al., 2001; Nosyreva and Huber, 2005). Correspondingly, feeding *dfmr1* mutant *Drosophila* with MPEP, as well as class II/III mGluR antagonists, can rescue some mutant phenotypes, including behavioral (courtship learning and memory) and morphological (mushroom body β-lobe over-extending) defects (McBride et al.,

2005). These data suggest a mechanistic connection between mGluR signaling, the translation regulatory function of FMRP, and AMPA GluR expression: a hypothesis termed “the mGluR theory of FXS” (Bear et al., 2004).

Aims and results in this work

This work employs the *Drosophila* model to study cellular and molecular mechanism of Fragile X syndrome, including dFMRP’s function on neuronal elaboration, synaptogenesis, and synaptic plasticity.

In the first part of this thesis work, I used a powerful genetic technique called Mosaic Analysis of Repressible Cell Marker (MARCM) to examine neuronal structure in *Drosophila* Mushroom Body (MB), a learning and memory center in the fly brain. Former results suggested dFMRP was a negative regulator of both axonal and dendritic elaboration in peripheral nerve system. My work examined this hypothesis in the central nervous system (CNS). I found that loss of dFMRP converts unipolar MB neurons into multipolar neurons. Both dendrites and axon display overgrowth and overbranching phenotypes in *dfmr1* null mutants, which is consistent with peripheral nervous system (PNS) phenotypes. Moreover, ultrastructure analysis of *dfmr1* mutants shows enlarged synaptic boutons, irregular bouton size, and abnormal vesicles accumulation in synaptic boutons, which indicate altered synaptogenesis and/or arrested synaptic function. Combined with former results, my data indicate that *Drosophila* FMRP is a negative regulator of the differentiation of neuronal architecture and synaptic connections in both PNS and CNS (Pan et al., 2004).

Beyond the cellular level, my next work investigated the molecular mechanisms underlying structural and functional defects in *dfmr1* mutant neurons. In a series of tests for synaptic protein levels at the *Drosophila* NMJ, I found that the levels of AMPA-like ionotropic glutamate receptor subunits were changed in *dfmr1* mutants. Associated with the “mGluR theory” hypothesis, I examined mechanistic links between dFMRP, DmGluRA and ionotropic GluR expression. Two GluR classes reside at this synapse, each containing common GluRIIC (III), IID and IIE subunits, and variable GluRIIA (A-class) or GluRIIB (B-class) subunits. In *dfmr1* null mutants, A-class GluRs accumulate and B-class GluRs are lost, whereas total GluR levels do not change, resulting in a striking change in GluR subclass ratio at individual synapses. DmGluRA is the sole *Drosophila* mGluR, and is expressed at the NMJ. In *dmGluRA* null mutants, both ionotropic GluR classes increase, resulting in an increase in total synaptic GluR content but no change in GluR subclass ratio. In *dfmr1; dmGluRA* double null mutants, there is an additive increase in A-class GluRs, and a similar additive impact on B-class GluRs, towards normal levels in the double mutants. By overexpressing dFMRP or DmGluRA at either pre- or post synaptic terminals, I found the mechanism of FMRP regulating ionotropic GluRs was postsynaptic. These results show that dFMRP differentially regulates different GluR subclasses within a single synaptic terminal that DmGluRA negatively regulates in common these GluRs, but the dFMRP mechanism is at least somewhat independent of mGluR signaling with the two pathways converging to jointly control synaptic GluR abundance.

To further elucidate the mechanistic relationship between dFMRP and

DmGluRA, I further tested behavioral performance, neuronal structure, and protein expression level, in both *dfmr1* and *dmGluRA* mutants. I found dFMRP is upregulated in *dmGluRA* mutant CNS, and vice versa. *dmGluRA* mutants display a behavioral defect in coordinated movement, as revealed by a “roll over” assay, which can be rescued by removing dFMRP expression. The *dfmr1* mutants display a series of neuronal structure defects at NMJ, including increased branch number, increased total bouton number, and increased total synaptic area. Blocking DmGluRA signaling can rescue the over-branching phenotype of *dfmr1* null, however with no significant effect on the increased total synaptic area. Conversely, the total bouton number is increased even more in absence of DmGluRA signaling in the *dfmr1* null mutants. These data strongly suggest that both overlapping and independent mechanisms exist between dFMRP function and DmGluRA signaling in neuronal/synaptic regulation.

Taken together, my studies showed that FMRP functions as a negative regulator of neuronal architecture. In addition, FMRP regulates synaptic function partially by interacting with metabotropic glutamate receptor signaling, and bring a new insight into the regulative function of FMRP to components of ionotropic glutamate receptors and neurotransmission control.

CHAPTER II

THE *DROSOPHILA* FRAGILE X GENE NEGATIVELY REGULATES NEURONAL ELABORATION AND SYNAPTIC DIFFERENTIATION

This paper has been published under the same title in *Current Biology*, 2004.

Luyuan Pan, Yong Q. Zhang, Elvin Woodruff and Kendal Broadie

Department of Biological Science, Kennedy Center for Research on Human Development, Vanderbilt University, Nashville, TN 37232

Summary

Fragile X Syndrome (FXS) is the most common form of inherited mental retardations. The disease is caused by silencing of the *fragile X mental retardation 1* (*FMR1*) gene, which encodes the RNA-binding, translational regulator FMRP. In FXS patients and *fmr1* knockout mice, loss of FMRP causes denser and morphologically altered postsynaptic dendritic spines. Previously, we established a *Drosophila* FXS model, and showed that dFMRP acts as a negative translational regulator of Futsch/MAP1B, and negatively regulates synaptic branching and structural elaboration in the peripheral neuromuscular junction (NMJ). Here, we investigate the role of dFMRP in the central brain, focusing on the Mushroom Body (MB), the learning and memory center. In MB neurons, dFMRP bi-directionally regulates multiple levels of structural architecture,

including process formation from the soma, dendritic elaboration, axonal branching and synaptogenesis. *Drosophila fmr1* (*dfmr1*) null mutant neurons display more complex architecture, including overgrowth, overbranching and abnormal synapse formation. In contrast, dFMRP overexpression simplifies neuronal structure, causing undergrowth, underbranching and loss of synapse differentiation. Ultrastructural studies of *dfmr1* mutant neurons reveal enlarged and irregular synaptic boutons with dense accumulation of synaptic vesicles. Taken together, these data show that dFMRP is a potent negative regulator of neuronal architecture and synaptic differentiation in both peripheral and central nervous system.

Introduction

The fragile X mental retardation protein (FMRP) is a negative translational regulator whose known targets include prominent regulators of the neuronal cytoskeleton such as Futsch/MAP1B (Zhang et al., 2001; Zalfa et al., 2003), Arc/Arg3.1 (Zalfa et al., 2003), α-CamKII (Zalfa et al., 2003) and FMRP itself (Schaeffer et al., 2001). Loss of FMRP is associated with abnormal postsynaptic dendritic spines in Fragile X Syndrome patients and in the mouse knockout model, which are denser and morphologically altered compared to normal (Rudelli et al., 1985; Hinton et al., 1991; Irwin et al., 2001). While dendritic spine abnormalities occur in other neurological diseases, including Down's Syndrome and Alzheimer's

Disease (Purpura, 1974; Fiala et al., 2002;), increased spine density appears to be a unique feature of FXS (Irwin et al., 2000; Kooy, 2003). Such defects in dendritic spine pruning and maturation may indicate that FMRP regulates experience-dependent synaptogenesis. While basal synaptic function appears relatively normal in mutant mice, hippocampal long-term depression (LTD) dependent on activation of metabotropic glutamate receptors is selectively enhanced (Huber et al., 2002). It is, therefore, enticing to speculate that synaptic structural and functional defects underlie fragile X mental retardation and cognitive deficits.

We previously established a *Drosophila* FXS model to test the hypothesis that FMRP regulates synaptic differentiation, utilizing the well-characterized neuromuscular junction (NMJ; Zhang et al., 2001). We showed that the level of *Drosophila* FMRP (dFMRP) regulates both structural complexity and synaptic transmission strength; *dfmr1* null mutants display overgrowth/overbranching and strengthened transmission, whereas dFMRP overexpression caused the opposite phenotype of undergrowth/underbranching (Zhang et al., 2001). Similar results were also reported in another peripheral nervous system model, dendritic arborization (DA) neurons, which are a subtype of *Drosophila* peripheral sensory neurons (Lee et al., 2003). In DA neurons, *dfmr1* mutants display increased higher-order sensory dendritic branching, whereas dFMRP overexpression inhibits dendritic branching and reduces the complexity of sensory processes.

While both NMJ and DA sensory neurons are tractable systems in which to study neuronal morphology, the mechanisms governing central neurons might be very different. In the adult *Drosophila* brain, dorsal cluster (DC) and lateral neurons (LNv) have been reported to display highly variable phenotypes in *dfmr1* mutants (Morales et al., 2002). In DC neurons, both null mutants and dFMRP overexpression reportedly result in similar phenotypes; decreased neuronal extension and irregular neuronal branching. However, in LNv processes, *dfmr1* mutants reportedly display over-extension phenotypes. In addition, axon guidance defects were reported in both DC and LNv neurons. At the same time, photoreceptor neurons are reportedly morphologically normal (Dockendorff et al., 2002; Morales et al., 2002). These results are confounding, suggesting that dFMRP may differentially regulate peripheral and central neurons, or play different roles in neuronal subtypes.

Given the importance of understanding the role of dFMRP in central neurons, particularly in behavioral circuits most relevant to FXS cognitive symptoms, we undertook an in-depth examination of the mushroom body, the learning and memory center of *Drosophila* brain (Davis and Han, 1996; Heisenberg, 1998; Heisenberg, 2003). Due to its inherent complexity, it is technically very difficult to study neuronal morphogenesis in the brain using conventional techniques. We therefore used the MARCM (mosaic analysis with a repressible cell marker) system developed by Lee and Luo (1999), which labels single homozygous

mutant neurons uniquely, to reveal the whole projections of labeled neurons in the intact brain. We show here that the level of dFMRP tightly regulates neuronal structure, including formation of cell body processes, dendritic elaboration, axon branching, and synapse formation in mushroom body neurons. These central phenotypes are strikingly similar to our earlier report of peripheral phenotypes at the NMJ (Zhang et al., 2001). Ultrastructure analysis of *dfmr1* mutants show enlarged synaptic boutons, irregular bouton size, and abnormal vesicles accumulation in synaptic boutons, which indicate altered synaptogenesis and arrested synaptic function. Taken together, these data suggest that dFMRP acts a negative regulator in the brain to control the differentiation of neuronal architecture and synaptic connections.

Results

dFMRP is expressed primarily in the neuronal soma in Mushroom Body

We previously showed in the *Drosophila* 3rd instar larva, that dFMRP is enriched in neuronal soma cytoplasm, undetectable in neuronal nuclei, and present at only a very low level in neuronal processes (Zhang et al., 2001). Likewise in larval sensory dendritic arborization (DA) neurons, dFMRP is highly enriched in soma and present at very low levels in sensory dendrites (Lee et al., 2003). Both mammalian and *Drosophila* FMRP is also enriched in adult brain,

specifically in neurons and glia progenitor cells but not mature glia (Devys et al., 1993; Morales et al., 2002; Wang et al., 2004). In rat brain, FMRP is found primarily in neuronal soma, absent from nuclei, with a very small percentage of the protein present in neuronal processes, including postsynaptic dendritic spines (Feng et al., 1997; Weiler et al., 1997). To understand if dFMRP plays a role in the mushroom body (MB), we first assayed the expression pattern of dFMRP in MB neurons.

To delineate MB neurons, we used the UAS-GAL4 system, in which a tissue-specific GAL4 transcription factor activates expression of a target gene by binding with its upstream activating sequence (UAS; Brand and Perrimon, 1993; Fischer et al., 1988). Here, UAS-mouseCD8-GFP driven by GAL4-OK107 labels the whole MB (Figure 2.1; Connolly et al., 1996). Double labeling of mushroom body with mCD8-GFP driven by OK107-GAL4 and anti-dFMRP antibody showed that dFMRP is expressed in the mushroom body neurons in a level similar to that of neighboring neurons (Figure 2.1A). dFMRP is prominently enriched in the soma of all MB neurons, but is undetectable in nuclei. The protein is clearly present at highest levels only within the cell body cytoplasm, with little or no detectable dFMRP in the dendrites and axonal lobes of MB neurons (Figure 2.1A). As a positive control, we labeled the MB with an antibody against Discs Large (DLG), a *Drosophila* homolog of postsynaptic density protein 95 (PSD95). Unlike dFMRP, DLG is prominently expressed in the dendritic arbor of MB neurons, as expected

Figure 2.1. dFMRP is primarily localized in the soma of Mushroom Body neurons.

The whole mushroom body is labeled by UAS-CD8-GFP (green) driven by GAL4-OK107. The cell bodies, dendrites and axons are indicated.

A. dFMRP expression (red) is predominantly present in soma, undetectable in dendrites and axons.

B. Discs Large (DLG; red), a synaptic maker, as a positive control. Expression clearly observed in the MB neuropil. Scale bar = 10 μm.

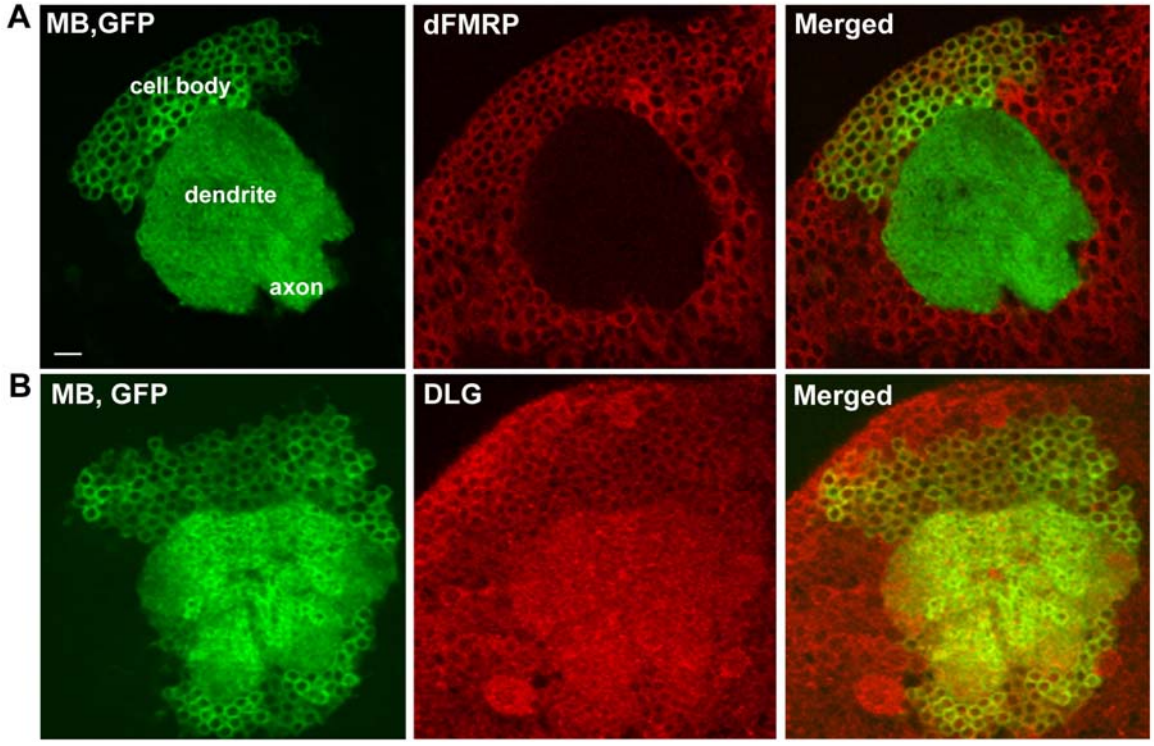
A
MB,GFP
cell body
dendrite
axon
dFMRP
Merged
B
MB, GFP
DLG
Merged

(Figure 2.1B). Thus, dFMRP is primarily restricted to neuronal soma.

Mushroom Body structure is largely normal in *dfmr1* null mutants

There are three types of neurons in the *Drosophila* MB: γ, α'/β', and α/β (Lee et al., 1999). In development, γ neurons are born first, soon after larval hatching, and their axonal projections form only one horizontal lobe in the adult MB. α'/β' neurons are born second, between the mid-3rd instar and puparium formation, and lastly α/β neurons are born after puparium formation. In contrast to the single horizontal projection of γ neurons, both α'/β', and α/β neurons have two axon projections, horizontal and vertical. The adult MBs display four specific structural clusters, including cell bodies, dendrites (also known as calyx), peduncle, and the axon lobes (Figure 2.2B). We took advantage of the relative simplicity of these MB neurons to analyze the requirement for dFMRP in their morphological differentiation. In this work, to make sure all phenotypes are caused by *dfmr1* mutation, we used two independently generated null mutant alleles of *dfmr1*, which represent over-lapping intragenic deficiencies; $dfmr1^{50M}$ (Zhang et al., 2001) and $dfmr1^{3}$ (Dockendorff et al., 2002) (Figure 2.2A). In addition, we overexpressed dFMRP in targeted MB neurons to examine the consequence of excess protein.

In both FXS patients and *fmr1* KO mice, brain morphology is grossly normal

Figure 2.2. dFMRP loss-of-function Mushroom Body has gross normal morphology.

A. Genomic structure of the *dfmr1* locus and the two independent *dfmr1* intragenic deletion mutants used in this study; $dfmr1^{50M}$ (Zhang, et al., 2001) and $dfmr1^{3}$ (Dockendorff, et al., 2002). Note that $dfmr1^{3}$ deletion reported here has verified breakpoints that differ from reported in Dockendorff, et al., 2002.

B. Whole mushroom morphology revealed by large neuroblast MARCM clones, labeled by UAS-CD8-GFP driven by GAL4-OK107. Wild type (WT) MB structure showing the labeled axon lobes (Lee et al., 1999). Occasional axon extension beyond the β lobe is observed. The *dfmr1* null mutants display grossly normal MB structure. Mild β lobe overgrowth was also observed at a slightly higher frequency than wild type. In contrast, dFMRP overexpression ($dfmr^{OE}$ mutant) caused a high frequency of apparently random growth of all axon lobes. Especially in β lobe, dramatic overgrowth was observed at high frequency. All scale bars = 25 μm.

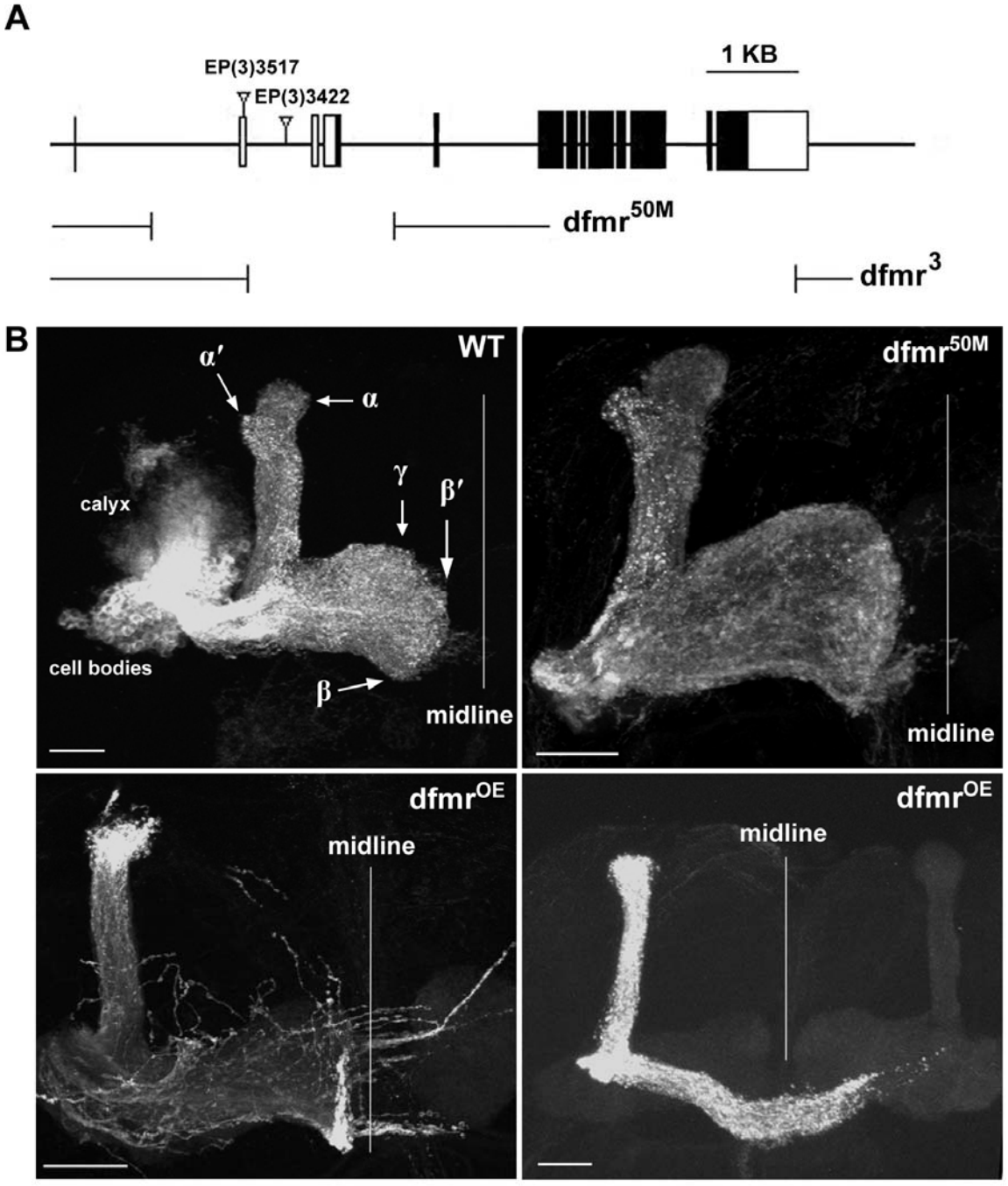
A
EP(3)3517
EP(3)3422
1 KB
dfmr50M
dfmr3
B
WT
α′
α
γ
β′
calyx
cell bodies
β
midline
dfmr50M
midline
dfmrOE
midline
dfmrOE
midline

with no detectable abnormalities in any specific brain regions (Bakker, 1994; Reyniers et al., 1999). Similarly, null *dfmr1* mutants display normal gross brain morphology, including an anatomically normal MB (Figure 2.2B). Mild overgrowth of the MB β lobe was observed in the null mutants. In contrast, dFMRP overexpression (OE) caused dramatic structural defects in MB axon lobes (Figure2.2B); the β lobe always over-extended across the midline, fusing the two MBs, the β' lobe often displayed an apparently random direction of axon projection outside of the normal MB domain, and the γ lobe always displayed a dramatic decrease in volume, or was even completely lost (Figure 2.2B). Thus, *dfmr1* null mutants display only subtle phenotypes at a gross MB level, whereas *dfmr1* OE mutants display dramatic defects. Since FXS is caused by loss of FMRP, we therefore turned our attention to the single cell and subcellular level to examine neuronal architecture.

Loss of dFMRP converts unipolar neurons into multipolar neurons

The MARCM technique (Lee and Luo, 1999) provides a uniquely powerful approach to examine homozygous mutant neurons *in situ* at a single cell level of resolution. In this technique, a repressor of GAL4 gene activation, the GAL80 gene, is placed *in trans* with the mutant gene, *dfmr1*. After induced mitotic recombination, homozygous mutant neurons express a GAL4-driven cell maker (e.g.UAS-GFP) because GAL80 is absent, whereas non-mutant neurons maintain

GAL80, silencing GAL4-drived gene expression (Figure 2.3). All the analyses presented in this study represent quantification from single cell clones, where only a single neuron in the mushroom body is labeled (Figure 2.3). We examine, in turn, each region of the mutant neuron, progressing from the cell body, through dendrites, axons and synapses.

Drosophila MB neurons are exclusively unipolar (Crittenden et al., 1998; Lee et al., 1999). The cell bodies of MB neurons extend only a single primary process, which subsequently branches to form distinctive dendrites and a single axon projection (Figure 2.3A). A minority of wild type cells displays 1-2 tiny hair-like projections, but these additional processes are always very short and thin compared with the primary process. In wild type animal, it is exceptionally rare for the secondary processes to contain any branches or varicosities indicating functional differentiation (Figure 2.3A). In contrast, *dfmr1* mutant cell bodies have a strong tendency to extend excess processes, thus always converting the characteristic unipolar neurons in wild type into multipolar neurons in mutants (Figure 2.3A). In addition, the supernumerary processes in *dfmr1* mutants are usually long and thick, posses a clear branching structure and usually contain varicosities characteristic of synaptic boutons (Figure 2.3A). Correspondingly, dFMRP overexpression (OE) mutants display even fewer processes than wild type neurons. With excess dFMRP protein, most MB cell bodies are extremely clean, with no excess processes in addition to the primary process (Figure 2.3A).

Figure 2.3. dFMRP loss-of-function results in aberrant multipolar neurons.

A. Representative images of α'/β' neuronal soma and processes in single-cell MARCM clones. Wild type (WT) neurons are typically unipolar, with at rare frequency 1-2 other short process (arrow). These tiny processes lack secondary branches. Overexpression of dFMRP (OE) results in a cleaner cell body, with no excess processes. In contrast, *dfmr1* null mutant neurons always display multiple processes (arrows), becoming characteristically multipolar. These supernumerary processes are almost always multiply-branched and contain varicosities resembling synaptic boutons. Scale bar = 5 μm.

B. Quantification of the number of processes projecting from cell bodies. Bars show mean ± SEM. Significance,: 0.001<P<0.05 (*); 0.0001<P<0.001 (**).

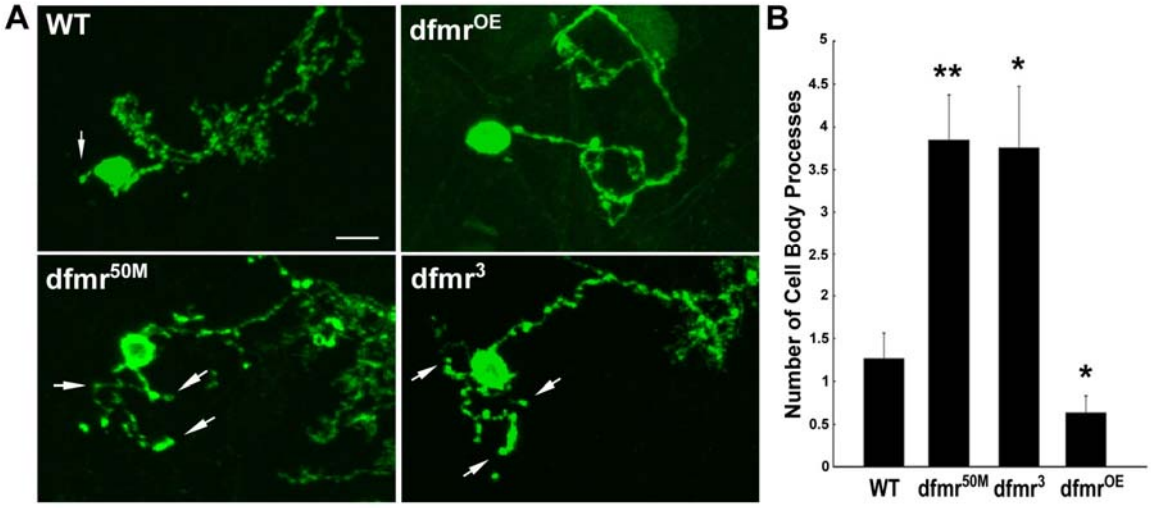
A
WT
dfmrOE
dfmr50M
dfmr3
B
Number of Cell Body Processes
0
0.5
1
1.5
2
2.5
3
3.5
4
4.5
5
**
*
*
WT
dfmr50M
dfmr3
dfmrOE

We quantified the number of supernumerary processes in single α'/β' neurons. Null mutants display a 3-fold increase in the number of cell body processes (WT, 1.27±0.3 (n=11); *dfmr1*^{50M}, 3.84±0.53 (n=19); *dfmr1*^{3}, 3.75±0.72 (n=12)), whereas dFMRP overexpression reduces the number of processes 2-fold (WT, 1.27±0.3 (n=11); *dfmr1*^{OE}, 0.64±0.2 (n=22)). Similar phenotypes were also observed in γ and α/β neurons. These data show that dFMRP strongly negatively regulates the generation of processes from neuronal cell bodies.

dFMRP negatively regulates dendritic branching and arbor elaboration

Although the dendritic arbors of all three types of MB neurons are elaborate and distinctive, common features of their dendritic structure aid in the description of the *dfmr1* mutant phenotypes. Late-born α/β neurons (mitotic recombination was induced >12 hours after pupa formation; Zhu et al., 2003) were used for comparative studies. Four features in particular were subject to analyses. First, wild type MB neurons have 3-4 primary dendritic branches. Second, wild type primary branches project from the main process with a regular spacing of ~7 μm. Third, wild type primary branches rarely contain higher-order branches. Finally, primary branches end with a fine dendritic terminal arbor, forming a highly characteristic "claw-like" structure (Figure 2.4; Zhu et al., 2003). We used these conserved features as a basis to analyze the effect of dFMRP levels on dendrite morphogenesis.

Dendrites on *dfmr1* null mutant neurons are consistently abnormal in morphology and projection, owing to changes in the number and arrangement of dendritic processes and increased variability of structural features (Figure 2.4). The number of primary dendritic branches are more variable in the mutant, ranging from 2-6 (compared to 3-4 in wild type). In addition, the spacing between these branches becomes extremely variable in the null mutant, from <3 μm to >20 μm, compared to the consistent ~7 μm spacing in wild type (Figure 2.4). More visually striking, most mutant dendrite processes have clear supernumerary higher-order branches, and the clustered fine dendritic arbors normally restricted to the extreme termini (the "claw-like" structure; Zhu et al., 2003), spread aberrantly along the entire length of dendritic branches. These excess fine dendritic processes convert the clear, orderly wild type dendrites into disordered, "cotton wool-like" dendrites in *dfmr1* mutants (Figure 2.4). On the other hand, dFMRP overexpression mutants lose the clustered fine dendritic arbors, and show severe reduction or complete loss of the claw-like structure at the terminal of dendritic branches (Figure 2.4). Excess dFMRP also results in longer, less structurally complex dendrites, which therefore take on the general appearance of axons. Thus, removal of dFMRP increases the branching and structural complexity of dendritic processes, whereas overexpression of dFMRP decreases dendritic branching and simplifies the arbor. These data show that dFMRP functions as a negative regulator of dendritic elaboration.

Figure 2.4. dFMRP negatively regulates dendrite elaboration.

Representative images of late-born α/β neuron dendrites in single-cell MARCM clones. Wild type (WT) dendrites typically display three primary branches, arranged in regular spacing of ~7μm. There are no high-order branches, but only a single, well-defined "claw-like structure" of fine processes at the termini (arrows). Three images of *dfmr1* null mutant neuron dendrites show more complex and disordered structure. Spaces between primary branches become extremely variable. Primary dendrites display clearly secondary branches. The fine dendritic processes normally restricted to the termini, spread aberrantly along the primary branches. These defects convert the orderly wild type dendrites into disordered, "cotton wool-like" structures. dFMRP overexpression results in loss of the claw-like termini. Arrows show the reduced or absent claw-like structures. Scale bar =10 μm.

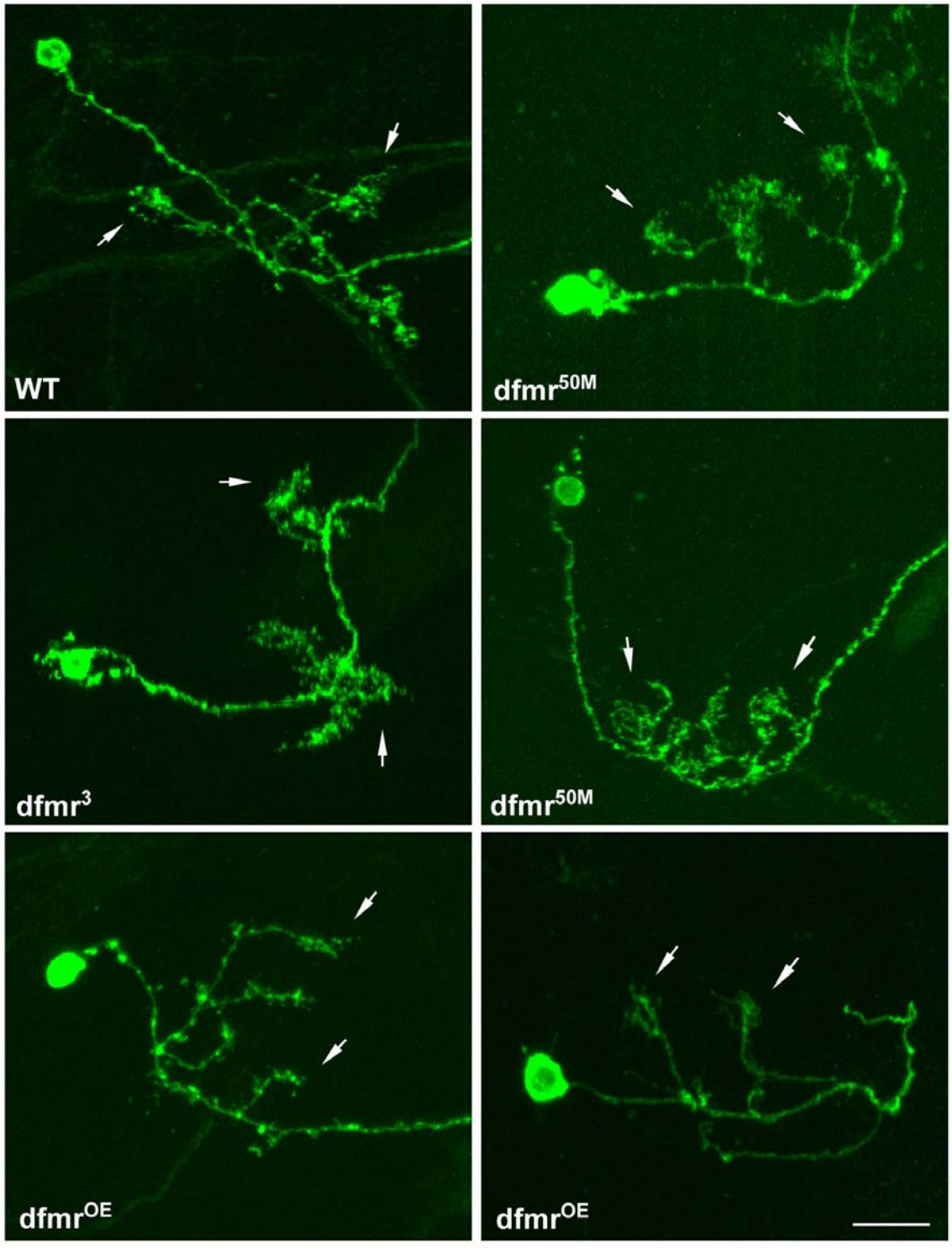
WT
dfmr50M
dfmr3
dfmr50M
dfmrOE
dfmrOE

dFMRP negatively regulates axonal branching

Progressing from the cell body and through the dendritic arbor, we next consider the role of dFMRP on axonal projection and structure. We first assayed the γ neuron because it has only one axonal branch and a particularly simple elaborative pattern in the adult MB. The wild type γ axon enters the horizontal MB axon lobe from the bottom edge, bends upwards to enter the γ lobe and terminates near the top boundary of the horizontal lobe (Figure 2.5A). The wild type γ neuron never branches prior to entering the γ lobe, but then typically has specific small branches along the main process (Lee et al., 1999). We assayed axonal morphology in *dfmr1* null mutant neurons and in neurons overexpressing dFMRP.

The axons of *dfmr1* null mutant γ neurons are more structurally elaborate the wild type cells. Mutant neurons always display significantly increased axonal branching, and always have significantly more and longer axonal branches (Figure 2.5A). These large, supernumerary branches do not follow the main axon trajectory, but rather extend in apparently random directions to invade inappropriate territory (Figure 2.5A). Mutant axons not only join the γ lobe and arrive at the top boundary of horizontal lobe, but also inappropriately enter the β lobe at the bottom boundary and the β' lobe at middle part of the horizontal lobe. Some of the excess branches in mutants are so large that it appears that the γ neuron possesses duplicated main axonal processes (Figure 2.5A). The number

Figure 2.5. dFMRP negatively regulates axonal branching.

A. Representative γ neuron axons in single-cell MARCM clones. The γ neuron axon normally enters the horizontal axon lobe from the bottom edge, bends upwards to enter the γ lobe and finally projects to the top boundary of horizontal lobe. In wild type (WT) neurons, the axon projection has only one main axonal branch with some specific small branches (arrows) along the main process. dFMRP over-expression (OE) causes dramatic underbranching of the axon. The γ neurons keep their processes along the bottom edge of the horizontal lobe and aberrantly invade the β lobe. The *dfmr1* null mutants display the opposite phenotype of axonal overbranching. Null mutant neurons always have more and longer axonal branches. These large branches don't follow the main axon direction, but rather extend in an apparently random direction (arrows). Scale bar =10μm.

B. Quantification of the large branches (>5μm) for a single γ axon.

C. Quantification of total branch length of a single γ axon. WT, n=19; $dfmr1^{50M}$, n=21; $dfmr1^{3}$, n=13; OE, n=24. Bars show mean ± SEM. Significance $0.001<P<0.05$ (*); $0.0001<P<0.001$ (**); $P<0.0001$ (***).

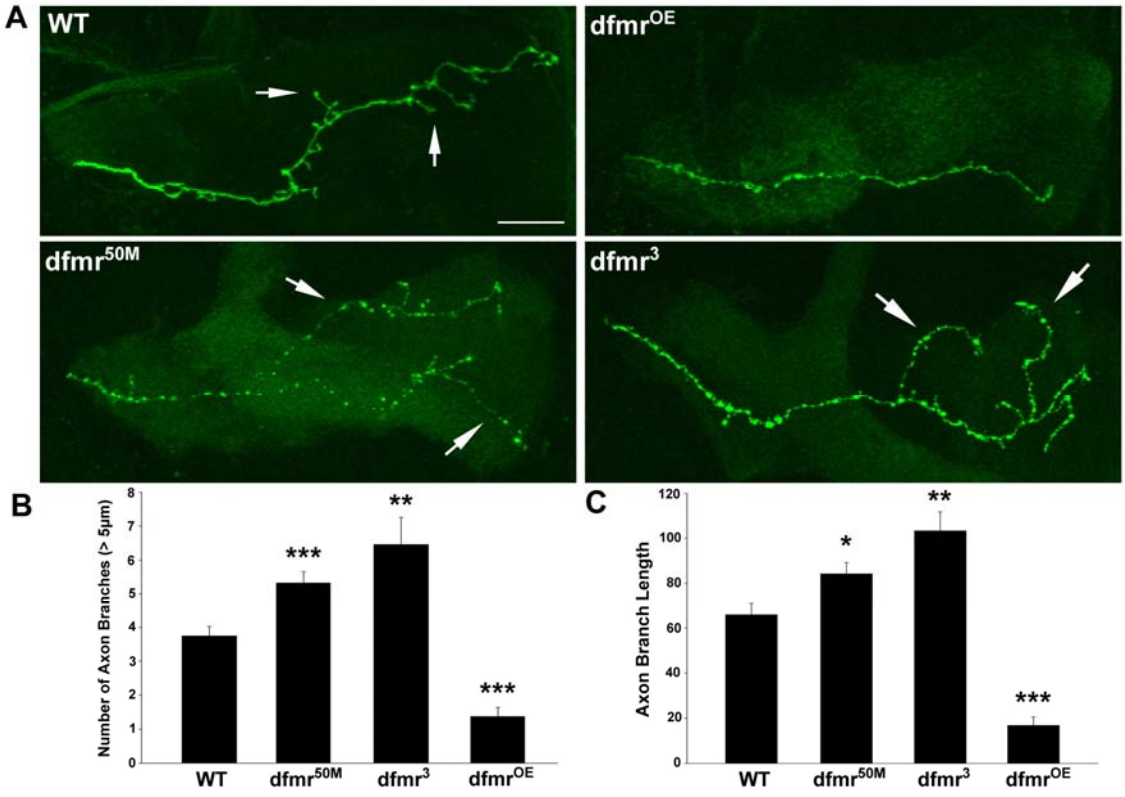
A
WT
dfmr^OE
dfmr^50M
dfmr^3
B
Number of Axon Branches (> 5μm)
0
1
2
3
4
5
6
7
8
***
**
***
WT
dfmr^50M
dfmr^3
dfmr^OE
C
Axon Branch Length
0
20
40
60
80
100
120
*
**
***
WT
dfmr^50M
dfmr^3
dfmr^OE

of these large branches (>5 μm in length) increased on average by >50% (WT, 3.74±0.28, n=19; *dfmr1*^{3}, 6.46±0.8, n=13; *dfmr1*^{50M}, 5.33±0.33, n=21; Figure 2.5B), and the total length of all axon branches also significantly increased (WT, 65.68±5.07 μm; *dfmr1*^{3}, 103.33±8.5 μm; *dfmr1*^{50M}, 84.29±5 μm; Figure 2.5C). Correspondingly, overexpression of dFMRP caused dramatic under-branching in the γ neuron axon. Overexpression (OE) mutant neurons lose most or all of the normal axonal branches (Figure 2.5A). At the same time, most dFMRP overexpression γ neurons maintain their processes along the bottom edge of the horizontal lobe and aberrantly invade the β lobe. With excess dFMRP, the number of axonal branches was decreased by 65% (WT, 3.74±0.28, n=19; *dfmr1*^{OE}, 1.38±0.26, n=24; Figure 2.5B) and the total axonal branch length was decreased by 75% (WT, 65.68±5.07 μm; *dfmr1*^{OE}, 16.86±3.8; Figure 2.5C). Thus, excess FMRP dramatically simplifies axonal projection and results in premature termination.

Similar phenotypes were observed in the other two classes of MB neurons. Wild type α'/β' neurons, for example, characteristically have one small side branch in the proximal quarter region of the primary axon process, and then small branches that cluster at the terminal of the horizontal lobes. Between this proximal branch and the terminal branching region, wild type α'/β' neurons never contain branches along the axon process (Figure 2.6A; Lee et al., 1999). In contrast, *dfmr1* null mutants display larger branches in both the proximal quarter region and

the terminal of α'/β' axons, and supernumerary branches in the interspace region (Figure 2.6A). Correspondingly, *dfmr1* OE mutants mostly lose this characteristic axonal branching pattern (Figure 2.6A). In addition, OE mutants often do not stop at the end of horizontal lobe, but usually turn up or down to form an aberrant hook at the terminus (Figure 2.6A). Similarly in α/β neurons, null *dfmr1* mutant display excessive α processes. These results demonstrate that dFMRP functions to negatively regulate axonal branching in MB neurons, resulting in defective axonal guidance and connectivity.

dFMRP regulates synaptic size and differentiation

Loss of dFMRP results in striking defects in neuronal architecture (Figure 2.3-2.6), suggesting that synaptic connectivity should be impaired. These structural defects may be the primary manifestation of the *dfmr1* mutation, or may be a secondary consequence of impaired synaptic differentiation. Recent work in mouse *fmr1* mutants have indicated defects in synaptic plasticity, suggesting specific problems in synaptogenesis, synaptic function or both (Huber et al., 2002). Likewise, our previous work on *dfmr1* mutants in the *Drosophila* NMJ and eye has strongly suggested specific defects at the synapse (Zhang et al., 2001). We therefore next examined synaptic differentiation in *dfmr1* mutant MB clones at both the light and electron microscopy levels.

In wild type animals, the axonal processes of MB neurons display a relatively

smooth profile, with only subtle swellings, or varicosities, marking the sites of presynaptic boutons forming *en passé* connections (Figure 2.5A (γ neuron) and 2.6A (α'/β' neuron)). In comparison, *dfmr1* mutant axons show a markedly discontinuous profile, with large puncta-like varicosity structures fairly evenly distributed along the axons, producing a highly characteristic "beads on a string" appearance (Figure 2.5A, 2.6A). The position and spacing of these varicosities strongly suggests that they represent enlarged or otherwise abnormal synaptic boutons. Correspondingly, overexpression of dFMRP resulted in reduction in the appearance of these presumptive synaptic boutons (Figure 2.5A, 2.6A). Thus, at a light microscope level, it appears that the level of dFMRP plays some prominent role in the regulation of synapse formation or differentiation.

To confirm the identity of these presumed synaptic boutons, and to examine in detail synaptic differentiation in *dfmr1* mutants, we next employed electron microscopy to examine MARCM mutant clones. For EM labeling, we used a peroxidase-conjugated anti-CD8 antibody followed by a Ni^{2+}-enhanced DAB reaction to produce an electron-dense, membrane-associated signal clearly marking the *dfmr1* mutant neurons (Figure 2.6D, and see Methods). We focused our analysis on α'/β' axons in the horizontal axon lobe (Figure 2.6C), which show an extensive over-branching phenotype and prominently enlarged varicosities at the light microscope level (Figure 2.6A).

Figure 2.6. Altered synaptogenesis in *dfmr1* mutants

A. Representative α'/β' neuron axon morphologies in single-cell MARCM clones. Wild type (WT) neurons characteristically have one small side branch in proximal quarter region, and branches clustered at the terminal of the horizontal lobes (arrowheads). Note that GFP distribution is relatively even along the axon, with only small varicosities. Two null *dfmr1* mutant neuron axons display over-branching. Axons have longer side branches in proximal quarter and the terminal region. Extra branches (arrowheads) are observed between the proximal quarter and the terminal branching region. The GFP distribution is strikingly altered, with enlarged puncta (arrows) distributed along the axons. dFMRP overexpression (OE mutant) causes the loss of the characteristic branches. There is no branch in proximal quarter and terminal branching region. Arrowheads indicate the positions should have typical branches in WT axon. Scale bar = 20 μm.

B. DAB stained brain revealing a large MARCM clone within the Mushroom Body. Scale bar = 100 μm.

C. Confocal image of the whole Mushroom Body MARCM clone. Quadrangle represents the plane of section through the horizontal lobe, where all electron micrographs were taken. Scale bar = 10 μm.

D&E. 11500X (D) and 40000X (E) electron micrograph of the Mushroom Body horizontal lobe. Labeled MARCM clone cells are marked with (L), unlabeled profiles (U), synaptic vesicles (SV), and mitochondria (M). Arrowheads indicate labeled membranes, and arrows indicate active zones. All scale bars = 500 nm.

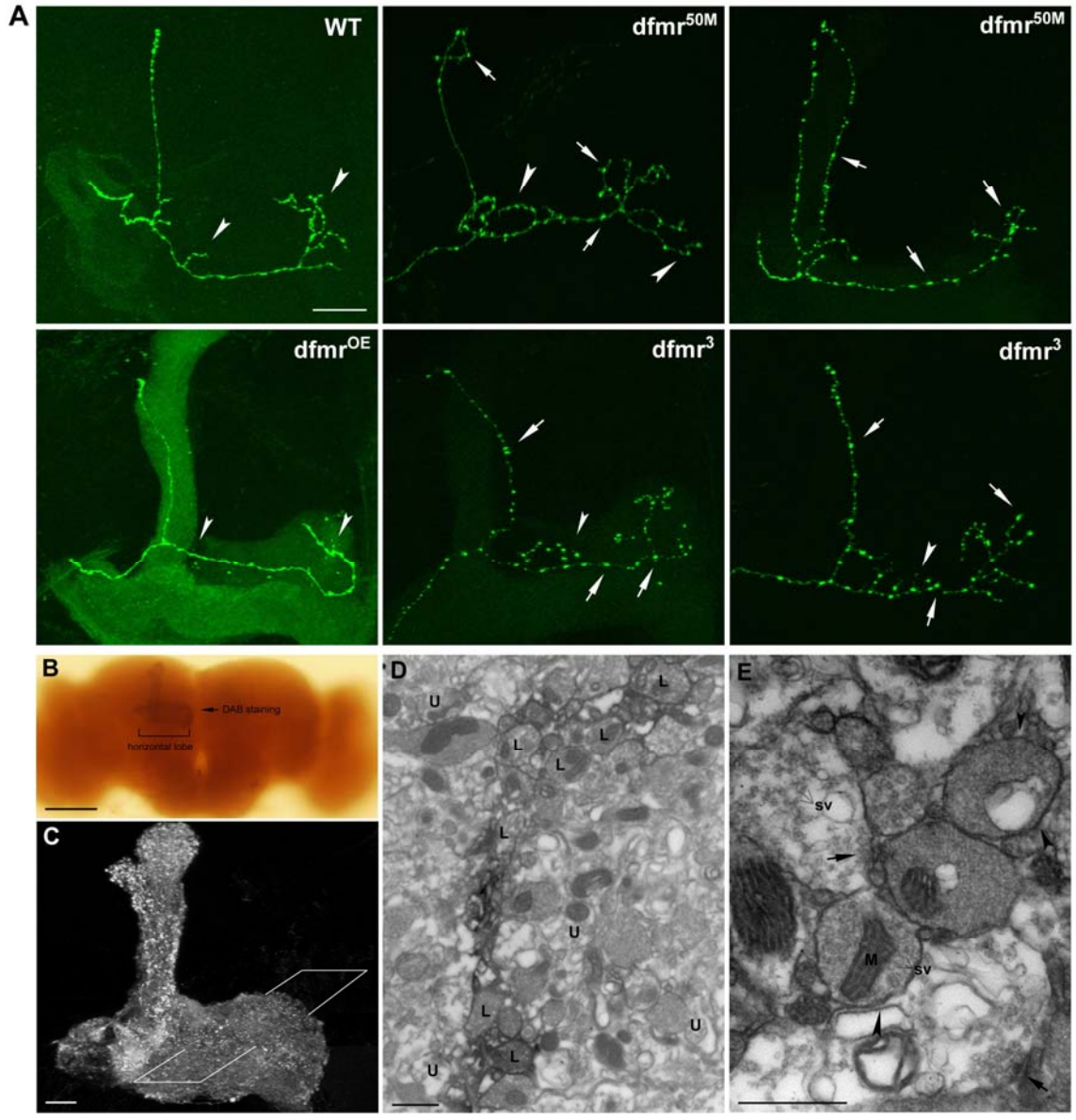
A
WT
dfmr50M
dfmr50M
dfmrOE
dfmr3
dfmr3
B
DAB staining
horizontal lobe
C
D
U
L
L
L
L
L
U
L
U
L
U
E
sv
M
sv

Presynaptic specializations were defined based on the presence of electron-dense T-bars at active zones (Broadie and Richmond, 2002). The first objective was to determine whether the enlarged varicosities observed in mutant neurons at the light microscope level represent synaptic boutons. We therefore serial sectioned labeled α'/β' axons and measured the cross-section area of any profile containing T-bar active zones (Figure 2.6D, E). The average bouton area of *dfmr1* mutant clones was significantly ($P<0.05$) enlarged compared to labeled wild type clones (WT, mean= 0.199 ± 0.012 μm^2, n=97; $dfmr1^{50M}$, mean=0.243 ± 0.018, n=108) (Figure 2.7B). These results confirmed the impression from light microscope analyses (Figure 2.6A). In addition, *dfmr1* null mutant boutons display a markedly more variable distribution of area than wild type boutons. In the 200+ boutons measured of both WT and mutant genotypes, the largest and smallest bouton ranges both occurred in mutant neurons (Figure 2.7B); the area of largest *dfmr1* bouton was >50% larger than the largest wild type bouton, and the area of smallest *dfmr1* bouton was ~35% decreased compared to the smallest wild type bouton. These results indicate that dFMRP negatively regulates the morphological differentiation of synaptic boutons, and also increases the fidelity of bouton size.

dFMRP regulates ultrastructural differentiation of synapses

Synaptic dysfunction may be a primary mutant phenotype in *dfmr1* mutants,

leading secondarily to branch sprouting, aberrant growth and further synaptic differentiation as compromised cells seek in vain for synaptic partners. We therefore examined the synaptic ultrastructure of MARCM-labeled *dfmr1* mutant MB neurons and performed a nearest-neighbor comparison with unlabeled control neurons. Labeled mutant α'/β' neuron axon profiles in the MB displayed thick, darkly labeled plasma membrane in the electron microscope, which unambiguously marked mutant cells relative to adjacent, unlabeled control cells (Figure 2.6D,E).

The immediately striking observation was that *dfmr1* mutant presynaptic boutons were almost filled with evenly-sized, electron-lucent synaptic vesicles, clearly several orders of magnitude more vesicles than in control boutons (Figure 2.6E, 2.7A and 2.7C). Indeed, vesicle density within the mutant boutons was so high that it often precluded the ability to resolve other features of the active zone and effectively prevented any ability to clearly resolve all individual vesicles for quantification. Therefore, to partially quantify the vesicle accumulation phenotype, we measured the area of bouton fully occupied by vesicles as a percentage of the total bouton area (Figure 2.7D). In control neurons, slightly less than 50% of the bouton area is normally occupied by synaptic vesicles, whereas in *dfmr1* mutant neurons nearly 75% of the bouton is occupied by vesicles. Thus, the average area occupied by vesicles is 50% increased ($P<0.001$) in *dfmr1* boutons compared to internal control boutons (Figure 2.6E and 2.7A, C, D). In fact, the

Figure 2.7. *dfmr1* mutants display enlarged synaptic boutons filled with vesicles.

A. Electron micrograph (25000X) of a Mushroom Body horizontal lobe with wild type (WT, left) and *dfmr1*^{50M} (right) MARCM clones. Arrows indicate the electron-dense labeled bouton membrane. Scale bars = 500 nm.

B. Quantification of labeled bouton area in both WT and *dfmr1*^{50M} clones. The *dfmr1* null mutant neurons display significantly enlarged average bouton area, and more variable distribution of bouton sizes than wildtype (WT, n=97; *dfmr*^{50M}, n=108, $P<0.05$).

C. High magnification of a single synaptic bouton from WT (left) and *dfmr1*^{50M} null mutant (right) neurons. The null mutant boutons show a dramatically increased density of synaptic vesicles (SV) throughout the bouton interior and at presynaptic active zones (arrows). Scale bars = 100 nm.

D. Quantification of vesicle density. Bars indicate the percentage of the total bouton area occupied by synaptic vesicles. (WT, n=25; *dfmr1*^{50M}, n=27, $P < 0.001$).

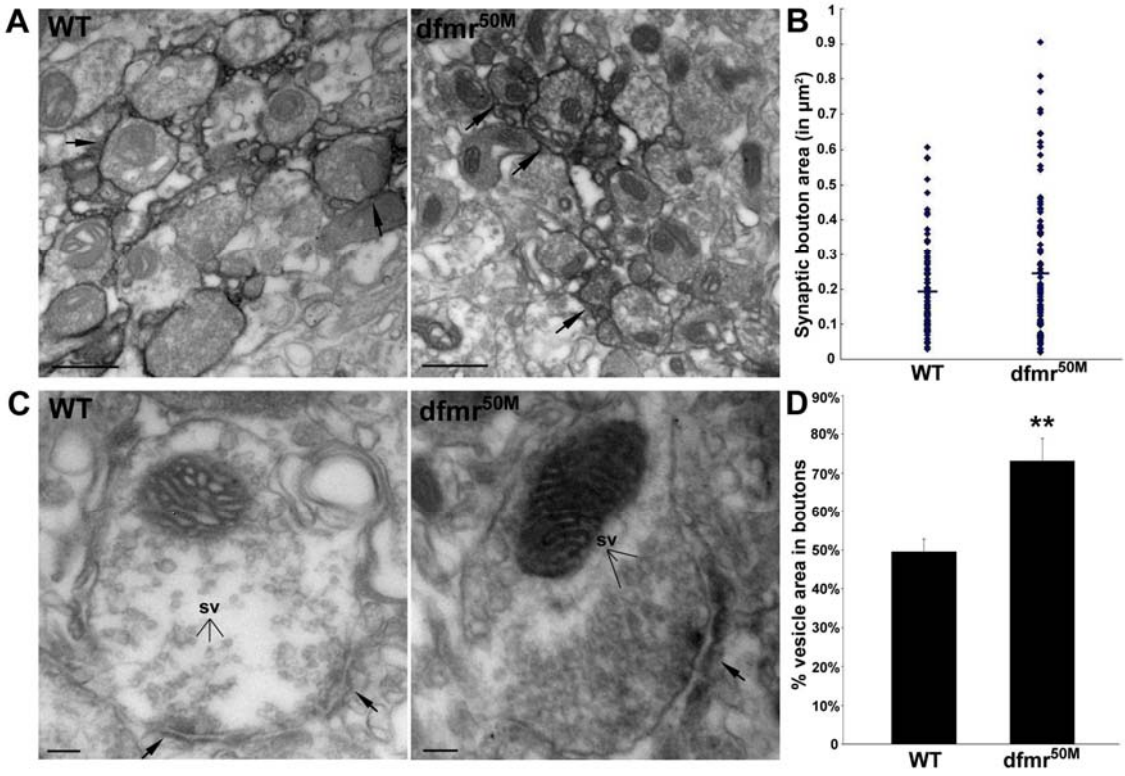
A
WT
dfmr50M
B
Synaptic bouton area (in µm²)
1
0.9
0.8
0.7
0.6
0.5
0.4
0.3
0.2
0.1
0
WT
dfmr50M
C
WT
dfmr50M
sv
sv
D
% vesicle area in boutons
90%
80%
70%
60%
50%
40%
30%
20%
10%
0
**
WT
dfmr50M

actual vesicle accumulation in mutant boutons is much greater than is reflected in these numbers, because vesicles in the mutant are much more densely accumulated, to the extent that normally prevent clear resolution of individual vesicles.

A vesicle accumulation defect of this severity has not before been reported in *Drosophila*. This defect could be due to hyperactive vesicle biogenesis, or an arrest in vesicular exocytosis, either resulting in increased vesicle density. Our previous studies have revealed synaptic vesicle accumulation only in mutants with severely impaired vesicular exocytosis and neurotransmitter release, such as *syntaxin*, *dUNC-13* and *dCAPs* mutants (Aravamudan et al., 1999; Broadie, 1996; Renden et al., 2001). Thus, *dfmr1* mutant synapses of MB neurons display severely aberrant ultrastructural profiles consistent with defective synaptic exocytosis and impaired neurotransmitter release.

Discussion

We have previously shown that dFMRP negatively regulates axonal branching and structural elaboration at the peripheral neuromuscular junction (Zhang et al., 2001). Similarly, dFMRP negatively regulates sensory dendrite branching and elaboration in peripheral sensory neurons (Lee et al., 2003). In contrast, the role of dFMRP in the central nervous system has received limited study, and the results have been confusing, including reports of similar

phenotypes in *dfmr1* null mutants and following dFMRP overexpression, neuronal overgrowth and undergrowth in different neurons, and no phenotypes at all in other neurons (Dockendorff et al., 2002; Morales et al., 2002). Does dFMRP have a role in regulating neuronal structure in the brain? If so, does dFMRP have a neuron type-specific role in regulating structure? Does dFMRP truly play a different role in the central versus the peripheral nervous systems?

To answer these questions, we have used the powerful MARCM clonal technique (Lee and Luo, 1999), to resolve the single-cell structure of *dfmr1* mutant neurons at both light and electron microscope levels. We analyzed all three classes of neurons in the Mushroom Body, the learning/memory center of *Drosophila* brain. Our results are in complete agreement with the previously reported roles of dFMRP in the larval peripheral nervous system, showing that dFMRP negatively regulates neuronal sprouting, branching and structural elaboration in the brain. We conclude, therefore, that dFMRP acts as a negative regulator of neuronal architecture throughout the entire nervous system; motor nerve terminals, sensory neuron dendrites and the cell body, dendrites and axons of central neurons in the brain.

dFMRP negatively regulates neuronal elaboration

The *Drosophila* Mushroom Body (MB) is an essential learning and memory center of the brain, which has been suggested to correspond functionally to the

hippocampus in mammals (Davis, 1993; Heisenberg, 1998; Heisenberg, 2003; Zars, 2000). Learning ability is strongly compromised in mutants impacting MB function, and lost altogether when the MB is ablated (de Belle and Heisenberg, 1994; McBride et al., 1999). In light of the cognitive impairments of FXS patients, the MB is therefore the most behaviorally relevant brain region to target for study in the *Drosophila* FXS model. As with FMRP expression in mammalian neurons (Devys et al., 1993; Verheij et al., 1993). dFMRP is enriched in the soma of all MB neurons, absent from nuclei, and present at only very low levels in any processes (dendrites or axons). Thus, the primary role of dFMRP is likely to be in the cell body. In *dfmr1* null mutants, we could detect only very mild defects in gross MB patterning. This contrasts with a recent study by Michel et al. (2004, in press) reporting that *dfmr1* mutants display grossly compromised MB structure. We did not observe any such phenotypes and therefore cannot validate the result. On the contrary, we did observe that dFMRP overexpression led to large-scale changes in MB structural integrity comparable to the report of Michel et al. (2004, in press). Nevertheless, since the dFMRP loss-of-function situation is our primary interest, modeling the FXS condition, we proceeded to focus at a single-cell level of resolution.

For completeness, we examined here all three neuronal classes comprising the MB, including γ, α'/β' and α/β neurons, in both *dfmr1* null mutants and with dFMRP overexpression. Loss of dFMRP causes increased structural complexity

throughout the entire neuron, including the extension of supernumerary processes from the cell body, the development of supernumerary higher-order branches in the dendritic arbor, overgrowth of the dendritic field, overbranching of axonal processes, overgrowth of axons and consequent defects in axonal projection. Correspondingly, overexpression of dFMRP causes simplification and decreased structural complexity throughout the entire neuron, including reduction of cell body processes, loss of dendritic branches, undergrowth of dendritic arbors, underbranching of axonal processes, undergrowth of axons and consequent defects in axonal connectivity. Thus, the level of dFMRP bidirectionally regulates growth and architectural elaboration throughout MB neurons, altering the availability of both synaptic input and output sites.

In mammals, the only neuronal morphological defect described in either FXS patients or *fmr1* mutant mice is longer, thinner, and structurally abnormal dendritic spines (Hinton et al., 1991; Irwin et al., 2002; Irwin et al., 2001; Nimchinsky et al., 2001). This defect may be variable in different brain regions, and may also be developmentally transient, with potentially complete recovery in older animals (Nimchinsky et al., 2001). Nevertheless, reports of mammalian structural defects are consistent with the results reported here in *Drosophila*; in both cases loss of FMRP/dFMRP results in increased structural complexity and a consequent increase in the availability of synaptic sites. Thus, from flies to mammals, FMRP acts as a negative regulator of neuronal complexity and synaptic availability. It is

not currently clear whether *Drosophila* displays more severe mutant phenotypes than mammals, or whether comparable studies in mammalian systems have simply not been done. Perhaps the higher complexity of the mammalian brain has hampered the ability to sufficiently resolve single cell structure? To our knowledge, studies of whole neuronal structure in *fmr1* mutant mice, comparable to those shown here in *Drosophila*, have not been published. Another possibility is that the requirement for dFMRP is indeed greater in flies, reflecting the fact that *Drosophila* has only one *fmr1* gene, compared to three related genes in mammals, which presumably allow diversification of FMR1-dependent functions in mammals.

dFMRP negatively regulates synapse differentiation

MB neurons possess periodic varicosities along the length of their axons that represent *en passé* presynaptic boutons (Watts et al., 2004). In *dfmr1* mutant neurons, the prominence of these varicosities is greatly enhanced, generating a distinctive “beads on a string” appearance, whereas dFMRP overexpression obscures these varicosities. Electron microscopy of these same neurons confirmed that loss of FMRP results in significantly enlarged synaptic boutons. In addition, bouton size is more variable, which may suggest that axons lose the control of bouton formation in absence of dFMRP. More strikingly, the enlarged mutant boutons were simply stuffed with densely accumulated synaptic vesicles.

Indeed, the density of synaptic vesicles in *dfmr1* mutant synapses is so high that other features of the bouton are frequently obscured and individual vesicles often cannot be resolved. This ultrastructural phenotype is strongly suggestive of altered synaptic function, including either abnormal vesicle biogenesis or impaired synaptic vesicle exocytosis and consequent neurotransmitter release. We have previously shown that vesicle accumulation occurs in mutants blocking the vesicular exocytosis pathway including *syntaxin*, *dUNC-13* and *dCAPs* mutants (Aravamudan et al., 1999; Broadie, 1996; Renden et al., 2001). In contrast, mutants showing vesicle accumulation as a consequence of increase biogenesis have not been revealed. Unfortunately, technical limitations currently prevent any direct investigation of synaptic function within the *Drosophila* MB, although we and others are working to overcome this restriction. Taken together, these studies strongly suggest that *dfmr1* mutants are defective in presynaptic differentiation in MB neurons, likely impairing normal neurotransmitter release.

In mammals, FMRP function has been clearly tied to synaptic mechanisms, although with a predominantly postsynaptic association. FMRP mRNA and protein are both found localized in dendritic spines in mouse brain (Antar et al., 2004; Weiler et al., 1997), and FMRP is locally translated in an activity-dependent mechanism that requires activation of metabotropic glutamate receptors (Todd et al., 2003; Weiler and Greenough, 1999; Weiler et al., 1997). FMRP is, in turn, required for mGluR-dependent translation (Greenough et al., 2001; Todd et al.,

2003). Mouse *fmr1* mutants have reduced GluR1 subunits at cortical synapses, but not in the hippocampus or cerebellum, and, similarly, long-term potentiation (LTP) is reduced in the cortex but not in the hippocampus (Li et al., 2002). Huber et al. (2002) showed that FMRP is also required for mGluR- dependent long term depression (LTD) in hippocampus. Although these results suggest primarily postsynaptic roles for FMRP, identification of FMRP mRNA targets has conversely suggested mostly presynaptic functions. Among presynaptic targets identified have been MUNC-13, NAP-22, SEC-7 and RAB-5 (Brown et al., 2001; Miyashiro et al., 2003). These putative FMRP targets suggests primarily presynaptic functions consistent with the presynaptic defects reported here and previously (Zhang et al., 2001) in *Drosophila*.

Acknowledgements

We are most particularly grateful to Dr. Ryan Watts and Dr. Jian Wang for answering endless questions on the MARCM technique, and to Dr. Liqun Luo and Dr. Tzumin Lee for kindly providing essential MARCM stocks. We thank Dr. T. Jongens and Dr. T. Dockendorff for providing *dfmr1*^{3} mutant stocks. We thank the Vanderbilt EM Core Lab. We thank the members of the Broadie lab for insightful discussions and comments on the manuscript. Y. Zhang was supported by a postdoctoral fellowship from the Vanderbilt Kennedy Center for Research on

Human Development. This work was supported by NIH grant HD40654 to K.B.

Experimental Procedures

Fly Stains and Genetics

All flies were maintained at 25^{o}C on standard medium. The following strains were generated by standard genetic methods and were used in this study: 1, *heatshock-FLP, mouse CD8-GFP; FRT82B, tubulin P-GAL80/TM3; GAL4-OK107*. 2, *y, w; FRT82B/TM3*. 3, *FRT82B, dfmr1^{50M}/TM6*. 4, *FRT82B, dfmr1^{dfmr3}/TM6*. 5, *FRT82B, UAS-dfmr1*. *GAL4-OK107* was used as the driver to visualize mushroom body clones in all situations (Connolly et al., 1996). *Mouse CD8-GFP* was used to label the mosaic clones. All *dfmr1^{50M}*, *dfmr1^{dfmr3}*, and *UAS-dfmr1* insertions (Zhang et al., 2001) were recombined to the *FRT82B* chromosome by classical genetic manipulation, based on the presence of *FRT82B* carrying the G418 resistance (Xu and Rubin, 1993) and PCR confirmation of all the genetic elements.

Immunohistochemistry

The following antibodies were used in this work: rat anti-mouse CD8a, 1:100 (Caltag); mouse anti-*Drosophila* Fasciclin II 1D4, 1:10 (Developmental Studies Hybridoma Bank); mouse anti-dFMRP, 1:1000 (Developmental Studies Hybridoma Bank); FITC-conjugated goat anti-rat IgG, 1:100 (Jackson); goat

Cy3-conjugated goat anti-mouse IgG, 1:100 (Jackson); rat anti-*Drosophila* DLG, 1:100 (V. Budnik). All fluorescent images were collected using a ZEISS LSM 510 META Laser Scanning Microscope and image-collection software. All image processing were done with Adobe Photoshop 7.0.

Mosaic analysis with a repressible cell maker (MARCM)

The MARCM technique was employed as described in Lee and Luo (1999). To generate MARCM clones in γ-neuron, embryos were collected within 5 hours window and cultured at 25 °C. 20 hours old embryos were heat-shocked at 37 °C for 1 hour. To generate α'/β' and α/β MARCM clones, the same heat-shock was done to 5 day old larvae and 8 day old pupa, respectively. Adult brains were dissected out from whole fly heads. All brains were from 3 days to 15 days adults after eclosion. Brains were dissected in 1XPBS, fixed in 4% paraformaldehyde 30 minutes, and processed with immuno-staining.

Morphological Quantification

All quantification data were come from single-cell MARCM clones. For γ-neuron axonal quantification, the primary axon branch was identified first and all other processes extended from this main trunk were counted as branches. The length of each branch was measured based on the 3D images obtained from confocal microscopy. All branch lengths of single axon branches were added

together to get the total cumulative length. For α'/β'-neuron cell body process quantification, all processes except the main process were counted. One branch was counted as one process. In mutants, branch numbers >10 (always difficult to tell apart) were counted as 10.

Electron Microscopy

Ultrastructural analyses of *Drosophila* brains were done using standard protocols (Barth et al., 1997; Yasuyama et al., 2002). Briefly, 1-3 days old adult brains with MB MARCM clones were dissected in 1XPBS buffer and immediately fixed for 30 minutes in 2% paraformaldehyde. The samples were subsequently rinsed with PBS-BSA buffer 3 hours in 4 ºC, stained with rat anti-mouse CD8 antibody (1:100) 12 hours in 4 ºC, washed with PBS-Horse serum buffer 3 hours in 4ºC , stained with biotinylated anti-rat IgG (1:50) 12 hours in 4 ºC, and washed in 1XPBS in 4ºC overnight. Brains were sequentially treated with Vectastain ABC kit (vector laboratories, Inc. Burlingame, CA), rinsed with in 1×PBS 1 hours in room temperature, stained with Vector peroxidase substrate DAB kit, and washed with PBS for 3 hours at 4ºC, and incubated in 1% glutemaldehyde 4ºC overnight. Samples were prepared for transmission electron microscopy (TEM) using standard techniques(Featherstone et al., 2001), with minor modifications. Briefly, samples were transferred to 2% glutaraldehyde for 45 minutes (2% glutaraldehyde in 0.2M phosphate buffer). Specimens were washed in phosphate

buffered sucrose 0.2M, transferred to 1% osmium tetroxide in ddH_2O for 1 hr, washed again in ddH_2O, and stained en bloc in 2% aqueous uranyl acetate for 1 hr, and washed in ddH_2O. Brains were dehydrated through an increasing series of ethanol (30%-100%), passed through propylene oxide for 20 minutes, and transferred to 50% / 50% propylene oxide and araldite for 30 minutes. Samples were placed in pure araldite for 30 minutes, under vacuum (-25psi). Finally specimens were transferred into fresh araldite overnight. Blocks were trimmed as close to the darkly stained mushroom bodies as possible. Ribbons of thin (~55 nm) sections were obtained using a Leica Ultracut UCT 54 Ultramicrotome and examined on a Phillips CM 12 TEM.

Ultrastructural Quantification

To assay bouton area, 25000X images were used to compare wild type and *dfmr1* mutant MARCM Mushroom Body clones. Areas were measured using NIH ImageJ software. To assay synaptic vesicle density, 25000X images were used. In *dfmr1* mutant MARCM Mushroom Body clones, 2 micron circles were centered over the labeled cell, and assays made of labeled bouton (*dfmr1* homozygous mutant) and unlabeled boutons (control) in a nearest neighbor comparison. Total bouton area and synaptic vesicle occupied bouton area were measured with NIH ImageJ software. The percentage of vesicle area was calculated by dividing vesicle area by total bouton area, giving the % vesicle area.

CHAPTER III

DROSOPHILA FRAGILE X MENTAL RETARDATION PROTEIN AND METABOTROPIC GLUTAMATE RECEPTOR A CONVERGENTLY REGULATE THE SYNAPTIC RATIO OF IONOTROPIC GLUTAMATE RECEPTOR SUBCLASSES

This paper has been published under the same title in *The Journal of Neuroscience,* 2007.

Luyuan Pan and Kendal Broadie

Department of Biological Sciences, Kennedy Center for Research on Human Development, Vanderbilt University, Nashville, TN 37232

Summary

A current hypothesis proposes that Fragile X Mental Retardation Protein (FMRP), an RNA-binding translational regulator, acts downstream of glutamatergic transmission, via metabotropic glutamate receptor (mGluR) G_q-dependent signaling, to modulate protein synthesis critical for trafficking ionotropic glutamate receptors (iGluRs) at synapses. However, direct evidence linking FMRP and mGluR function with iGluR synaptic expression is limited. In this study, we use the *Drosophila* Fragile X model to test this hypothesis at the well-characterized glutamatergic neuromuscular junction (NMJ). Two iGluR classes reside at this synapse, each containing common GluRIIC (III), IID and IIE

subunits, and variable GluRIIA (A-class) or GluRIIB (B-class) subunits. In *dfmr1* null mutants, A-class GluRs accumulate and B-class GluRs are lost, whereas total GluR levels do not change, resulting in a striking change in GluR subclass ratio at individual synapses. The sole *Drosophila* mGluR, DmGluRA, is also expressed at the NMJ. In *dmGluRA* null mutants, both iGluR classes increase, resulting in an increase in total synaptic GluR content at individual synapses. Targeted postsynaptic *dmGluRA* over-expression causes the exact opposite GluR phenotype to the *dfmr1* null, confirming postsynaptic GluR subtype-specific regulation. In *dfmr1; dmGluRA* double null mutants, there is an additive increase in A-class GluRs, and a similar additive impact on B-class GluRs, towards normal levels in the double mutants. These results show that both dFMRP and DmGluRA differentially regulate the abundance of different GluR subclasses in a convergent mechanism within individual postsynaptic domains.

Introduction

Fragile X Syndrome (FXS) is the leading known genetic cause of both mental retardation and autism spectrum disorders. The disease also produces hyperactivity, hypersensitivity to sensory stimuli and epileptic seizures (O'Donnell and Warren, 2002; Bagni and Greenough, 2005; Garber et al., 2006). FXS is caused by silencing of the *fragile X mental retardation 1* (*fmr1*) gene, which encodes the RNA-binding, translational regulator Fragile X Mental Retardation

Protein (FMRP) (Jin and Warren, 2000; Brown et al., 2001; Li et al., 2001). In *fmr1* knockout mice, hippocampal long-term depression (LTD) dependent upon activation of the group I class 5 metabotropic glutamate receptor (mGluR) is selectively enhanced (Huber et al., 2002; Koekkoek et al., 2005). This LTD is caused by loss of surface AMPA GluRs, a mechanism requiring protein synthesis (Huber et al., 2000; Huber et al., 2001; Nosyreva and Huber, 2006; Pfeiffer and Huber, 2006). Similarly, cerebral cortex long-term potentiation (LTP) is reduced concomitant with reduced GluR1 expression (Li et al., 2002; Larson et al., 2005; Zhao et al., 2005). Two major FXS phenotypes in *fmr1* knockout mice, reduced habituation in open field tests and increased sensitivity to audiogenic seizures, can be rescued by the mGluR5 antagonist MPEP (Yan et al., 2005).

In a negative feedback loop, FMRP suppresses its own translation in postsynaptic terminals, in a mechanism regulated by group I mGluRs, whose activation is a potent stimulus for synaptic protein synthesis (Weiler et al., 1997; Todd et al., 2003b; Weiler et al., 2004). Both FMRP synaptic localization and expression are increased by glutamatergic activity, and this regulation is blocked by MPEP (mGluR5 antagonist) and increased by DHPG (agonist) (Weiler et al., 1997; Antar et al., 2004; Weiler et al., 2004; Hou et al., 2006). mGluR5-dependent LTD is normally completely dependent on new translation, but in the absence of FMRP, mGluR5 activation does not trigger protein synthesis (Weiler et al., 2004; Aschrafi et al., 2005). The anisomycin (translation inhibitor) response is lost and

the DHPG-induced increase of synaptic proteins synthesis is reduced in *fmr1* KO mice (Hou et al., 2006; Nosyreva and Huber, 2006). A primary target of mGluR5 activation is to regulate trafficking of AMPA GluRs (Carroll et al., 1999; Snyder et al., 2001; Xiao et al., 2001; Nosyreva and Huber, 2005). These data suggest a mechanistic connection between mGluR signaling, the translation regulatory function of FMRP, and AMPA GluR expression: a hypothesis termed “the mGluR theory of FXS” (Bear et al., 2004).

We developed a *Drosophila* FXS model through mutation and over-expression of *Drosophila fmr1* (*dfmr1*) (Zhang et al., 2001; Pan et al., 2004; Zhang and Broadie, 2005). In support of the mGluR theory, feeding *dfmr1* mutants with MPEP, as well as class II/III mGluR antagonists, can rescue some mutant phenotypes, including behavioral (courtship learning and memory) and morphological (mushroom body structure) defects (McBride et al., 2005). A great advantage for testing the mGluR theory in *Drosophila* is that the genome encodes only a single mGluR, DmGluRA (Parmentier et al., 1996; Bogdanik et al., 2004; Mitri et al., 2004). We characterized DmGluRA to show it is synaptically localized and regulates synaptic structure and activity-dependent function at the neuromuscular junction (NMJ) (Bogdanik et al., 2004). This glutamatergic NMJ contains five AMPA-like GluR subunits, GluRIIA-E. Three subunits (GluRIIC, IID and IIE) are essential for all GluRs, whereas the other two subunits define two GluR classes; A-class (GluRIIA) and B-class (GluRIIB), which are differentially

regulated, subsynaptically localized, and possess distinct functional properties, including differential conductance and opening kinetics (Schuster et al., 1991; Petersen et al., 1997; DiAntonio et al., 1999; Sigrist et al., 2002; Marrus et al., 2004; Featherstone et al., 2005; Qin et al., 2005b).

The purpose of this study was to genetically test the mGluR theory of FXS in the *Drosophila* model; specifically mechanistic links between dFMRP, DmGluRA and ionotropic GluR expression. In *dfmr1* null mutants, A-class GluRs accumulate and B-class GluRs are lost, significantly altering the GluR class ratio in single synapses. In *dmGluRA* null mutants, both GluR classes increase, showing that the metabotropic receptor negatively regulates both ionotropic receptors. Targeted rescue experiments demonstrate that *dfmr1* defects are due to a postsynaptic requirement. Postsynaptic over-expression of DmGluRA causes the exact opposite GluR class-specific changes to the *dfmr1* null. In *dfmr1; dmGluRA* double null mutants, there are additive effects on both GluR classes. These results show that DmGluRA glutamatergic signaling and dFMRP regulatory function converge to control the GluR class ratio in the postsynaptic domain, but that the two pathways are at least partially independent.

Results

dFMRP differentially regulates GluR classes

Subunit-specific antibodies were used to examine three GluR populations at the NMJ; A-class receptors only (anti-GluRIIA), B-class receptors only (anti-GluRIIB) and the total GluR population (anti-GluRIIC) (Yoshihara and Littleton, 2002; Marrus et al., 2004; Liebl et al., 2005; Qin et al., 2005a). Fluorescence intensity was compared to an internal fluorescent signal marking the NMJ synaptic terminal: anti-HRP labels a carbohydrate epitope in the neuronal membrane of NMJ boutons (Katz et al., 1988; Wang et al., 1994; Sun and Salvaterra, 1995). The *dfmr1* null and w^{1118} genetic background control (WT) animals were processed simultaneously and imaged using identical microscope settings. All quantification was done on type IB synaptic boutons in the muscle 4 NMJ in segment A3. Fluorescence intensity was calculated at each NMJ terminal and then averaged between the two A3 hemisegments to generate each data point for each genotype. Representative images and quantification results are shown in Figure 3.1.

Synaptic A-class GluRs were very significantly increased in *dfmr1* null mutants compared to matched controls (Figure 3.1A). Average fluorescence intensity in NMJ synaptic boutons was increased by 30% in mutant terminals relative to controls (WT, 96.3±5.03; *dfmr1*, 124.62±4.84; N=15 for each genotype;

Figure 3.1: dFMRP differentially regulates A- and B-class GluRs

Third instar NMJs were probed using subunit-specific anti-GluRs (green: IIA, IIB, IIC) and anti-HRP (red) antibodies. The HRP antibody recognized a neural membrane epitope, and thus labels the NMJ synapse and acts as an internal fluorescence control for intensity quantification. Type IB boutons on muscle 4 in abdominal segment A3 were used for all quantified analysis.

A-C. Representative images of GluRIIA, IIB and IIC expression in WT (w^{1118}) and *dfmr1* null mutant (*dfmr1*^{50m}).

D-F. Fluorescence intensity quantification of all three GluR subunits and the HRP internal standard.

D. The GluRIIA subunit expression is significantly increased in *dfmr1* mutants. (N=15 for both WT and *dfmr1*).

E. The GluRIIB subunit expression is significantly decreased in *dfmr1* mutants. (N=10 for both WT and *dfmr1*).

F) The GluRIIC subunit expression is comparable in WT and *dfmr1* mutants. (N=10 for both WT and *dfmr1*).

0.0001<P<0.001(**); P<0.0001(***).

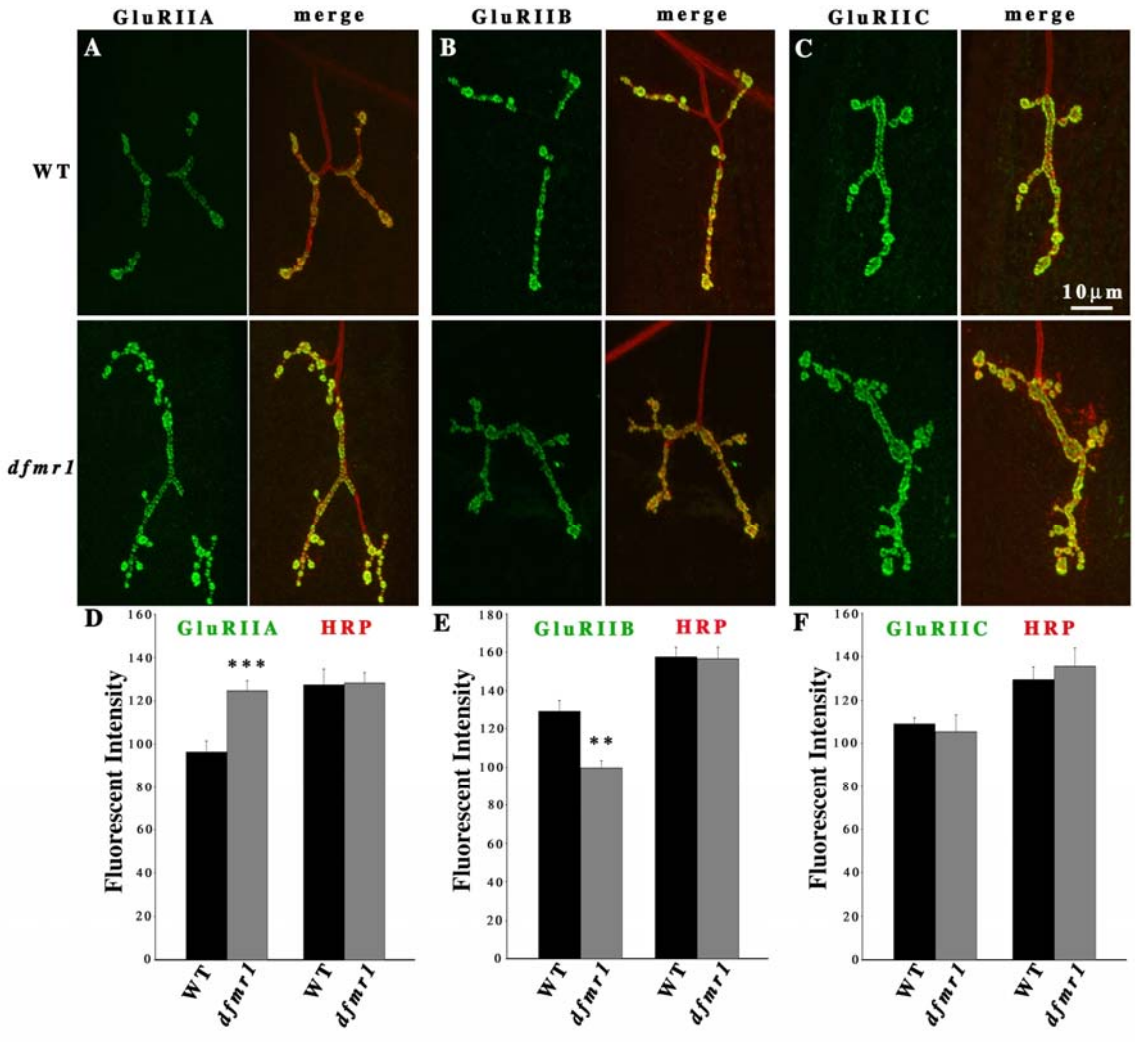
GluRIIA
merge
GluRIIB
merge
GluRIIC
merge
A
B
C
WT
dfmr1
10μm
D
GluRIIA
HRP
E
GluRIIB
HRP
F
GluRIIC
HRP
Fluorescent Intensity
***
**
WT
dfmr1
WT
dfmr1

P<0.0001; Figure 3.1D). There was no difference in HRP fluorescent intensities between mutants and controls (Figure 3.1D). In contrast, B-class GluRs were very significantly decreased in *dfmr1* null mutants compared to matched controls (Figure 1B). GluRIIB levels were decreased to a similar level (23%) in *dfmr1* null terminals relative to controls (WT, 129.3±5.67; *dfmr1*, 99.62±3.81; N=10 for each genotype; P=0.0004; Figure 1E). There was no difference in HRP fluorescent intensities between mutants and controls (Figure 1E). Total GluR content at the same synaptic terminals was assayed using an antibody against the common GluRIIC subunit (Figure 1C). Since the two GluR classes displayed similar opposing abundance changes, as might be predicted there was no significant difference in total GluR abundance between *dfmr1* and control synapses (WT, 108.94±2.95; *dfmr1*, 105.34±7.83; N=10 for each genotype; P=0.76; Figure 1F). These data show that the two GluR classes are differentially modulated in opposite directions in the absence of dFMRP function, with A-class GluRs increasing, B-class GluRs decreasing, but total GluR levels remaining normal.

All GluR classes decreased by *dfmr1* over-expression in postsynaptic muscle

Neuronal over-expression of the dFMRP protein results in synaptic structural and functional defects that are largely the inverse of *dfmr1* null mutant phenotypes, in both the NMJ and in the central nervous system (Zhang et al., 2001; Pan et al., 2004). However, roles of dFMRP in the postsynaptic muscle have not been

investigated. To begin to assay whether GluR phenotypes in *dfmr1* null mutants arise through postsynaptic dysfunction, as predicted, and to determine whether GluR phenotypes are also inversely correlated in loss and gain of function conditions, GluR levels were next quantified in dFMRP over-expression (OE) mutants. The UAS-*dfmr1* transgenic line was crossed with neuronal specific (ELAV-Gal4) and muscle specific (MHC-Gal4) drivers to induce dFMRP over-expression in either presynaptic (in neuron, NOE) or postsynaptic (in muscle, MOE) compartments (Figure 3.2). As above, fluorescence intensities for all three GluR populations were compared relative to the internal HRP fluorescence control. Over-expression of *dfmr1* in the muscle had no significant impact on the presynaptic HRP fluorescence in any of these experiments.

As predicted, dFMRP acts in the postsynaptic muscle to regulate the postsynaptic expression of A-class GluRs, and there is an inverse relationship between the increase observed in the *dfmr1* null (Figure 3.1A, D) and the decrease caused by *dfmr1* muscle over-expression (MOE) in the postsynaptic cells (Figure 3.2A, D). GluRIIA levels were decreased 15% compared to controls, a highly significant (P=0.0008) reduction. Further as expected, neural over-expression (NOE) of *dfmr1* in the presynaptic compartment caused no change in the abundance of the postsynaptic A-class GluRs (Figure 3.2A, D). In contrast, the situation with the B-class GluRs was more complex. Over-expression of *dfmr1* in the muscle caused a 27% decrease in GluRIIB

Figure 3.2: Total GluR abundance is decreased by *dfmr1* over-expression in muscle

Third instar NMJs were probed using subunit-specific anti-GluRs (green) and anti-HRP (red) antibodies. Type IB boutons on muscle 4 in A3 were used for all imaging analysis.

A-C. Representative images of GluRIIA, IIB and IIC expression in dFMRP muscle over-expression (MOE) and neuronal over-expression (NOE).

D-F. Fluorescence intensity quantification for each GluR subunit.

D. GluRIIA is decreased in *dfmr1* MOE mutants, but unchanged in *dfmr1* NOE mutants (N=11 for all genotypes).

E. GluRIIB is decreased in both *dfmr1* MOE and NOE mutants (N=13 for all genotypes).

F. The GluRIIC subunit is decreased in *dfmr1* MOE mutants, but not changed in *dmfr1* NOE mutants (N=10 for all genotypes).

0.0001<P<0.001(**); P<0.0001(***).

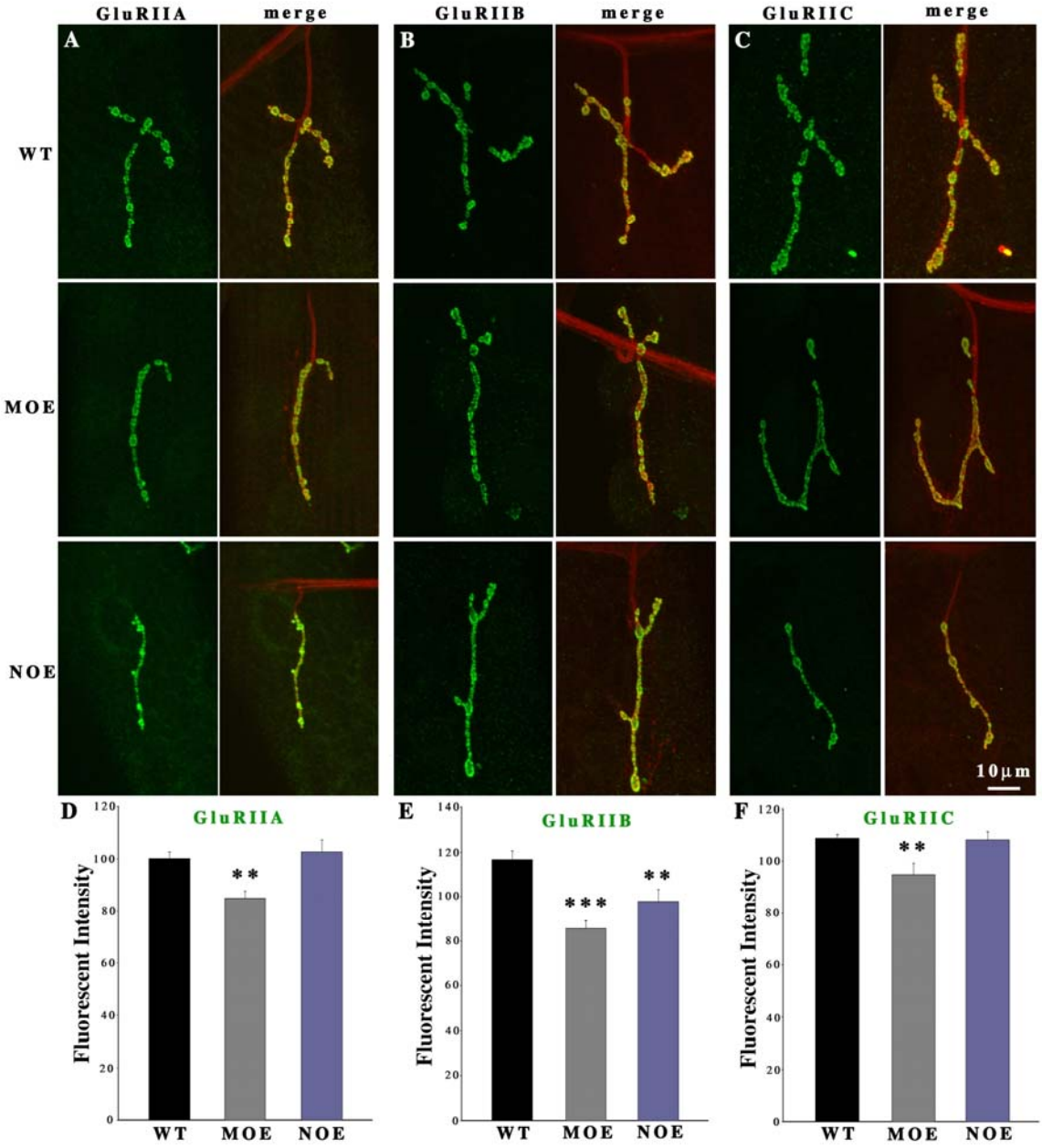
GluRIIA
merge
GluRIIB
merge
GluRIIC
merge
A
B
C
WT
MOE
NOE
10μm
D
GluRIIA
Fluorescent Intensity
**
WT
MOE
NOE
E
GluRIIB
***
**
F
GluRIIC
**

expression (Figure 3.2B, E), which resembled the decrease observed in the *dfmr1* null synapses (Figure 3.1B, E). Moreover, presynaptic *dfmr1* over-expression also caused a smaller (15%), but still significant (P=0.008), decrease in GluRIIB expression (Figure 3.2B, E). The change in the total GluR population was largely consistent with the combined changes of the two subclasses. The total GluR level also significantly (P<0.01) decreased by over-expression of *dfmr1* in the muscle (Figure 3.2C, F). Neural over-expression of *dfmr1* in the presynaptic terminal had no distinguishable impact on total GluR abundance in the postsynaptic domain (Figure 3.2C, F). These data support a primary role for dFMRP within the postsynaptic cell regulating the postsynaptic abundance of GluRs, but also show that presynaptic dFMRP levels can impact postsynaptic GluRIIB.

All ionotropic GluRs increase in the absence of metabotropic GluR signaling

Mammals possess three types of metabotropic GluRs (mGluRs) and eight specific mGluR classes. Activation of different mGluR classes differentially regulates synaptic AMPA GluR expression (Snyder et al., 2001; Nosyreva and Huber, 2005). Recently, mounting evidence has suggested a connection between type I mGluR (mGluR5) activation and the translational regulatory function of FMRP to promote down-regulation of synaptic AMPA GluR1 (Hou et al., 2006; Nosyreva and Huber, 2006). The situation in *Drosophila* is much simpler. The *Drosophila* genome encodes only a single mGluR, DmGluRA. We previously

showed that this receptor is localized to the glutamatergic NMJ and that *dmGluRA* null mutants display strikingly elevated short-term synaptic facilitation and augmentation (Bogdanik et al., 2004). In that earlier work, we identified a P-element deletion excision line, 112b, as a null mutant (hereafter called *dmGluRA*) and a companion precise excision line, 2b, as a genetic background control. Here, these lines were used to investigate the role of mGluR signaling in the regulation of ionotropic GluR abundance in the NMJ synaptic terminal.

The three different GluR populations were examined in the *dmGluRA* null mutant compared to its 2b genetic background control (Figure 3.3). All three tested GluR subunits were significantly increased in *dmGluRA* mutants: GluRIIA was increased 15% (WT, 107.5±4.2; *dmGluRA*, 123.5±3.2; N=13 for each genotype; P=0.006; Figure 3.3A, D), GluRIIB was increased 11% (WT, 98.21±3.24; *dmGluRA*, 109.12±3.27; N=16 for each genotype; P=0.03; Figure 3.3B, E) and GluRIIC was increased 15% (WT, 109.08±4.38; *dmGluRA*, 124.7±3.42; N=13 for each genotype; P=0.0096; Figure 3.3C, F). The HRP internal fluorescence standard displayed no change between the *dmGluRA* null and the 2b genetic background control in any of the experimental trials (Figure 3.3). These data show that loss of all mGluR signaling results in the upregulation of total ionotropic GluR abundance in the postsynaptic domain, and that A- and B-class GluRs are similarly suppressed by DmGluRA glutamatergic signaling.

Figure 3.3: Total GluR abundance is increased in the absence of mGluR signaling

Third instar NMJs were probed using subunit-specific anti-GluRs (green) and anti-HRP (red) antibodies. Type IB boutons on muscle 4 in A3 were used for all imaging analysis.

A-C. Representative images of GluRIIA, IIB and IIC expression in WT (2b, p-element precise excision line) and *dmGluRA* null mutant (*dmGluRA*^{112b}, imprecise deletion line).

D-F. Fluorescence intensity quantification of all three GluR subunits and the HRP internal standard. All three tested GluR subunits (GluRIIA, GluRIIB, and GluRIIC) were increased in *dmGluRA* mutants, while HRP showed no significant change in any trial (N=13 for both genotypes in GluRIIA and GluRIIC tests, N=16 for both genotypes in GluRIIB test).

$0.001<P<0.05$(*); $0.0001<P<0.001$(**).

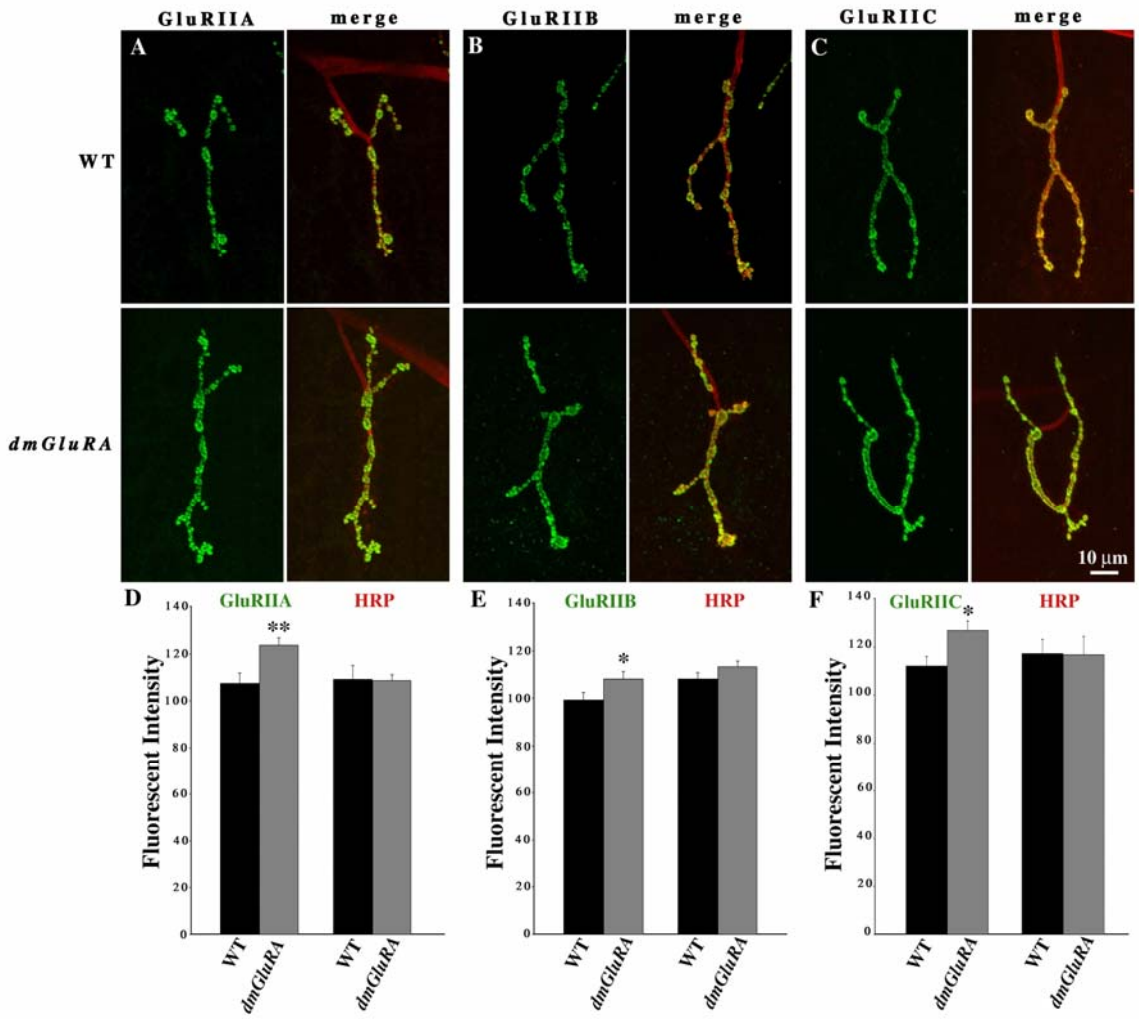
GluRIIA
merge
GluRIIB
merge
GluRIIC
merge
A
B
C
WT
dmGluRA
10 μm
D
GluRIIA
HRP
E
GluRIIB
HRP
F
GluRIIC
HRP
Fluorescent Intensity
WT
dmGluRA

Postsynaptic DmGluRA over-expression induces GluR class-specific changes

To determine whether the regulatory function of DmGluRA on ionotropic GluRs reflects pre- or postsynaptic signaling, GluR levels were next examined in targeted DmGluRA over-expression (OE) mutants. As above, the UAS-*DmGluRA* transgenic line (Bogdanik et al., 2004) was driven by neural ELAV-Gal4 or muscle MHC-Gal4 to induce DmGluRA over-expression in either presynaptic (NOE) or postsynaptic (MOE) cells. The results are displayed in Figure 3.4.

Postsynaptic over-expression of DmGluRA changes GluR class abundance in exactly the opposite direction of the *dfmr1* null; A-class GluRs are decreased and B-class GluRs are increased (compare Figures. 3.1 and 3.4). GluRIIA expression was decreased 10% in DmGluRA muscle over-expression (Figure 3.4A, C; N=15, P=0.003), and GluRIIB was similarly increased by 10% (Figure 3.4B, D; N=12, P=0.05). As in the *dfmr1* null with opposing GluR class changes, there are no change in total GluR based on the common GluRIIC subunit. In addition, however, presynaptic over-expression of DmGluRA down-regulates both A- and B-class GluRs, which is an opposite phenotype to the *dmGluRA* null (compare Figs. 3 and 4). The expression of GluRIIA was decreased 10% (Figure 3.4A, C; N=15, P=0.015), and GluRIIB was decreased 20% (Figure 3.4B, D; N=12; P=0.006). These data show that presynaptic DmGluRA function indirectly

Figure 3.4: DmGluRA postsynaptic over-expression causes the opposite GluR class changes to the *dfmr1* null.

NMJs probed using subunit-specific anti-GluRs (green) and anti-HRP (red) antibodies. Type IB boutons on muscle 4 in A3 were used for all imaging analysis. Representative images of GluRIIA (A) and GluRIIB (B) with DmGluRA muscle over-expression (MOE) and neuronal over-expression (NOE).

C, D. Fluorescence intensity quantification for each GluR class.

C. GluRIIA is decreased with both DmGluRA MOE and NOE (N=15 for all genotypes).

D. GluRIIB is increased with MOE but decreased with NOE mutants (N=12 for all genotypes).

0.001<P<0.05(*).

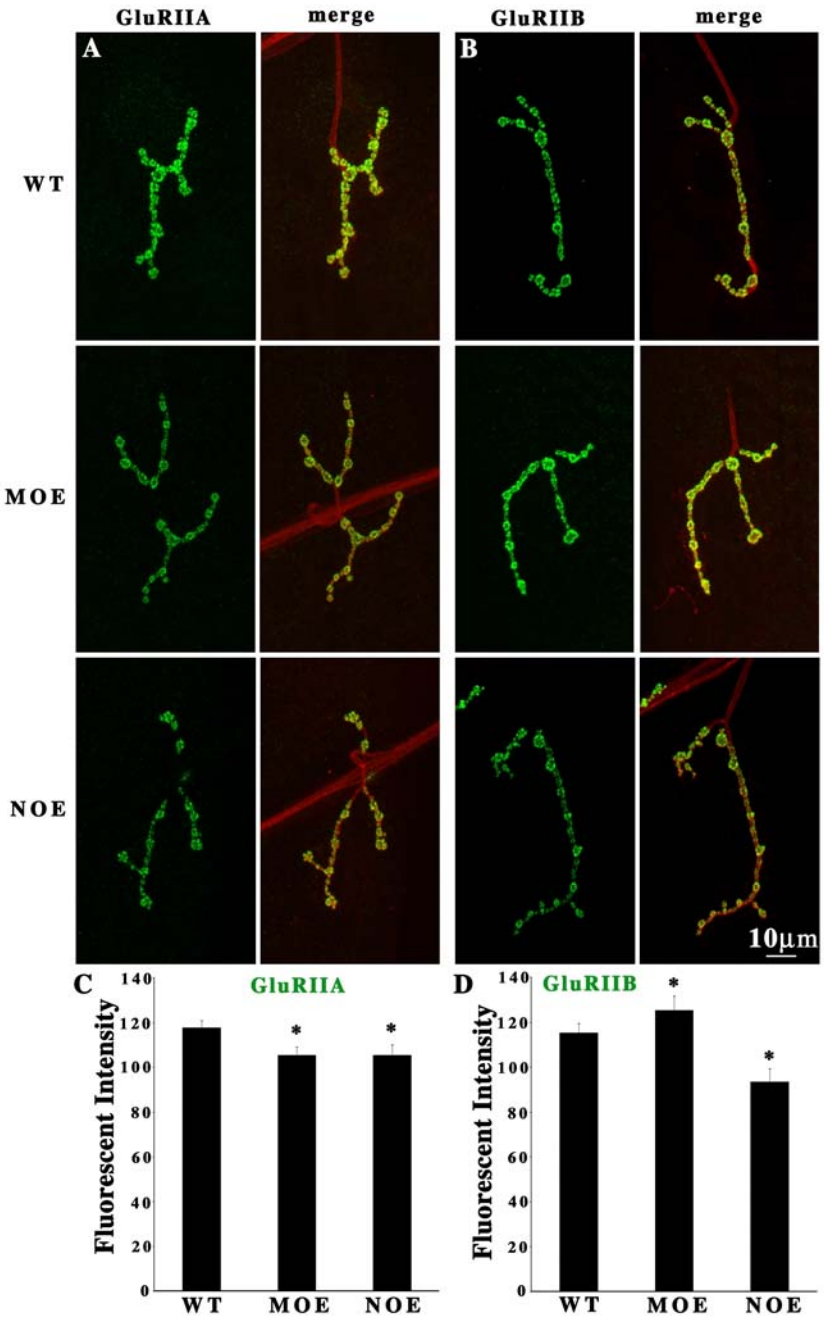
GluRIIA
merge
GluRIIB
merge
A
B
WT
MOE
NOE
10μm
C
GluRIIA
Fluorescent Intensity
140
120
100
80
60
40
20
0
*
*
WT
MOE
NOE
D
GluRIIB
Fluorescent Intensity
140
120
100
80
60
40
20
0
*
*
WT
MOE
NOE

Indirectly regulates postsynaptic GluR abundance, presumably via a homeostatic mechanism (Paradis et al., 2001; Fong et al., 2002; Wierenga et al., 2005).

dFMRP regulates the ratio of A- to B-class GluRs in single postsynaptic domains

We next queried where dFMRP and DmGluRA regulate A- and B-class within individual synaptic boutons. The two GluR classes exhibit largely overlapping expression patterns in distinct postsynaptic membrane domains directly apposing presynaptic active zones (Figure 3.5). There are approximately 20 of these punctate GluR postsynaptic domains within each type IB NMJ bouton. It has been reported, however, that the two GluR classes can also spatially segregate in non-overlapping puncta in a minority of cases (Marrus et al., 2004). By staining for the two class-specific subunits simultaneously, the distribution and fluorescence intensities of A- and B-class GluRs were directly compared in both *dfmr1* and *dmGluRA* mutants (Figure 3.5).

As might be predicted, the GluRIIA/GluRIIB ratio at individual synaptic boutons is dramatically altered by the absence of dFMRP. The IIA/IIB ratio is roughly equal in control synapses (1.07±0.03), with the two GluR subclasses showing a similar distribution in the punctate postsynaptic domains (Figure 3.5A). In quite evident contrast, the *dfmr1* null mutant displayed a coincident strong elevation in GluRIIA and downregulation in GluRIIB, dramatically altering the GluR presentation within single synaptic boutons and in individual postsynaptic

punctate domains (Figure 3.5B). As a result, the IIA/IIB ratio was strongly shifted towards the A-class receptor (1.53±0.08; P<0.0001; N=9 for each genotype; Figure 3.5C). Comparing highly magnified images of *dfmr1* null and control boutons, there was no detectable shift in the distribution pattern of the two GluR classes. Specifically, there was no evidence of the appearance/disappearance of new postsynaptic puncta, or a differential change in the ratio of IIA/IIB within subclasses of postsynaptic puncta (Figure 3.5). Therefore, the strongly skewed IIA/IIB receptor ratio represents an increase of A-class GluR and decrease of B-class GluR within the same postsynaptic receptor domains in the absence of dFMRP function.

The IIA/IIB ratio was similarly examined in the *dmGluRA* null mutants. As might be predicted, there was no apparent difference between the WT (2b) control and *dmGluRA*, with the mutant showing a coincident increase in both A- and B-class GluRs without apparent change in ratio or distribution (data not shown). Quantification of the IIA/IIB receptor ratio showed no significant change between the mutant and control (P=0.14; N=11 for each genotype; Figure 3.5D). These results show that DmGluRA signaling negatively regulates A- and B-class GluRs in common within single synaptic boutons, whereas dFMRP bidirectionally regulates the two receptor classes to determine the IIA/IIB expression ratio within single postsynaptic punctate domains.

Figure 3.5: Ratio of A- to B-class GluRs is dramatically changed in *dfmr1* mutants

Third instar NMJs were probed using subunit-specific anti-GluRIIA (green), anti-GluRIIB (red), and anti-HRP (purple) antibodies. Type IB boutons on muscle 4 in A3 were used for all imaging analysis.

A, B. Representative images of WT (w^{1118}) and *dfmr1* mutant NMJs at a high magnification showing individual punctate GluR postsynaptic domains. GluRIIA is highly increased and GluRIIB is highly decreased within overlapping punctate domains in *dfmr1* mutants. There was no detectable spatial shift in GluR classes relative to each other in *dfmr1* mutants compared to control.

C, D. Fluorescence intensity ratio of GluRIIA to GluRIIB.

C. IIA/IIB ratio is 50% increased in *dfmr1* compared to control (N=9 for both genotypes).

D. IIA/IIB ratio is shows no significant change in *dmGluRA* mutants (WT=2b; N=11 for both genotypes).

P<0.0001(***).

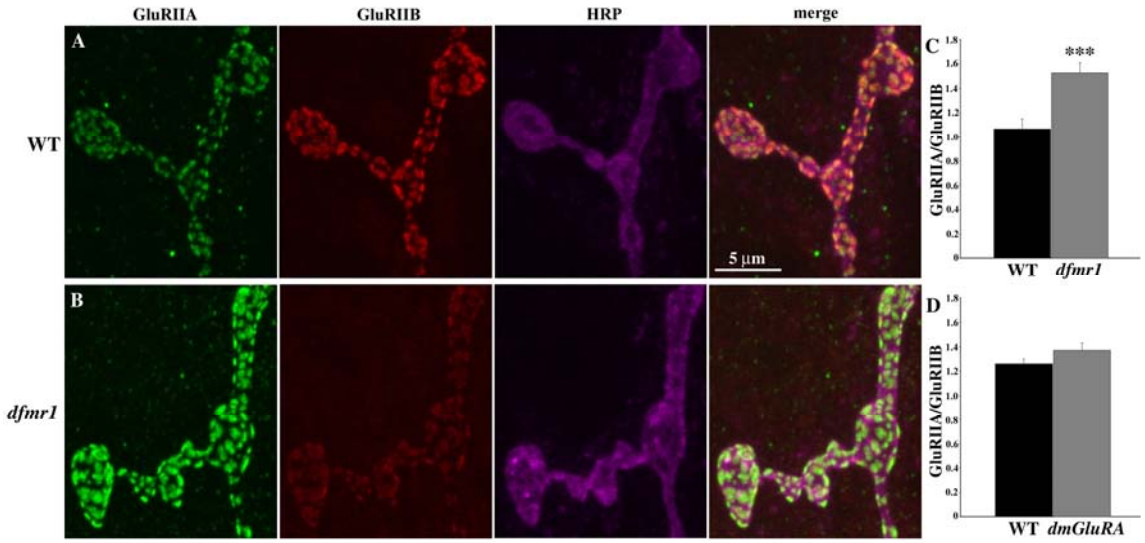
GluRIIA
GluRIIB
HRP
merge
A
WT
B
dfmr1
5 μm
C
***
GluRIIA/GluRIIB
WT
dfmr1
D
GluRIIA/GluRIIB
WT
dmGluRA

The postsynaptic regulatory function of dFMRP

Transynaptic signaling strongly modifies synapse assembly at the *Drosophila* NMJ. The level of glutamate release from presynaptic terminals can alter the abundance of postsynaptic GluRs (Featherstone et al., 2002; Chen and Featherstone, 2005) and, conversely, GluR over-expression can feedback to alter active zone assembly and function (Sigrist et al., 2002). Since dFMRP function is known to regulate presynaptic glutamate release (Zhang et al., 2001) and increase postsynaptic A-class GluR abundance (Figure 3.1), it is critical to examine possible transynaptic mechanisms for these changes. To further determine whether dFMRP regulates GluRs by pre- or postsynaptic mechanisms, two experiments were performed to examine presynaptic consequences of dFMRP loss.

Presynaptic active zones were assayed with a probe for NC82/bruchpilot, an ELKS/CAST protein at the active zone (Figure 3.6; (Kittel et al., 2006; Wagh et al., 2006). Each NC82-positive punctum was counted as one active zone within a synaptic bouton area, which was defined by presynaptic membrane HRP staining. Compared to control, *dfmr1* null mutants display significantly more active zones per bouton (WT=18.8±0.75; N=164; *dfmr1*=23.1±1.2; N=152; P=0.003; Figure 3.6A, C). However, *dfmr1* mutants possess significantly larger synaptic boutons than controls (WT=6±0.25; N=164; *dfmr1*=7.7±0.46; N=152; P=0.0009). When active zone density is considered (number pre area, μm^2), there was no difference

Figure 3.6: Presynaptic active zone density normal in *dfmr1* and *dmGluRA* mutants

Third instar NMJs probed using anti-NC82 (green), and anti-HRP (red) antibodies. Type IB boutons on muscle 4 in A3 were used for all imaging analysis. Bouton area was defined by the boundary of HRP staining. A) Representative images of WT (w^{1118}) and *dfmr1* mutant. B) Representative images of WT (2b) and *dmGluRA (112b)* mutant. C, D) Quantification of both the number of active zones per bouton and the active zone density per area (μm^2). C) The active zone number per bouton is increased in *dfmr1* mutants, but there is no difference in active zone density. D) Both active zone number and density are not changed in *dmGluRA* mutants. $0.001<P<0.05$(*).

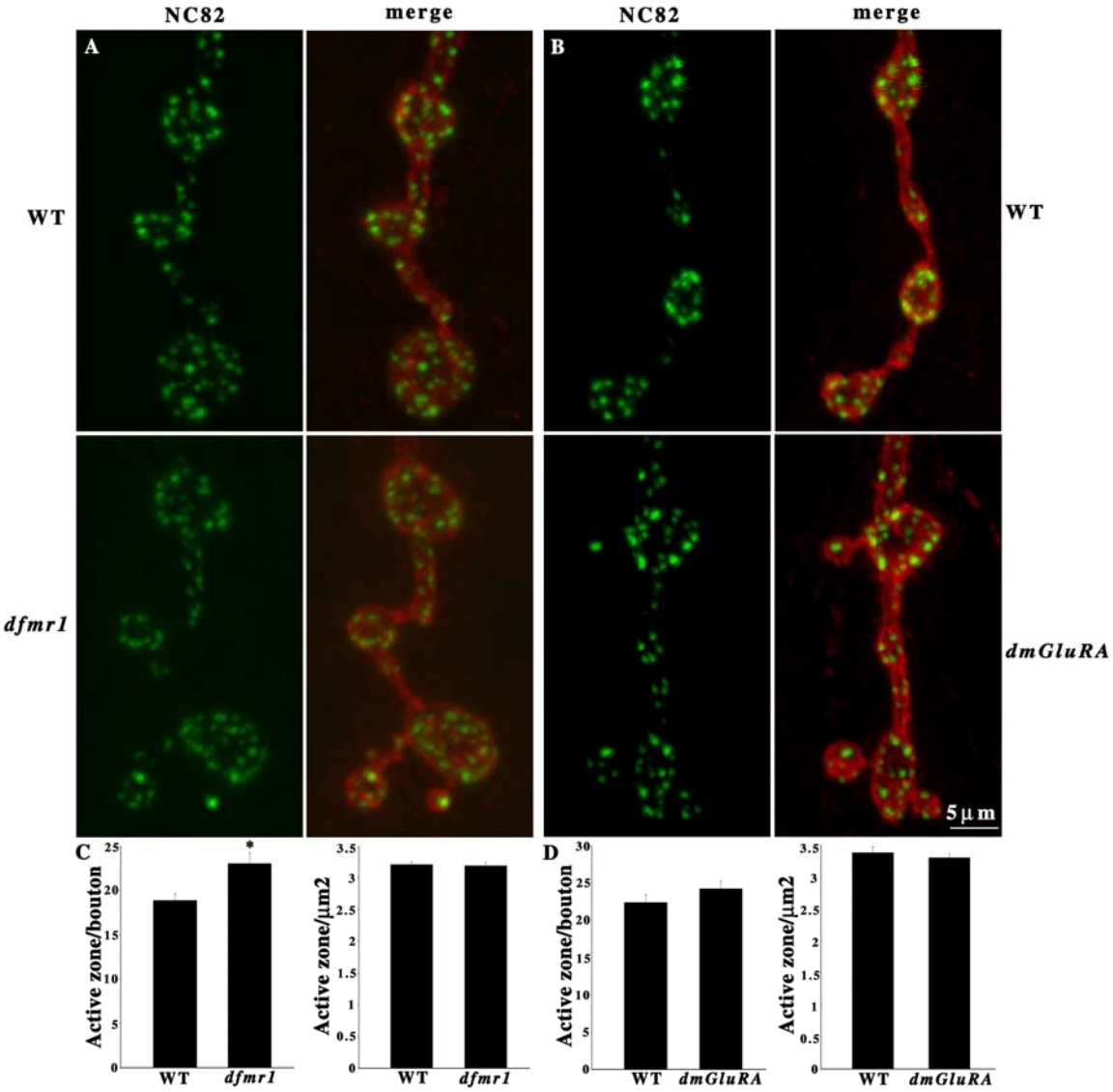
NC82
merge
NC82
merge
A
B
WT
WT
dfmr1
dmGluRA
5μm
C
D
Active zone/bouton
Active zone/μm2
Active zone/bouton
Active zone/μm2
WT
dfmr1
WT
dfmr1
WT
dmGluRA
WT
dmGluRA

in *dfmr1* mutants, which had identical density to controls (WT=3.2±0.04, N=152; *dfmr1*=3.2±0.06,N=164; P=0.73). In *dmGluRA* mutants, there was no change in either active zone number or density (Figure3.6B,D; N=103 WT; N=114 *dmGluRA*). Note that in all GluR measurements, fluorescent density per synaptic area was assayed, and therefore the changes in GluR class abundance occur over an area in which active zone density was unchanged.

To directly test a possible presynaptic dFMRP role, targeted presynaptic dFMRP expression was driven in the *dfmr1* null to assess the impact on the GluR phenotypes. The neural ELAV-Gal4 driver was crossed into the *dfmr1* null background with a recombinant line of UAS-*dfmr1*. This combination strongly expressed dFMRP in the presynaptic neurons, whereas dFMRP was undetectable in the postsynaptic muscles (data not shown). The two controls were ELAV-GAL4 in the heterozygous background (+/*dfmr1*), and the *dfmr1* null (null in both pre- and postsynaptic cells). The presynaptic-only expression of dFMRP failed to rescue either GluRIIA or GluRIIB phenotypes (Figure 3.7). The A-class GluRs were increased in this single-side rescue (+/*dfmr1*=118±4.88; *dfmr1*=130.8±4.56; presynaptic rescue=139.5±3.87; N=9 for all genotypes; P=0.002 between +/*dfmr1* and presynaptic rescue; Figure 3.7A, C). The B-class GluRs were decreased in single-side rescue (+/*dfmr1*=134.63±3.65; *dfmr1*=124.16±5; presynaptic rescue=112.56±3.58; N=10 for all genotypes; P=0.004 between +/*dfmr1* and presynaptic rescue; Figure 3.7B, D). No significant

Figure 3.7: Targeted presynaptic dFMRP expression in *dfmr1* null mutants

Third instar NMJs probed using subunit-specific anti-GluRs (green) and anti-HRP (red) antibodies. Type IB boutons on muscle 4 in A3 were used for all imaging analysis. Representative images of GluRIIA (A) and GluRIIB (B) in heterozygous mutant (+/*dfmr1*), *dfmr1 null*, and presynaptic-only rescue of dFMRP expression.

C, D. Fluorescence intensity quantification of each GluR subunit and the HRP internal standard.

C. GluRIIA is significantly increased in *dfmr1* mutants, and is not rescued by presynaptic expression of dFMRP (N=9 for all genotypes).

D. GluRIIB is significantly decreased in *dfmr1* mutants, and is not rescued by presynaptic expression of dFMRP (N=10 for all genotypes).

$0.001<P<0.05$(*); $0.0001<P<0.001$(**).

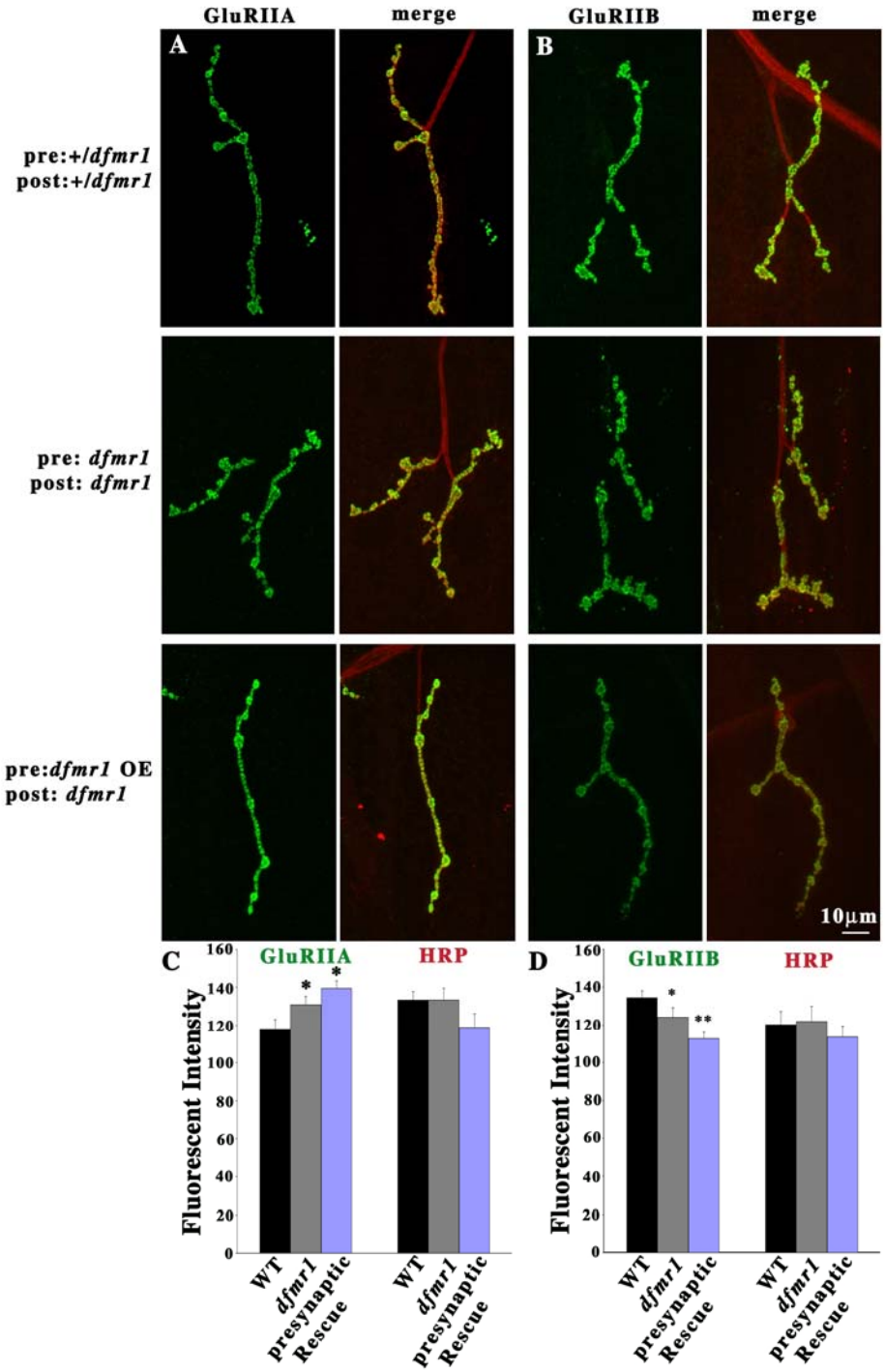
GluRIIA
merge
GluRIIB
merge
A
B
pre:+/dfmr1
post:+/dfmr1
pre: dfmr1
post: dfmr1
pre:dfmr1 OE
post: dfmr1
10μm
C
GluRIIA
HRP
Fluorescent Intensity
160
140
120
100
80
60
40
20
0
*
*
WT
dfmr1
presynaptic
Rescue
WT
dfmr1
presynaptic
Rescue
D
GluRIIB
HRP
Fluorescent Intensity
*
**
WT
dfmr1
presynaptic
Rescue
WT
dfmr1
presynaptic
Rescue

changes were detected on GluRIIC levels in either *dfmr1* null and presynaptic rescue conditions (data not shown).

DmGluRA and dFMRP functions converge to regulate synaptic GluR expression

The above results demonstrate that both dFMRP and DmGluRA function to regulate GluR abundance in the postsynaptic compartment. Loss of function of these two genes increases A-class GluRs, whereas B-class GluRs are down-regulated in the absence of dFMRP and upregulated in the absence of DmGluRA. The best possible test for interactions between these two proteins is to generate double null mutants, in order to determine whether GluR phenotypes may cancel out, be additive, or show a synergistic interaction. If the two proteins function in the same signaling pathway, the prediction is that an epistatic interaction will be observed, with the downstream function epistatic to the upstream function. In this case, dFMRP translation regulation function is clearly predicted to be downstream of DmGluRA glutamatergic signaling. If the two proteins act in pathways that converge on GluR regulation, then mutant phenotypes are predicted to be additive, without any epistasis. To test these two possibilities, we generated a *dfmr1; dmGluRA* double null mutant. We crossed *dfmr1* into both the 2b (*dmGluRA* background control) and *dmGluRA* null mutant backgrounds. There was no significant difference between the original single *dfmr1* and *dfmr1; 2b* in

Figure 3.8: GluR expression in *dfmr1; dmGluRA* double null mutants

Third instar NMJs were probed using subunit-specific anti-GluRs (green) and anti-HRP (red) antibodies. Type IB boutons on muscle 4 in A3 were used for all imaging analysis.

A-C. Representative images of GluRIIA, IIB and IIC expression in WT (2b), *dfmr1;2b* single mutants, and *dfmr1;dmGluRA* double mutant NMJs. D-F) Fluorescence intensity quantification of each GluR subunit and the HRP internal standard in independent trials.

D. GluRIIA is significantly increased in *dfmr1* single mutants and the *dfmr1; dmGluRA* double mutants display an additive, highly significant level of GluRIIA expression (N=27 for *dfmr1;2b* and *dfmr1;dmGluRA*).

E. GluRIIB is very significantly decreased in *dfmr1* single mutants, and the *dfmr1; dmGluRA* double mutants display a reduced, less significant change in GluRIIB expression, indicating an additive interaction (N=18 for *dfmr1;2b* and *dfmr1,dmGluRA*).

F. GluRIIC showed no significant change in *dfmr1* single or *dfmr1; dmGluRA* double mutants (N=13 for *dfmr1;2b* and *dfmr1,dmGluRA*). In all independent trials, there was no significant change of HRP levels among the three genotypes.

$0.001<P<0.05$(*); $0.0001<P<0.001$(**).

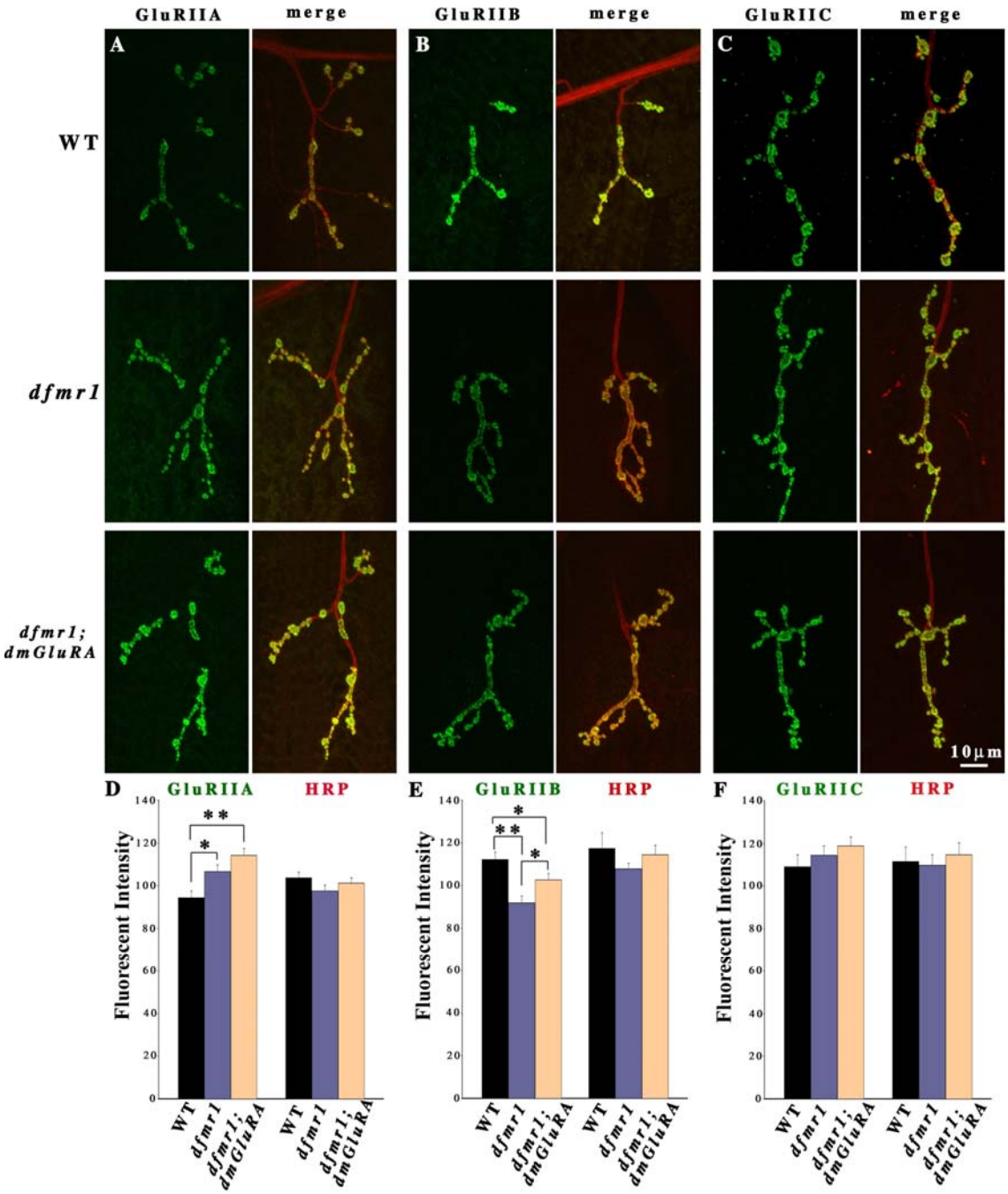
GluRIIA
merge
GluRIIB
merge
GluRIIC
merge
A
B
C
WT
dfmr1
dfmr1;
dmGluRA
10μm
D
GluRIIA
HRP
E
GluRIIB
HRP
F
GluRIIC
HRP
Fluorescent Intensity
0
20
40
60
80
100
120
140
*
**
WT
dfmr1
dfmr1;
dmGluRA

any assays (data not shown), therefore genetic background is not a complicating factor. All three GluR populations were assayed in all mutant combinations (Figure 3.8).

For both GluR classes, the *dfmr1; dmGluRA* double null mutant showed the additive phenotypes of *dfmr1* and *dmGluRA* single null mutants. For GluRIIA, the *dfmr1; 2b* single mutant displayed a significant increase and the double mutant displayed a significantly larger, further elevation in A-class receptor expression (*dfmr1; dmGluRA*, 114.24±3.24; N=27; P=0.004; Figure 3.8A, D). For GluRIIB, the *dfmr1; dmGluRA* double mutant similarly showed an additive phenotype. The *dfmr1* single mutant displayed a 20% decrease in GluRIIB level compared to WT (2b) controls (*dfmr1; 2b*, 91.92±23.16; WT (2b), 112.29±3.32; N=18, P=0.0007; Figure 3.8B, E). However, the *dmGluRA* single mutant displayed an apposing 11% increase in GluRIIB (see Figure 3.3B, E). The *dfmr1; dmGluRA* double mutant displayed an intermediate, additive phenotype, with a 12% increase in B-class GluRs relative to the *dfmr1* single mutant (*dfmr1; 2b*, 91.92±23.16; *dfmr1;DmGluRA*, 102.74±2.88; N=18 for both, P=0.016; Figure 3.8B, E). Thus, the double mutant displayed only an 8% decrease in GluRIIB compared to the control, a significant difference (P=0.05) compared to the *dfmr1* single mutant. For GluRIIC, there were no significant changes between any of the genotypes (WT (2b), 109.03±5.67, N=8; *dfmr1; 2b*, 114.54±4.46; *dfmr1; dmGluRA*, 118.93±4.11; N=13 for both mutants; P=0.48 between WT and *dfmr1*; P=0.45 between *dfmr1*

and *dfmr1; dmGluRA*; Figure 3.8C, F). Similarly, the ratio of GluRIIA/GluRIIB subunits in *dfmr1; 2b* single mutants and *dfmr1; dmGluRA* double mutants was not significantly different (*dfmr1; 2b*, 1.51±0.05; *dfmr1; dmGluRA*, 1.42±0.06; N=9 for each genotype; P=0.24). These data show an additive interaction between DmGluRA signaling and dFMRP function, which suggests convergent mechanisms on GluR regulation.

Discussion

The finding of elevated Group I mGluR5-dependent hippocampal LTD in the *fmr1* knockout mouse (Huber et al., 2002) has elicited a great deal of attention and excitement. This type of LTD is caused by loss of surface-expression of AMPA GluRs, in a mechanism requiring protein synthesis (Huber et al., 2000; Huber et al., 2001; Nosyreva and Huber, 2006; Pfeiffer and Huber, 2006). Since synaptic protein translation is regulated by FMRP (Weiler et al., 1997; Todd et al., 2003a; Antar et al., 2004; Weiler et al., 2004; Aschrafi et al., 2005; Qin et al., 2005b), these observations suggest a mechanistic connection between mGluR signaling and FMRP translation regulation in the control of GluR expression at the synapse, and indicate that this pathway may be a critical regulator of functional synaptic plasticity. This idea has been formally expressed as the ‘mGluR theory of FXS’ (Bear et al., 2004). Our study directly investigates this hypothesized connection between mGluR signaling, FMRP regulatory function and the synaptic

expression of GluRs using the *Drosophila* FXS model. In *Drosophila*, there is a single FMR1 protein (dFMRP; (Wan et al., 2000; Zhang et al., 2001) and a single mGluR (DmGluRA; Parmentier et al., 1996; Bogdanik et al., 2004). dFMRP structure, expression and regulative functions closely resemble mammalian FMRP (Wan et al., 2000; Zhang et al., 2001; Dockendorff et al., 2002; Morales et al., 2002; Lee et al., 2003; Schenck et al., 2003; Ling et al., 2004; Reeve et al., 2005; Zhang et al., 2005). In contrast, DmGluRA is more homologous to mammalian Group II/III mGluRs (Parmentier et al., 1996), not the Group I mGluRs implicated in the FMRP mechanism. However, these mGluR class distinctions may mean little in *Drosophila*, with its single mGluR. The mammalian group I mGluR antagonist MPEP rescues morphological and behavioral phenotypes in *dfmr1* null mutants (McBride et al., 2005), and DmGluRA modulates synaptic architecture (Bogdanik et al., 2004), which is a known function of mammalian Group I mGluRs (Vanderklish and Edelman, 2002). These findings suggest that DmGluRA likely occupies the Group I mGluR niche in *Drosophila*. In any case, DmGluRA is the only mGluR capable of mediating glutamatergic signaling in the *Drosophila* system.

We previously showed that both *dfmr1* and *dmGluRA* mutants have strong defects in glutamatergic synaptic function at the *Drosophila* NMJ (Zhang et al., 2001; Bogdanik et al., 2004). Neurotransmission at this synapse is mediated by A- and B-class AMPA-type GluRs, which have distinctive functional properties,

subsynaptic distributions and are regulated by distinct mechanisms (Schuster et al., 1991; Petersen et al., 1997; Sigrist et al., 2002; Marrus et al., 2004; Featherstone et al., 2005; Qin et al., 2005a). Here, we show in *dfmr1* null mutants that A-class GluRs accumulate and B-class GluRs are lost (Figure 3.9A). The total GluR content does not change, but rather there is a striking shift in the GluR class ratio within single postsynaptic domains. This subclass-specific regulation of GluRs is a novel finding. In *dmGluRA* null mutants, we show that both GluR classes, and therefore the total GluR population, are significantly increased (Figure 3.9A). This is a novel finding for DmGluRA, but consistent with findings in mammals showing that GluR1 AMPA receptors are decreased in synaptic terminals when mGluR activity is induced (Snyder et al., 2001; Xiao et al., 2001). Moreover, we show that postsynaptic over-expression of DmGluRA induces exactly opposite changes of A- and B-class GluRs compared to *dfmr1* null mutants. By testing active zone density and targeted presynaptic rescue of dFMRP in the *dfmr1* null, we show that the regulatory function of dFMRP on the GluR classes is a postsynaptic mechanism. Finally, we show in *dfmr1; dmGluRA* double null mutants that both GluR class phenotypes are additive (Figure 3.9A); A-class GluRs increase further with the additive increases of *dfmr1* and *dmGluRA* single mutants, and B-class GluRs tend toward normal levels, with the additive downregulation in the *dfmr1* single mutant and upregulation in the *dmGluRA* single mutant. These results suggested that DmGluRA signaling and dFMRP

Figure 3.9: mGluR and dFMRP pathways converge in the regulation of iGluRs

A. Comparison of *dfmr1* and *dmGluRA* single mutants, and *dfmr1; dmGluRA* double mutants in the expression of the three GluR subunits. The WT control is set as zero and each bar represents percent change in expression.

B. Model relating mGluR signaling and FMRP translation regulatory function controlling synaptic expression of ionotropic GluR classes. DmGluRA negatively regulates both A- and B-class GluRs. dFMRP negatively regulates A-class GluRs and positively regulates B-class GluRs. Genetic tests (part A) show that the regulation of these two pathways is additive, and therefore that the pathways converge on the regulation of these GluR classes. The mGluR theory of FXS postulates that these pathways both regulate local postsynaptic mRNA translation; activated by mGluR signaling and inhibited by dFMRP. Some newly synthesized proteins (Pool 1 mRNA) promote synaptic expression of A-class GluRs, whereas others (Pool 2 mRNA) depress synaptic expression of B-classes GluRs. Thus, the postsynaptic ratio of A- to B- class GluRs is independently regulated.

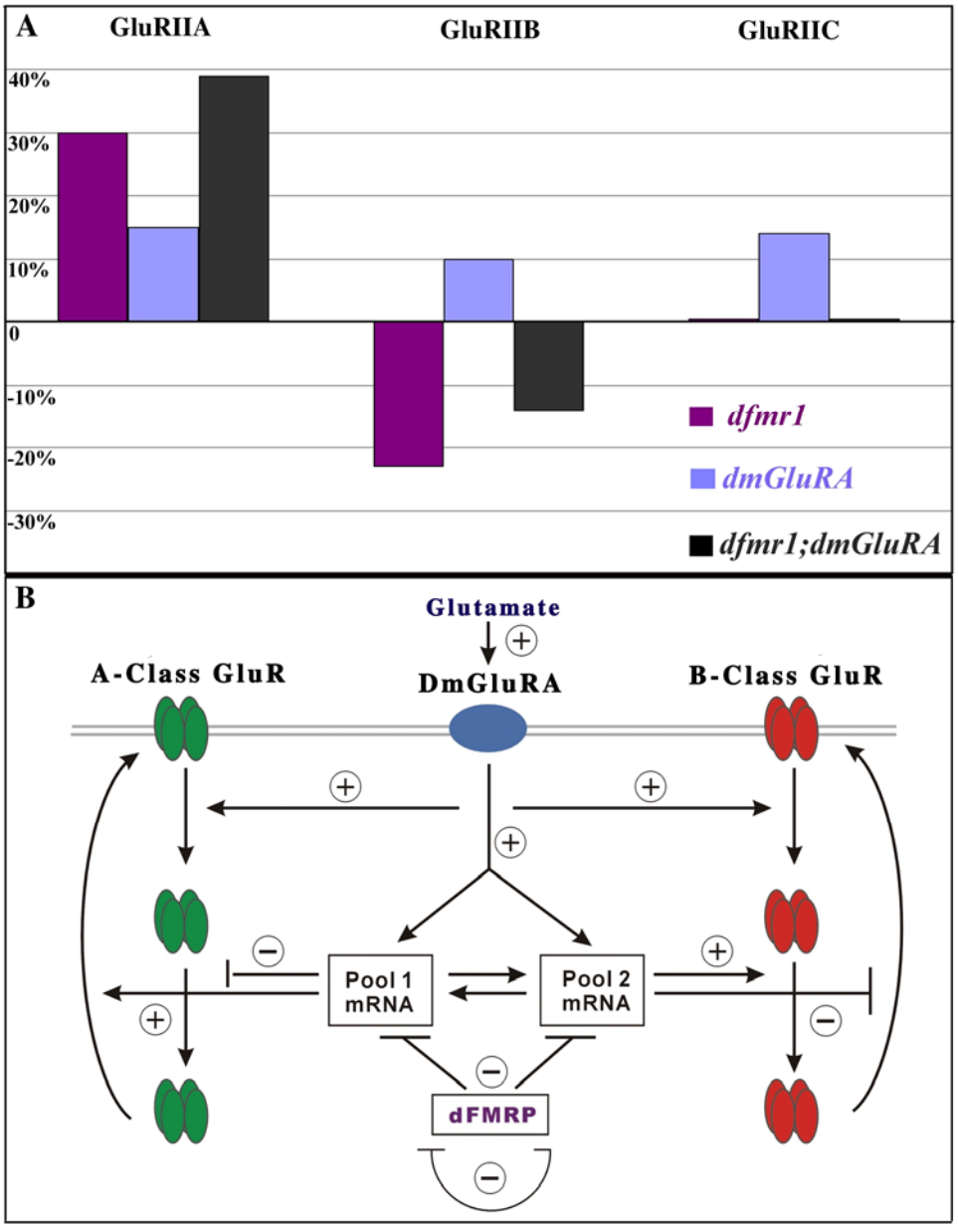
A
GluRIIA
GluRIIB
GluRIIC
40%
30%
20%
10%
0
-10%
-20%
-30%
dfmr1
dmGluRA
dfmr1;dmGluRA
B
Glutamate
A-Class GluR
DmGluRA
B-Class GluR
Pool 1 mRNA
Pool 2 mRNA
dFMRP

function converge to regulate the synaptic expression of these two GluR classes, but that independent pathways of DmGluRA signaling and dFMRP function also exist.

Pre- and postsynaptic functions; overlapping and independent mechanisms

This study suggests that dFMRP and DmGluRA perform in both overlapping and independent pathways in the regulation of postsynaptic GluR classes (Figure 3.9B). Targeted presynaptic expression of dFMRP in the *dfmr1* null fails to provide any rescue of class-specific GluR misregulation, showing that the dFMRP requirement is in the postsynaptic compartment. Consistently, targeted postsynaptic over-expression of DmGluRA causes the opposite class-specific GluR misregulation of the *dfmr1* null, suggesting an intersection of DmGluRA signaling and dFMRP function in the postsynaptic compartment (Figure 3.9B). In the *dfmr1* null, quantal size is increased (Zhang et al., 2001), a hallmark postsynaptic defect. A mechanistic cause suggested by this study is the elevated A-class GluR level, consistent with former reports that GluRIIA over-expression increases quantal size. Moreover, GluRIIA over-expression increases active zone number per bouton, based on the NC82/bruchpilot probe, but does not alter active zone density (Sigrist et al., 2002), which is identical to the phenotype reported here for *dfmr1* mutants. These results support the conclusion that both dFMRP and DmGluRA function in the postsynaptic domain in class-specific GluR

regulation (Figure 3.9B), and that this mechanism may feedback to alter presynaptic properties.

In addition to the postsynaptic mechanism, there appears to also be presynaptic roles of both dFMRP and DmGluRA that can impact the postsynaptic GluR domains. We have shown previously that both proteins are expressed in the presynaptic neuron of the *Drosophila* NMJ (Zhang et al., 2001; Bogdanik et al., 2004). Single null mutants show differential misregulation, with the *dfmr1* null displaying the class-specific change reflecting its postsynaptic function, but the *dmGluRA* null increasing both GluR classes in common. This must reflect a presynaptic function for DmGluRA. Consistently, presynaptic over-expression of DmGluRA depresses the level of both A- and B-class GluRs, the opposite phenotype as the *dmGluRA* null. Likewise, presynaptic over-expression of dFMRP also reduces B-class GluR expression, although it does not change the abundance of A-class receptors. Presumably, these presynaptic roles reflect the know functions of dFMRP and DmGluRA in regulating presynaptic glutamate release properties, which we have shown previously (Zhang et al., 2001; Bogdanik et al., 2004), and therefore the GluR changes reflect transynaptic signaling in a homeostatic mechanism.

By strict genetic criteria, the prediction for the interaction of two proteins within a common regulatory pathway is that the mutant phenotype for the gene product downstream in the pathway should be epistatic to that of the gene product

upstream in the pathway. Clearly, the FMRP translation regulatory activity should be downstream of mGluR surface glutamate reception. Such a strict epistatic relationship is not observed for DmGluRA and dFMRP in the control of GluR expression. Rather, the null mutant phenotypes are obviously additive in double mutants (Figure 3.9A). The A-class GluR goes up in both single mutants, and goes up further in the double mutant. The B-class GluR goes down in *dfmr1* and up in *dmGluRA*, and shows an intermediate, additive level in the double mutant. Such additive phenotypes show that dFMRP and DmGluRA have overlapping functions but can be operating in the independent pathways (Figure 3.9B). Taken together, our results suggest that dFMRP and DmGluRA pathways converge on the regulation of GluR synaptic expression, and that this involves both pre- and postsynaptic interactions.

Acknowledgements

We are most grateful to Dr. Aaron DiAntonio for the generous gift of GluRIIB and GluRIIC antibodies. We thank the Iowa Developmental Studies Hybridoma Bank for providing the GluRIIA and NC82 antibodies. We also thank members of Broadie Lab for discussion, especially Dr. Charles Tessier and Dr. Cheryl Gatto for comments on the manuscript, and Dr. Jeffrey Rohrbough for imaging advice. This work was supported by NIH grants HD40654 and GM54544 to K.B.

Experimental Procedures

Drosophila Genetics

All *Drosophila* stocks were maintained at 25^{o}C on standard food under standard conditions. The w^{1118}; $dfmr1^{50M}$ null mutant strain was used as the *dfmr1* single mutant (Zhang et al., 2001), and w^{1118} was used as its genetic background control. The P-element imprecise excision $dmGluRA^{112b}$ null mutant was used as the *dmGluRA* single mutant, and $dmGluRA^{2b}$ (hereafter called 2b), a p-element precise excision line from the same screen, was used as its genetic background control (Bogdanik et al., 2004). For targeted over-expression studies, lines used included *w;* UAS-*dfmr1* (Zhang et al., 2001; Pan et al., 2004), *w*; UAS-dmGluRA (Bogdanik et al., 2004), and the tissue-specific Gal4 drivers ELAV-Gal4 (neural specific) and MHC-Gal4 (muscle specific). The following strains were generated by standard genetic methods for this study: 1) the $dfmr1^{50M}$; $dmGluRA^{112b}$ double null mutant, 2) the $dfmr1^{50M}$; 2b genetic background control combination, 3) the ELAV-GAL4; $dfmr1^{50M}$ and 4) $dfmr1^{50M}$, UAS-*dfmr1*.

Immunohistochemistry

Wandering 3rd instar larvae were dissected in Ca^{2+}-free standard saline containing 2mM L-glutamate, followed by ice-cold methanol fixation for 5 minutes. The monoclonal mouse antibody against GluRIIA (8B4D2, used at 1:20) was

obtained from the Developmental Studies Hybridoma Bank (University of Iowa). The polyclonal rabbit antibodies against GluRIIB (used at 1:2000)(Marrus et al., 2004) and GluRIII/IIC (used at 1:2000)(Marrus et al., 2004) were a generous gift from Dr. Aaron DiAntonio (Washington University). The specificity of these GluR subunit-specific antibodies has been rigorously demonstrated in western blot analyses and genetic tests in subunit-specific null mutants (Yoshihara and Littleton, 2002; Marrus et al., 2004; Liebl et al., 2005; Qin et al., 2005a). The monoclonal mouse antibody against NC82/bruchpilot (used as 1:200) was obtained from the Iowa Developmental Studies Hybridoma Bank (Wagh et al., 2006). All primary antibodies were visualized using fluorescent dye-conjugated secondary antibodies, including Alexa Fluor 488 goat anti-mouse IgG (1:200; Molecular Probes), Alexa Fluor 488, 546, and 633 goat anti-rabbit IgG (1:200; Molecular Probes), Cy5- and Texas Red- conjugated anti-Horseradish Peroxidase (1:200; Jackson). All fluorescent images were collected using a Zeiss LSM 510 meta laser scanning confocal microscope and image-collection software. All image processing was done with Adobe Photoshop 7.0.

Fluorescent intensity quantification

For any given experiment, animals of control and mutant genotypes were simultaneously processed, together in the same tube, and imaged using identical confocal settings. A neuronal membrane specific probe, anti-HRP, was used in all

experiments to label the NMJ synapse and as an internal fluorescence staining control. All images used in fluorescent intensity quantification were 3D-projections from complete Z-stacks through the entire NMJ on the lateral, longitudinal muscle 4 in abdominal segment A3. Data from the two-paired hemisegments were averaged for each animal, to produce each single data point. All images were analyzed using LSM 5 Confocal Image Examiner software in the “histogram” display mode. Synaptic regions were user-defined with the closed free shape curve drawing tools, defined by the boundary of HRP staining. For quantification, multiple synaptic regions were defined, and the fluorescence intensity calculated as an average of all regions. The software output reports fluorescence intensity for each fluorescent channel and the calculated area for each region. Thus, all reports are density measurements. In the direct ratio tests, green channel (GluRIIA) intensity was divided by red channel (GluRIIB) intensity to determine GluRIIA/GluRIIB ratio in the same synaptic regions. Statistical analysis was done using GraphPad InStat 3 software. Significance levels in figures were represented as $0.001<P<0.05$(*); $0.0001<P<0.001$(**); $P<0.0001$(***). All error bars represent SEM (Standard Error of Mean), appropriate for comparison of the mean of means distribution.

CHAPTER IV

MECHANISTIC RELATIONSHIPS BETWEEN *DROSOPHILA* FRAGILE X MENTAL RETARDATION PROTEIN AND METABOTROPIC GLUTAMATE RECEPTOR A SIGNALING

This paper is submitted under the same title to *Molecular and Cellular Neuroscience*.

Luyuan Pan, Elvin Woodruff and Kendal Broadie

Department of Biological Science, Kennedy Center for Research on Human Development, Vanderbilt University, Nashville, TN 37232

Summary

Fragile X Syndrome (FXS), the most commonly inherited mental retardation disorder, is caused by loss of Fragile X Mental Retardation Protein (FMRP), an mRNA-binding regulator of protein translation. A current hypothesis proposes that FMRP functions downstream of metabotropic glutamate receptor (mGluR) signaling to regulate protein synthesis driving structural/functional changes in synapse development and plasticity. Using our *Drosophila* FXS model, we investigate here the mechanistic relationship between dFMRP and the sole *Drosophila* mGluR (DmGluRA) by assaying protein expression, behavioral

performance and neuronal structure in brain Mushroom Body (MB) neurons and the peripheral NMJ; in *dfmr1* and *dmGluRA* single null mutants, double null mutants and with a pharmacological mGluR antagonist. At the protein level, dFMRP is upregulated in the *dmGluRA* null mutant, and DmGluRA is upregulated in the *dfmr1* null mutant, demonstrating a mutual negative feedback loop. Null *dmGluRA* mutants display behavioral defects in coordinated movement behavior, which are rescued by also removing dFMRP expression in the double mutant. Null *dfmr1* mutants display increased synaptic structural complexity at the NMJ, which is partially rescued by blocking mGluR signaling in *dmGluRA* double mutants or with an mGluR antagonist. Ultrastructurally, *dfmr1* null mutants display elevated presynaptic vesicle pools, which is also partially rescued in *dmGluRA* double mutant combinations. In the brain MB learning/memory center, *dfmr1* null neurons display increased presynaptic architectural complexity, which is also partially rescued by treating mutants with mGluR antagonist. These data show overlapping mechanisms between DmGluRA signaling and dFMRP function in the regulation of neuronal architecture and presynaptic properties.

Introduction

Fragile X syndrome (FXS) is a broad-spectrum neurological disease with symptoms including hyperactivity, hypersensitivity to sensory stimuli, mental retardation and autism (Turner et al. 1996; Rogers et al. 2001; Visootsak et al.

2005). The disease is caused solely by loss of expression of the *fragile X mental retardation 1* (*fmr1*) gene, which encodes FMRP, an mRNA-binding protein that associates with polyribosomes and acts as a negative translational regulator (Garber et al. 2006). A prominent neuronal structure defect found in FXS patients and *fmr1* knockout mice is denser, longer and immature appearing postsynaptic dendritic spines in the cortex, a defect also found in other mental retardation diseases (Purpura 1974; Hinton et al. 1991; Irwin et al. 2002; Grossman et al. 2006). FMRP similarly negatively regulates presynaptic growth and differentiation, with increased filipodial extensions from axon growth cones in an *fmr1* mouse culture system (Antar et al., 2006) and altered presynaptic synaptogenesis in a mosaic mouse model of FXS (Hanson and Madison, 2007). FMRP also regulates synaptic functional plasticity. A prominent defect in *fmr1* knockout mice is enhanced long term depression (LTD) in the hippocampus, a group I class 5 metabotropic glutamate receptor (mGluR) signaling-induced event (Huber et al. 2002). This form of LTD requires *de novo* protein synthesis induced by mGluR signaling, which is sensitive to translational inhibitors and dependent on FMRP (Huber et al. 2000; Koekkoek et al. 2005; Nosyreva and Huber 2006). Based on these findings, a hypothesis has been proposed suggesting that FMRP regulates synaptic properties by regulating the level of protein synthesis downstream of mGluR signaling; “the mGluR theory of FXS” (Bear et al. 2004; Pfeiffer and Huber 2006).

Drosophila provides a powerful genetic model system to test this hypothesis. The *Drosophila* genome contains only one *fmr1* homolog (*dfmr1*) and encodes a single functional mGluR (DmGluRA) (Parmentier et al. 1996; Wan et al. 2000; Zhang et al. 2001; Bogdanik et al. 2004). Null mutants of both genes are viable and therefore accessible to neurological studies throughout life. As in the mammalian system, null *dfmr1* mutants display structural overgrowth and overbranching of both presynaptic and postsynaptic processes, which has been well-characterized in both the larval glutamatergic neuromuscular junction (NMJ) and the adult central brain Mushroom Body (MB) learning/memory center (Zhang et al. 2001; Lee et al. 2003; Michel et al., 2004; Pan et al. 2004; McBride et al., 2005). Loss of dFMRP also causes altered synaptic differentiation and/or function in the visual system, brain MB and NMJ (Zhang et al. 2001; Pan et al. 2004; Zhang and Broadie 2005). DmGluRA is synaptically localized in both CNS synaptic neuropil and at the NMJ (Parmentier et al. 1996; Bogdanik et al. 2004). DmGluRA is a sequence ortholog of mammalian group II/III mGluRs but, as the sole *Drosophila* mGluR, presumably takes on all GluR signaling functions subdivided between group I-III mGluRs in mammals. Null *dmGluRA* mutants display altered synaptic architecture at the NMJ and also strong defects in activity-dependent functional plasticity at the NMJ (Bogdanik et al. 2004). Roles of DmGluRA in the CNS have not yet been investigated. These data show that dFMRP and DmGluRA modulate synaptic architecture and function in the same

or closely related processes.

Treatment with a group I mGluR antagonist (MPEP) can rescue two major FXS behavioral phenotypes in *fmr1* knockout mice, habituation in open field tests and increased sensitivity to audiogenic seizures (Yan et al. 2005). Similarly, treating *dfmr1* null mutant flies with either MPEP (Group I mGluR antagonist), or LY341495, MPPG, or MTPG (Group II/III mGluR antagonists), can effectively rescue behavioral and gross brain morphological defects, including male courtship learning/memory defects and β-lobe fusion in the Mushroom Body (McBride et al. 2005). These results have strongly supported a mechanistic relationship between DmGluRA signaling and dFMRP function. The fact that antagonists of different mammalian mGluR classes can equally rescue *dfmr1* null phenotypes (McBride et al. 2005), suggests that DmGluRA does indeed mediate group 1 mGluR signaling or, alternatively, that the connection between FMRP function and mGluR signaling might be broader than is currently appreciated. The identification and elucidation of the molecular and cellular relationships between mGluR signaling and FMRP will significantly increase understanding on the mechanism of FXS, and provide insights into potential therapeutic treatments for the disease.

In this study, we examine mechanistic relationships between DmGluRA signaling and dFMRP function at the genetic, molecular and cellular levels. We find that dFMRP protein is increased in *dmGluRA* null mutant CNS, and that

DmGluRA protein is similarly increased in *dfmr1* null mutants, showing a molecular feedback regulation mechanism. DmGluRA and dFMRP interact in the regulation of coordinated movement behavior, and in the regulation of synaptic architecture at the NMJ. Ultrastructure analyses show greatly increased synaptic vesicle pools in *dfmr1* null synaptic boutons, which are largely restored to normal by also removing DmGluRA function. In the brain, blocking DmGluRA signaling rescues single-cell architectural defects in *dfmr1* null neurons. Taken together, these data suggest that convergent cross-talk between DmGluRA signaling and dFMRP function controls neuron structure and presynaptic differentiation.

Results

DmGluRA and dFMRP mutual negative feedback loop

Previous work has shown that dFMRP and DmGluRA are both localized in the nervous system (Parmentier et al. 1996; Ramaekers et al. 2001; Zhang et al. 2001; Dockendorff et al. 2002), but the spatial relationship between them has not been clear. Just like mammalian FMRP, dFMRP appears to be pan-neuronally expressed with similar levels in most/all neurons, and is primarily localized in the neuronal soma cytoplasm with little/no detectable expression in the nucleus and only very faint expression in distal neuronal processes (Verheij et al., 1993; Feng et al., 1997; Zhang et al., 2001; Antar et al., 2004; Pan et al., 2004; Bagni and

Greenough 2005). In the *Drosophila* larval CNS, dFMRP is concentrated in all neuronal soma, including midline motor neuron soma, but largely undetectable in the synaptic neuropil (Figure 4.1A). In direct contrast, DmGluRA is specifically concentrated at synaptic connections (Bogdanik et al., 2004). In the *Drosophila* larval CNS, DmGluRA is undetectable in neuronal soma but appears throughout the synaptic neuropil (Figure 4.1A). DmGluRA therefore also appears pan-neuronal, although this is impossible to say for sure in the absence of neuronal soma localization. Thus, dFMRP is primarily localized in neuronal cell bodies, whereas DmGluRA is primarily localized in synaptic neuropil (Figure 4.1A). The two proteins have a largely non-overlapping expression pattern in the same neurons.

The mGluR theory of FXS proposes that FMRP expression is negatively regulated by mGluR signaling (Bear et al. 2004; Pfeiffer and Huber 2006). We therefore first asked whether DmGluRA signaling may regulate dFMRP by examining dFMRP protein expression in the *dmGluRA*^{112b} null mutant with a companion precise excision line, 2b, as the genetic background control (Figure 4.1A; top, green). The antibody against dFMRP does not produce any signal in *dfmr1* null mutants (data not shown), proving antibody specificity. The level of dFMRP is clearly and consistently upregulated in *dmGluRA* null mutants (Figure 4.1A). There is no detectable change of the expression pattern, but rather just a greatly heightened dFMRP expression in neuronal soma. Given this evident

regulation, we next asked whether dFMRP may also regulate DmGluRA protein levels. The *dfmr1*^{50M} null mutant was assayed, with *w*^{1118} as the genetic background control (Figure 4.1A; bottom, red). The antibody against DmGluRA does not produce any signal in *dmGluRA*^{112b} (data not shown), proving antibody specificity. The synaptic neuropil expression of DmGluRA is increased in the *dfmr1* null mutants (Figure 4.1A). As in the case of dFMRP, there is no detectable change in the pattern of expression, just an increase in the DmGluRA protein level in the synaptic neuropil.

To further examine the interaction between dFMRP and DmGluRA, we performed immunocytochemistry at an electron microscope level on ultrathin sections through the third instar CNS (Figure 4.1B). Both primary antibodies were visualized by secondary antibodies directly conjugated to gold beads (10nm diameter). In null mutant controls, the background level of adherent gold beads was virtually undetectable (data not shown), once again demonstrating antibody specificity. The dFMRP label was localized to cellular cytoplasm in neurons, often with several gold particles localized on or near large (~100nm), uniform dense-core granules resembling stress granules or P-bodies (Figure 4.1B, top). In the *dmGluRA*^{112b} null mutant, the density of dFMRP gold particle label was clearly increased compared to controls (Figure 4.1B; top, arrows). The CNS neuropil is densely packed with many synaptic structures, including prominent synaptic terminals filled with mitochondria and synaptic vesicles. The synaptic

Figure 4.1. DmGluRA and dFMRP display mutual negative regulation.

A. Representative images of dFMRP (green) and DmGluRA (red) expression patterns in third instar larval CNS in wildtype (WT), *dfmr1* null mutant, and *dmGluRA* null mutant. Both dFMRP and DmGluRA are highly enriched in CNS neurons, with dFMRP primary localized in neuronal cell bodies (cb), and DmGluRA primary localized in synaptic neuropil (np). Expression was assayed for each protein in the respective opposing null mutant. dFMRP level is clearly increased in *dmGluRA* null mutants, and DmGluRA level is also increased in *dfmr1* null mutants. The scale bar is 10μm.

B. Immuno-EM localization of dFMRP and DmGluRA in third instar larval CNS. Wildtype (WT), *dfmr1* and *dmGluRA* null mutants immuno-labeled with 10nm gold particles against dFMRP (top) and DmGluRA (bottom). Arrows indicate representative clusters of immunogold particles in each case. Insets show higher magnification images of the gold label in each case. In *dmGluRA* mutants, there is a clear increase of gold particle number of dFMRP labeling. Similarly, a clear increase of DmGluRA labeling is also observed in *dfmr1* null mutants. The scale is 250nm.

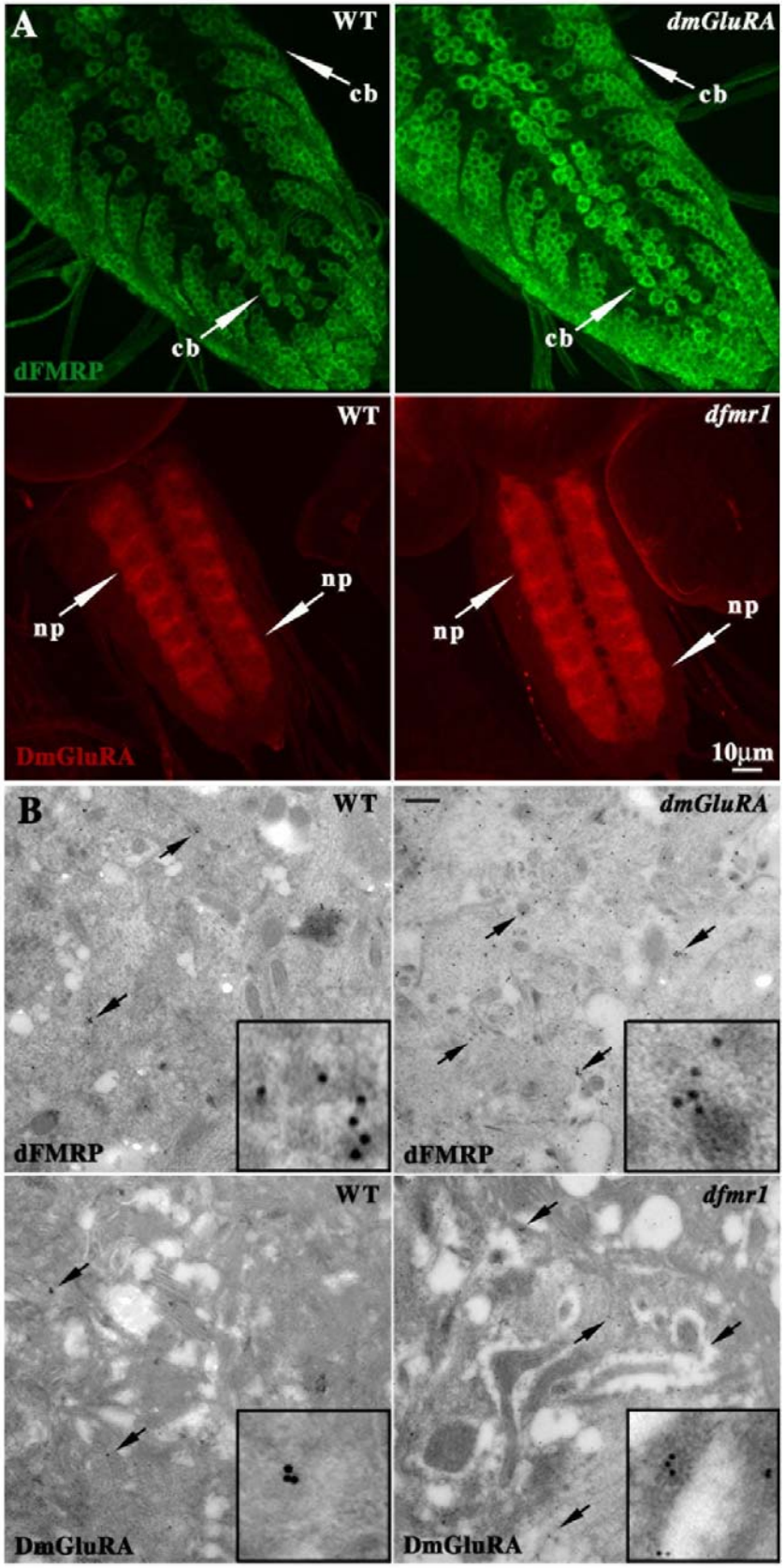
A
WT
cb
cb
dFMRP
dmGluRA
cb
cb
WT
np
np
DmGluRA
dfmr1
np
np
10μm
B
WT
dFMRP
dmGluRA
dFMRP
WT
DmGluRA
dfmr1
DmGluRA

arborizations are very small (<500nm mean diameter) with a packing density that exceeds by several fold the highest density found among vertebrate neurons (Strausfeld 1998). Immunogold labeling of DmGluRA shows a moderate level of protein associated with synaptic membranes (Figure 4.1B, bottom). In the *dfmr1*^{50M} null mutant, the density of DmGluRA gold particle label was clearly increased compared to the genetic control (Figure 4.1B; bottom, arrows). Taken together, both fluorescent confocal microscopy and immunogold electron microscopy reveal that dFMRP and DmGluRA negatively regulate each other's expression in the same neurons. This reciprocal regulation between dFMRP and DmGluRA shows a negative feedback mechanism exists between DmGluRA signaling and dFMRP expression.

DmGluRA and dFMRP genetically interact in behavioral movement regulation

Behavioral tests of coordinated movement involve the integration of several sensory input modalities, coupled to sequential motor output driving the appropriate movement response. We previously devised a simple but effective test called the "roll-over" assay to measure such coordinated behavior in the *Drosophila* larva (Bodily et al. 2001). This assay involves placing wandering third instar larva on a smooth agar plate, turning the animal to a totally inverted position and then measuring the time the animal takes to fully right itself to the normal position. This behavior requires the integration of sensory stimuli and

coordinated bilateral motor control to produce the necessary sequence of movements. We used this assay to test *dfmr1* and *dmGluRA* single null mutants for possible defects in coordinated movement behavior, and then double null mutant combinations for modulation of behavioral responses.

Loss of DmGluRA signaling strongly impairs coordinated movement behavior, with the average response time lengthened by 50% (Figure 4.2). In individual animals, the behavioral defect was clearly evident as a combination of inappropriate movement responses and defects in cooperative motor control. The *dmGluRA* mutant animals appear to “struggle” during a period of continuous, spastic muscle contractions that do not aid in the tuning over behavior, while wildtype animals always display smooth, cooperative motor control to turn over quickly. Quantitatively, *dmGluRA* null mutants display a very significantly slowed performance compared to the genetic wildtype (WT) control in this coordinated behavior (WT=12.4±0.7 sec, N=46; *dmGluRA*=18.4±1.15 sec, N=49; P<0.0001; Figure 4.2). In contrast, removal of dFMRP alone causes no defect in this coordinated behavior. We used two independent *dfmr1* null mutant lines, $dfmr1^{50M}$ and $dfmr1^{3}$ (Zhang et al. 2001; Dockendorff et al. 2002), and crossed them into the same genetic control (2b) background shared with *dmGluRA*. Both $dfmr1^{50M}$ and $dfmr1^{3}$ null mutants perform comparably to the control in this coordinated movement assay (WT=12.4±0.7 sec, N=46; $dfmr1^{50M}$=12.9±1.04 sec, N=43, P=0.71; $dfmr1^{3}$=12.3±0.65, N=33; P=0.92; Figure 4.2). Therefore, loss of dFMRP

alone does not detectably impair the coordinated movement in the roll-over assay.

To examine the relationship between DmGluRA signaling and dFMRP function in coordinated movement behavior, we tested the performance of two double mutant combinations; *dfmr1*^{50M}*; dmGluRA* and *dfmr1*^{3}*; dmGluRA* (Figure 4.2). Both double null mutant lines displayed a remarkable rescue of the behavioral impairment caused by loss of mGluR signaling. In individual double mutant animals, the roll-over behavioral response was smooth and efficient, with a significantly shorter "struggle" time compared to the *dmGluRA* null. Quantitatively, the double null mutant showed comparable behavior to the wildtype control, with a very significant rescue of the impaired performance compared to the *dmGluRA* single mutant (*dfmr1*^{50M}*;dmGluRA*=9.0±0.62 sec, N=45, P<0.0001 to *dmGluRA*; *dfmr1*^{3}*;dmGluRA*=14.2±0.69 sec, N=34, P=0.007 to *dmGluRA*; Figure 4.2). It is not clear why the *dfmr1*^{50M} combination actually shows improved response time compared to the control, but the average response time for the two double null mutants (11.6 seconds) is quite comparable to the wildtype performance (12.4 seconds), with no significant difference. Therefore, the coordinated movement behavior defect in the *dmGluRA* null mutant can be effectively rescued by removing dFMRP function.

Figure 4.2. DmGluRA and dFMRP genetically interact in coordinated movement.

Coordinated movement behavior requires integration of sensory input and motor output. One test for this integration is the larval roll-over assay in which larvae are inverted and their righting time measured. Null *dmGluRA* mutants show a highly significant increase in response time, indicating grossly slowed performance. Two independent *dfmr1* null alleles behave normally. However, both double mutant combinations significantly rescue the slow performance of the *dmGluRA* null. 0.001<P<0.05(*); P<0.0001(***).

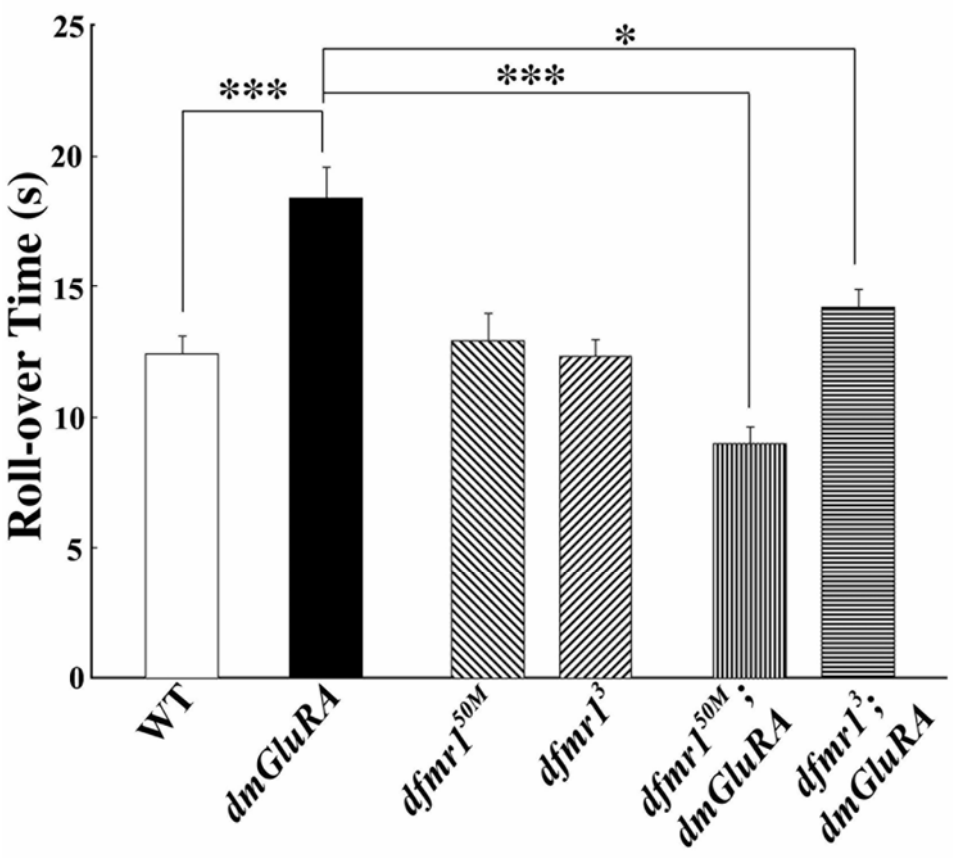
Roll-over Time (s)
25
20
15
10
5
0
***
***
*
WT
dmGluRA
dfmr1 50M
dfmr1 3
dfmr1 50M ; dmGluRA
dfmr1 3 ; dmGluRA

DmGluRA and dFMRP genetically interact in regulating NMJ structure

Treating *dfmr1* null flies with the mammalian group I mGluR antagonist MPEP rescues gross brain anatomical defects (McBride et al. 2005), suggesting that dFMRP and DmGluRA may be involved in the same mechanisms regulating neuronal structure. The *Drosophila* glutamatergic NMJ is an ideal system to test this hypothesis, since previous work has shown that both *dfmr1* and *dmGluRA* single mutants display significant NMJ structure defects (Zhang et al., 2001; Bogdanik et al., 2004). The availability of the *dfmr1; dmGluRA* double mutant combinations produced here provides the opportunity for the most rigorous genetic test of the relationship between dFMRP and DmGluRA in this synaptic architectural patterning. NMJ structure was examined in *dfmr1* and *dmGluRA* single null mutants, *dfmr1; dmGluRA* double mutants, and MPEP treated *dfmr1* null mutants and controls. The muscle 4 NMJ in abdominal segment A3 was used in all studies, with NMJs co-labeled for the presynaptic marker HRP (Figure 4.3, red) and the postsynaptic marker DLG (Figure 4.3, green). NMJ synaptic structure was quantified by measuring synaptic branch number, synaptic terminal area and synaptic bouton number (Figure 4.4).

For synaptic branch number, *dfmr1* single mutants display a very highly significant overbranching phenotype, while *dmGluRA* single mutants display branching comparable with the genetic control (WT=2.89±0.11, N=15; *dfmr1*=6.32±0.33, N=15, P<0.0001; *dmGluRA*=3.4±0.35, N=11, P=0.15; Figure

4.3A-C, 4.4A). The *dfmr1; dmGluRA* double mutants display a tendency towards the normal level of synaptic branching with a significant rescue of the *dfmr1* mutant defect (*dfmr1; dmGluRA*=5.5±0.38, N=11; P=0.039 to *dfmr1*; Figure 4.3F, 4.4A). Consistently, treating *dfmr1* null mutants with the mGluR antagonist MPEP, which blocks mGluR signaling, also effectively rescues the *dfmr1* overbranching phenotype with no difference remaining with the control (MPEP-treated WT=3.5±0.3, N=11; MPEP-treated *dfmr1*=3.63±0.29, N=11, P=0.62 to treated WT; Figure 4.3D-E, 4.4A). Thus, blocking DmGluRA signaling significantly rescues the synaptic overbranching phenotype of *dfmr1* mutants.

For synaptic terminal area, *dfmr1* single mutants display a very significant increase in total area, while *dmGluRA* mutants display a slight, marginally significant decrease in synaptic area compared to the genetic control (WT=458.52±12.96μm^2, N=15; *dfmr1*=597.45±29.61μm^2, N=15, P=0.0007; *dmGluRA*=426.61±10.89μm^2, N=11, P=0.078; Figure 4.3A-C, 4.4B). The *dfmr1; dmGluRA* double mutants do not show any rescue of the increased synaptic area characteristic of *dfmr1* alone, which therefore remains highly elevated compared to control (*dfmr1; dmGluRA*=622.88±15.77μm^2, N=11; P=0.46 to *dfmr1*; Figure 4.3F, 4.4B). The *dfmr1* null mutants treated with the mGluR antagonist MPEP do display significantly decreased synaptic area compared to non-treated mutants (MPEP-treated *dfmr1*=499.95±24.88μm^2, N=11, P=0.0048 to non-treated *dfmr1*). However, MPEP-treated control animals display a similar decrease compared to

Figure 4.3. DmGluRA and dFMRP genetically interact in regulating NMJ structure.

Wandering 3rd instar NMJs were probed using anti-HRP (red) and anti-DLG (green) antibodies, to reveal pre- and postsynaptic domains respectively. Representative images of the NMJ on muscle 4 in abdominal segment A3 are shown.

A. The wildtype (WT) 2b genetic background control.

B. Null *dfmr1* mutant allele $dfmr1^{50M}$ in the 2b genetic background.

C. Null *dmGluRA* mutant allele $dmGluRA^{112b}$ in the 2b genetic background.

D. WT animal fed 68 μM MPEP. E. Null *dfmr1* mutant fed 68 μM MPEP. F. Double mutant $dfmr1^{50M}$; $dmGluRA^{112b}$ in the 2b genetic background. Null *dfmr1* mutants display increased NMJ synaptic branch number, terminal area and synaptic bouton number. MPEP-treatment and *dfmr1; dmGluRA* double mutant rescue the increased branch number, but not the other two defects. The scale bar is 10μm.

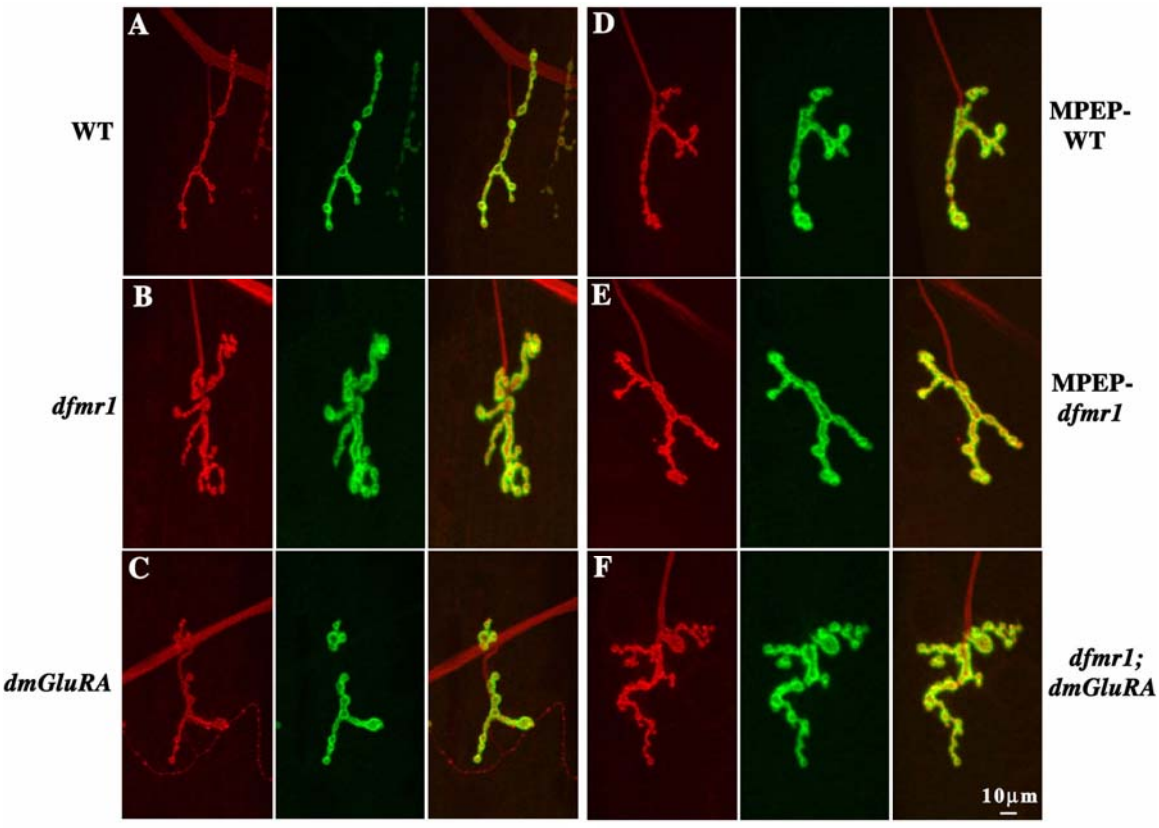
A
D
WT
MPEP-
WT
B
E
dfmr1
MPEP-
dfmr1
C
F
dmGluRA
dfmr1;
dmGluRA
10μm

non-treated control, and therefore the difference between the MPEP-treated wildtype control and the MPEP-treated *dfmr1* null mutant is still extremely significant (MPEP-treated WT=330.53±21.81μm^2, N=11, P<0.0001; Figure 4.3D-E, 4.4B). Therefore, blocking DmGluRA signaling does not significantly rescue the increased synaptic terminal area characteristic of *dfmr1* mutants.

For synaptic bouton number, *dfmr1* single mutants display a very highly significant increase, whereas *dmGluRA* mutants display a small, opposing decrease in bouton number compared to control animals (WT=29.7±1.48, N=15; *dfmr1*=36.5±1.5, N=15, P=0.001; *dmGluRA*=24.94±1.17, N=11, P=0.02 to WT; Figure 4.3A-C, 4.4C). Surprisingly, the *dfmr1; dmGluRA* double mutants do not show the additive effects of the opposite phenotypes of the two single mutants, but rather display an even more severe, synergistic increase in synaptic bouton number compared to the *dfmr1* single mutants (*dfmr1; dmGluRA*=42.3±2.09, N=11; P=0.037 to *dfmr1*; Figure 4.3F, 4.4C). Consistently, treating *dfmr1* null mutants with the mGluR antagonist MPEP also does not rescue the increased bouton defect of the *dfmr1* mutant. Indeed, the difference between MPEP-treated control and MPEP-treated *dfmr1* is more significant than the comparison of non-treated control and non-treated *dfmr1* (MPEP-treated WT=28.27±2.14, N=11; MPEP-treated *dfmr1*=39.27±1.51, N=11, P=0.0004, Figure 4.3D-E, 4.4C). Thus, either genetic or pharmacological block of DmGluRA signaling further exaggerates the synaptic bouton over-proliferation caused by loss of dFMRP.

Figure 4.4. Quantification of NMJ structure in single and double mutants.

A. Quantification of NMJ synaptic arbor branch number for all genotypes. Null *dfmr1* mutants display a highly significant increase of branch number, which can be rescued by blocking DmGluRA signaling genetically (double mutant) and pharmacologically (MPEP).

B. Quantification of terminal synaptic area for all genotypes. Null *dfmr1* mutants display a very significant increase of synaptic area, which is unaltered by blocking DmGluRA signaling in double mutant combination or with MPEP antagonist.

C. Quantification of total synaptic bouton number for all genotypes. Null *dfmr1* mutants display a very significant increase of bouton, whereas *dmGluRA* mutants display a significant decrease. Double mutants and MPEP-treated *dfmr1* mutants display synergistically increased bouton number. $0.001<P<0.05$(*); $0.0001<P<0.001$(**); $P<0.0001$(***).

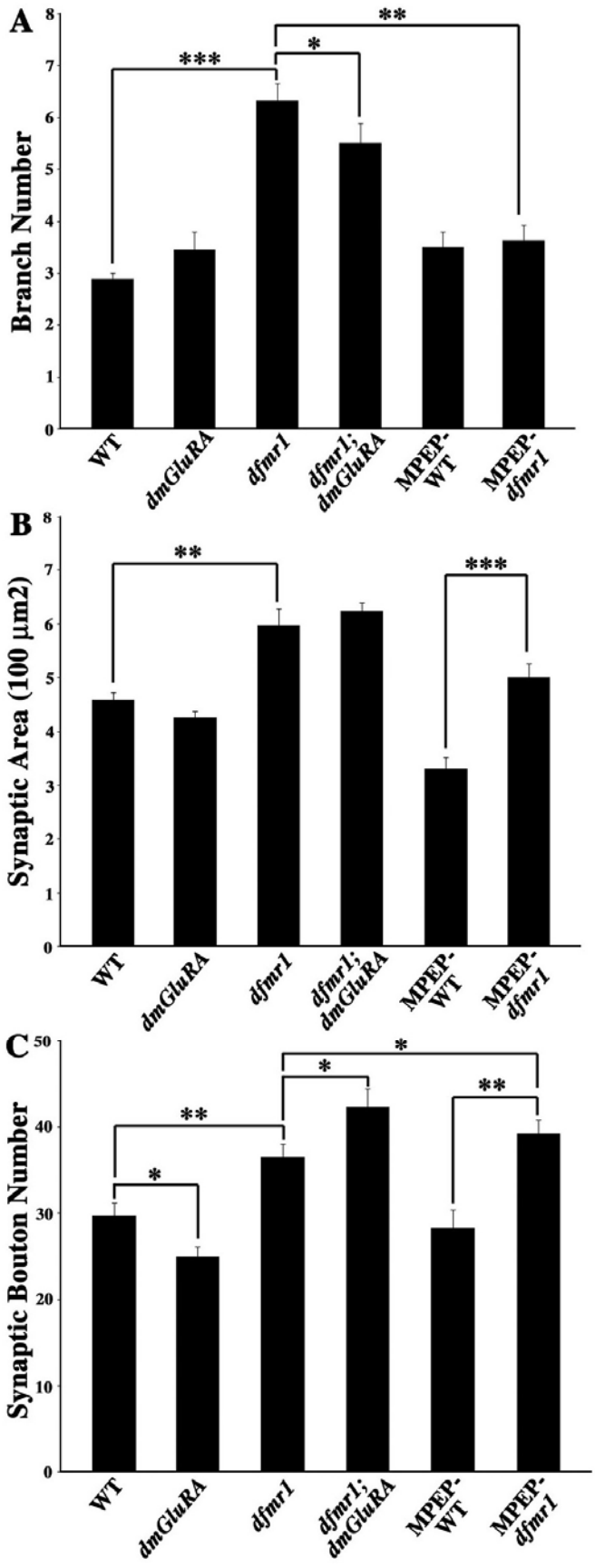
A
Branch Number
0
1
2
3
4
5
6
7
8
***
*
**
WT
dmGluRA
dfmr1
dfmr1; dmGluRA
MPEP-WT
MPEP-dfmr1
B
Synaptic Area (100 μm2)
0
1
2
3
4
5
6
7
8
**
***
WT
dmGluRA
dfmr1
dfmr1; dmGluRA
MPEP-WT
MPEP-dfmr1
C
Synaptic Bouton Number
0
10
20
30
40
50
*
**
*
**
*
WT
dmGluRA
dfmr1
dfmr1; dmGluRA
MPEP-WT
MPEP-dfmr1

Taken together, these results show a complex interaction between dFMRP and DmGluRA in regulating different aspects of presynaptic architecture. Whereas the synaptic over-branching caused by loss of dFMRP can be rescued by co-removal of DmGluRA or pharmacological block of mGluR signaling, the supernumerary boutons formed in the absence of dFMRP proliferate even more wildly when DmGluRA signaling is blocked. Thus, dFMRP and DmGluRA functions overlap in common mechanisms, but not in a simply interpretable manner.

DmGluRA and dFMRP genetically interact in regulating synaptic ultrastructure

Electron microscopy is the best means available to assay the complex assemblage occurring as a product of synaptic differentiation (Figure 4.5). The presynaptic NMJ bouton is characterized by multiple, large mitochondria, dense accumulations of ~40nm synaptic vesicles, an electron-dense active zone, and clustered vesicles around and docked adjacent to the T-bar presynaptic fusion sites. This bouton is deeply embedded in muscle and surrounded by the maze-like subsynaptic reticulum (SSR), which demarcates the postsynaptic domain (Figure 4.5A). A detailed ultrastructural examination includes multiple parameters such as presynaptic bouton area and appearance, postsynaptic SSR area and appearance, mitochondria area and appearance, size and structure of the active zone and quantification of the different presynaptic vesicle pools

(Figure 4.5). At the ultrastructural level, the overall appearance of bouton and the postsynaptic SSR morphology appears normal in both *dfmr1* and *dmGluRA* single null mutants. Quantitatively, there is no significant difference in bouton size, mitochondria size, active zone size/number or the postsynaptic SSR parameters between control and mutants (Figure 4.5A and data not shown). However, there is a clear change in presynaptic vesicle density in the *dfmr1* mutant, which we therefore carefully assayed in single and double mutant combinations.

Null *dfmr1* mutants display significant increases of synaptic vesicle density throughout the synaptic bouton, clustered vesicle number surrounding active zones and docked vesicle number at the T-bar membrane (Figure 4.5A, B). For synaptic vesicle density, single *dfmr1* null mutant display a highly significant ~30% increase in overall vesicles, whereas *dmGluRA* mutants show vesicle density comparable to the genetic control (WT=56.36$\pm$5.6 vesicles/μm^2, N=61; *dfmr1*=87.89$\pm$5.6 vesicles/μm^2, N=40, P=0.0002; *dmGluRA*=59.94$\pm$4.4 vesicles/μm^2, N=51, P=0.62; Figure 4.5A, C). The *dfmr1; dmGluRA* double mutants show a very significant rescue of this elevated vesicle density phenotype (*dfmr1; dmGluRA*=64.22$\pm$2.8 vesicles/μm^2, N=75, P=0.001 to *dfmr1*, P=0.14 to WT, Figure 4.5A, C). Therefore, removing DmGluRA signaling can rescue the abnormal presynaptic vesicle accumulation characteristic of *dfmr1* null synapses.

The synaptic vesicles clustered around the active zone form a local pool that can quickly replenish vesicles used during transmission (Figure 4.5B). These

vesicles are quantified by drawing a circle of 250nm around the electron dense T-bar and counting the number of synaptic vesicles within this radius. Null *dfmr1* mutants display a highly significant ~50% increase in the pool of clustered vesicles, whereas *dmGluRA* mutants make vesicle pools comparable to control (WT=13.1±0.8; *dfmr1*=18.8±0.7, P=0.0001; *dmGluRA*=14.6±0.8, P=0.22; Figure 4.5B, D). The *dfmr1; dmGluRA* double mutants display a significant reduction in the clustered vesicle pool compared to the *dfmr1* single mutant, and thus very significantly rescue the *dfmr1* mutant phenotype (*dfmr1; dmGluRA*=16.3±0.4, P=0.005 to *dfmr1*; Figure 4.5B,D). Therefore, removing DmGluRA signaling can also effectively rescue the increased clustered synaptic vesicle pool of the *dfmr1* null mutant.

To provide for the rapidity of synaptic transmission, a subset of synaptic vesicles are maintained docked at active zones, where they form a pool that is immediately releasable upon arrival of an action potential. Electron microscopy reveals a population of synaptic vesicles morphologically adjacent to the presynaptic electron-dense membrane, which are considered to be these docked vesicles (Figure 4.5B, arrows; Couteaux and Pecot-Dechavassine, 1970). Null *dfmr1* mutants display a highly significant ~85% increase in the number of docked vesicles at the active zone, whereas *dmGluRA* mutants appear totally normal (WT=1.5±0.12; *dfmr1*=2.8±0.18, P=0.0001; *dmGluRA*= 1.5±0.14, P=0.92, Figure 4.5B, E). In contrast to the above two vesicle pools, removing DmGluRA signaling

Figure 4.5. DmGluRA and dFMRP genetically interact in presynaptic ultrastructure.

A. Representative TEM images of NMJ boutons in 2B genetic background control (WT), *dfmr1* and *dmGluRA* single null mutants, and the *dfmr1; dmGluRA* double mutant. The *dfmr1* mutant has a slightly larger bouton size but comparable synaptic morphology and postsynaptic SSR. Normal active zones (AZ) are visible in all panels as electron-dense synaptic membranes and T-bars. Null *dfmr1* mutants display a striking increase of synaptic vesicles throughout the terminal. The scale bar is 500nm.

B. High magnification images of individual synaptic active zones. In control animals (far left) the clustered area (250nm radius from T-bar center) has ~13 vesicles localized around the T-bar and ~2 docked vesicles (white arrow) contacting the presynaptic membrane adjacent to the T-bar. In *dfmr1* mutants (second from left) there is an increased number of clustered vesicles and docked vesicles (arrows). The *dmGluRA* null mutants (second from right) display no detectable differences from control. In double mutants (far right), synaptic vesicle density and clustered synaptic vesicle number are comparable to control, but the docked synaptic vesicle number is still increased. The scale bar is 100nm.

C-E) Quantitative analysis of ultrastructural phenotypes, including synaptic vesicle density (C), clustered synaptic vesicles (D; <250nm from active zone) and docked synaptic vesicles (E; <20nm from active zone). Significance indicated as $0.001<P<0.05$(*); $0.0001<P<0.001$(**); $P<0.0001$(***).

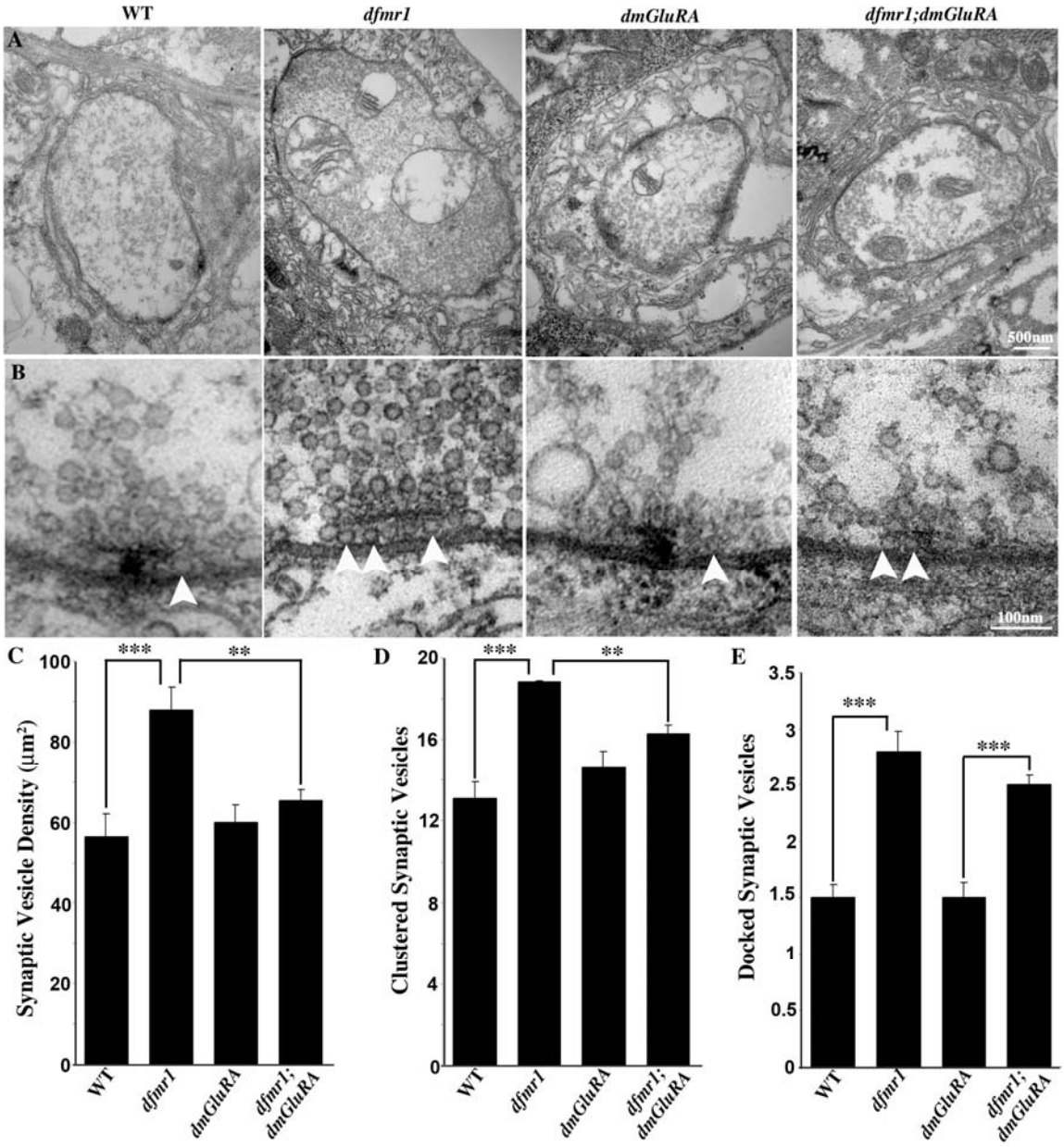
WT
dfmr1
dmGluRA
dfmr1;dmGluRA
A
500nm
B
100nm
C
Synaptic Vesicle Density (μm²)
***
**
D
Clustered Synaptic Vesicles
E
Docked Synaptic Vesicles

does not detectably rescue the increased docked vesicle number characteristic of the *dfmr1* null mutants. The *dfmr1; dmGluRA* double mutants, the elevation in docked vesicle number is indistinguishable from the *dfmr1* single mutant alone (*dfmr1; dmGluRA*=2.5±0.09; P=0.19 to *dfmr1*, P=0.0001 to WT, Figure 4.5B, E). Thus, removing DmGluRA signaling does not rescue the increased docked vesicle pool characteristic of *dfmr1* mutants.

Taken together, these data also suggest that there is a complex interaction between dFMRP and DmGluRA signaling in regulating presynaptic differentiation. Loss of dFMRP results in large increases of presynaptic vesicle pools. Removing DmGluRA function alone has no effect on these vesicle pools, however removing DmGluRA in the double mutant condition can effectively rescue the enhanced overall vesicle density and increased clustered vesicle pools of the *dfmr1* null mutant. In contrast, the number of docked vesicles remains elevated. These results suggest partially overlapping mechanisms between dFMRP and DmGluRA in the regulation of presynaptic differentiation at the peripheral NMJ.

DmGluRA and dFMRP interact in regulating central neuron structure

The Mushroom Body (MB) is a learning and memory center in the *Drosophila* brain (Heisenberg 1998; Heisenberg 2003). Our previous work has shown that *dfmr1* null mutant MB neurons display increased overall architectural complexity, including axonal overgrowth and overbranching (Pan et al. 2004). The

Mosaic Analysis of Repressible Cell Marker (MARCM) clonal technique provides a uniquely powerful means to examine homozygous mutant neurons *in situ* at a single cell level of resolution and therefore to study the cell autonomous functions for the mutant gene (Lee and Luo 1999). To test the mechanistic relationship between dFMRP and DmGluRA in central nervous system, we asked whether blocking DmGluRA signaling can rescue the architectural defects in single cell MARCM clones of *dfmr1* null MB neurons. The *dfmr1* gene is located on the third chromosome, while the *dmGluRA* gene is on fourth chromosome. It is technically not possible to do MARCM analysis for double mutants. However, our NMJ work shows that MPEP mGluR antagonist treatment totally mimics the effects of removing DmGluRA expression in all cases studied. Therefore, we used MPEP to treat MARCM clonal animals to assay the effect of blocking DmGluRA signaling on *dfmr1* null MB neurons.

In MARCM clone brains, the MB axon lobes were visualized with an antibody against Fasciclin II (FasII, red), and the single-cell γ neuron MARCM clones identified by GFP (green) expression (Figure 4.6A). The MB γ neuron contains a single primary axon projection in control animals (Figure 4.6A; left, box) (Lee et al. 1999). The branching features of the γ neuron axon projection can be quantified both by branch number and total branch length. Null *dfmr1* mutant MB neurons display obvious axon overgrowth; both the axon branch number (WT=6.2$\pm$0.5, N=10; *dfmr1*=10$\pm$0.7, N=12; P=0.0008) and the total axon branch

Figure 4.6. Blocking mGluR signaling rescues *dfmr1* null neuron defects in brain.

A. Representative image of single cell MARCM clone of a Mushroom Body γ neuron. The Mushroom Body axon lobes are labeled with an antibody against Fasciclin II (FasII, red). The single γ neuron is visualized by MARCM technique-induced GFP expression (green). The boxed area indicates the axonal projection shown in the B panels.

B. Representative images of axons in a non-treated WT cell, a non-treated *dfmr1* null mutant cell, a MPEP-treated WT cell and a MPEP-treated *dfmr1* null cell. The non-treated *dfmr1* null γ neuron axon displays significant over-growth and over-branching, which is effectively rescued by MPEP treatment.

C-D. Quantification of axon branch number (C) and total axon branch length (D) in both genotypes, with or without MPEP treatment. Compared to the significant increase of both axonal branch number and cumulative axon length in non-treated *dfmr1* null, MPEP-treated *dfmr1* mutant neurons display significant rescue of over-growth phenotypes. $0.001<P<0.05$(*); $0.0001<P<0.001$(**).

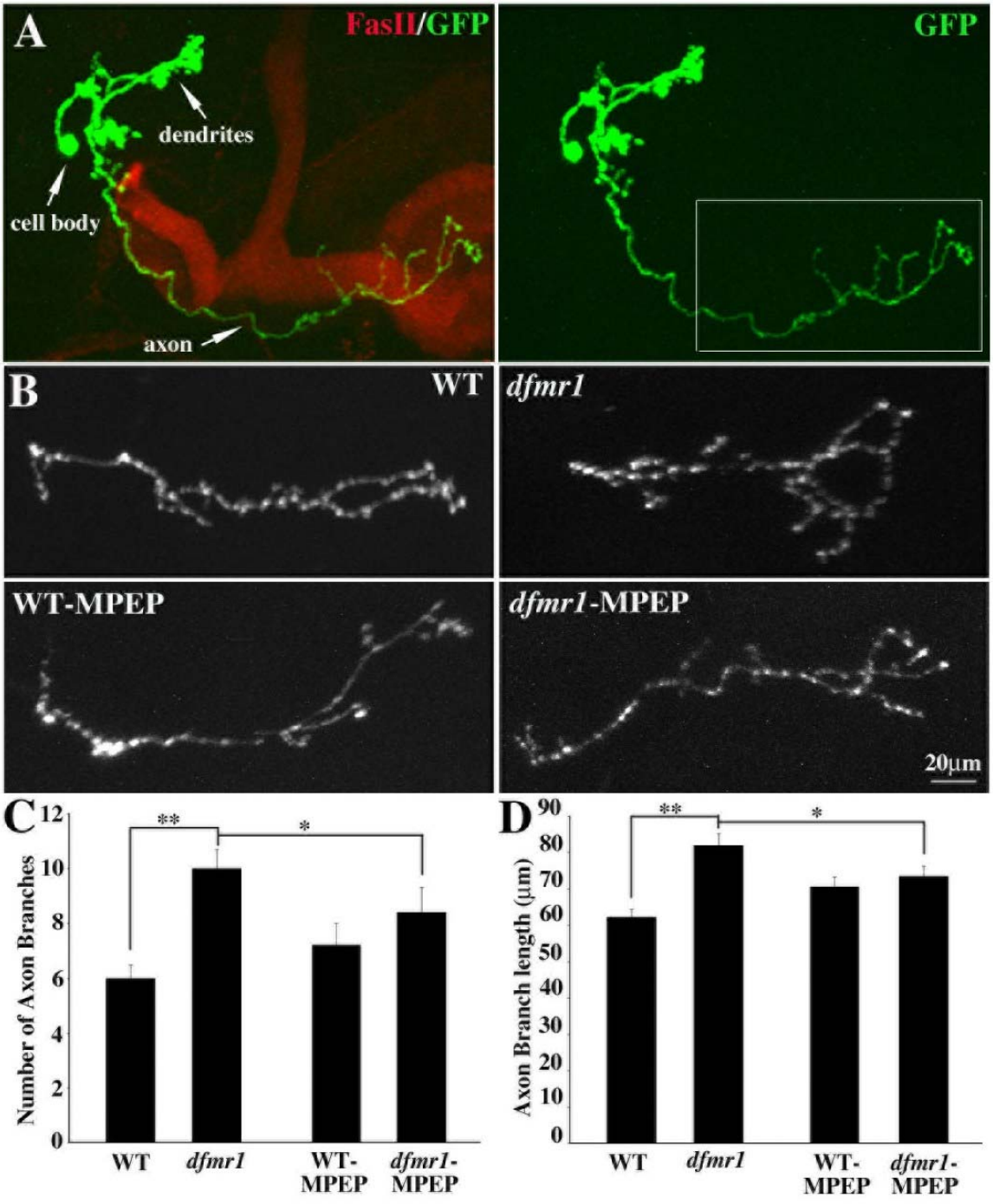
A
FasII/GFP
dendrites
cell body
axon
GFP
B
WT
dfmr1
WT-MPEP
dfmr1-MPEP
20μm
C
Number of Axon Branches
0
2
4
6
8
10
12
**
*
WT
dfmr1
WT-MPEP
dfmr1-MPEP
D
Axon Branch length (μm)
0
10
20
30
40
50
60
70
80
90
**
*
WT
dfmr1
WT-MPEP
dfmr1-MPEP

length (WT=62.2±2.3 μm; *dfmr1*=82±3.2 μm; P=0.0006) are very significantly increased in *dfmr1* null neurons (Figure 4.6B-D). Treating MARCM clone animals with the mGluR antagonist MPEP can effectively rescue the axon overgrowth defects of *dfmr1* null mutant neurons. Blocking mGluR signaling with MPEP produces a significant rescue of the increased axon branching defect in *dfmr1* null neurons (MPEP-*dfmr1*=8.4±0.9, N=8, P=0.05 to non-treated *dfmr1*=10±0.7). Similarly, the axon overgrowth defect is countered by MPEP treatment (MPEP-*dfmr1*=73.4±2.9 μm, P=0.06 to non-treated *dfmr1*=82±3.2 μm). Thus, MPEP-treated *dfmr1* mutant neurons resemble control neurons compared to non-treated *dfmr1* mutants, although the rescue provided by MPEP treatment is partial. Therefore, blocking mGluR signaling by MPEP can rescue the central neuron presynaptic over-elaboration defect of *dfmr1* null mutants.

Discussion

Drosophila is a powerful system to test the mGluR theory of Fragile X Syndrome. There is one *Drosophila* homolog of the 3-member mammalian FMRP gene family (dFMRP) (Wan et al. 2000; Zhang et al. 2001) and one *Drosophila* homolog of the 8-member mammalian mGluR family (DmGluRA) (Parmentier et al. 1996; Bogdanik et al. 2004). Therefore, the double mutant combination of the two *Drosophila* null alleles provides a unique opportunity to test the relationship between all FMRP family function and all mGluR signaling throughout the

nervous system. Of course this is a two-edged argument; *Drosophila* does not provide the means to test family member specific functions within or between these gene families, and so this sophistication of the mammalian system cannot be addressed. Nevertheless, *Drosophila* provides an excellent opportunity to comprehensively test interactions between mGluR signaling and FMRP functions in the *in vivo* context of the whole nervous system.

The mGluR theory of FXS proposes that FMRP functions downstream of mGluR signaling to regulate the synthesis of proteins critical for synaptic structural modeling and functional synaptic plasticity (Bear et al., 2004; Bagni and Greenough, 2005; Grossman et al., 2006; Pfeiffer and Huber, 2006). FMRP is a negative regulator of translation, and most known FMRP targets are constitutively upregulated in the absence of FMRP (Brown et al., 2001; Laggerbauer et al., 2001; Sung et al., 2003; Bagni and Greenough, 2005). One FMRP target is its own message, providing an interesting negative feedback loop on FMRP expression (Ashley et al., 1993; Sung et al., 2000; Schaeffer et al., 2001). In this work, we find that dFMRP and DmGluRA also mutually negatively regulate each other's expression levels (Figure 4.1). The protein level of dFMRP is increased in the *dmGluRA* null mutant, and the DmGluRA level is increased in the *dfmr1* null mutant, providing bidirectional negative feedback regulation between the two proteins. Although these two proteins are co-expressed in the same neurons, consistent with their mutual co-regulation, they occupy quite distinct subcellular

domains (Figure 4.1); dFMRP is highly enriched in the soma cytoplasm and is largely undetectable at synapses, whereas DmGluRA is highly enriched in the synaptic plasma membrane and is largely undetectable in the soma. This protein distribution suggests that the effect of mGluR signaling on dFMRP expression must be somewhat indirect, involving a long-distance second messenger mechanism. The increase in dFMRP level in the absence of mGluR signaling is somewhat surprising in light of mammalian studies showing that increased synaptic activity increases FMRP expression and, more specifically, that mGluR activation increases FMRP expression (Weiler et al., 1997; Todd et al., 2003). The current study suggests instead that the overall role of mGluR signaling is to strongly suppress FMRP expression in the nervous system, at least in *Drosophila*. The increase in the DmGluRA in the absence of dFMRP indicates that the receptor is negatively regulated by dFMRP function. Some studies have suggested that mGluR transcripts may be direct targets for FMRP binding and, presumably, negative translation regulation. Such a mechanism would be consistent with the findings of this study. However, such direct regulation is not required, as there is obviously numerous possibilities of indirect regulation. In any case, the existence of this mutual negative feedback loop shows that mGluR signaling and FMRP function clearly interact to mutually repress each other in the *Drosophila* nervous system, providing molecular support for the theory of their functional interaction.

Both Group I and Group II/III mGluRs have been shown to play roles in the generation of locomotor activity and regulation of movement behavior (Vezina and Kim, 1999; Cauli et al., 2005; Nistri et al., 2006). In *Drosophila*, mGluR signaling is similarly required for effective performance in coordinated movement behavior (Figure 4.2). Null *dmGluRA* mutants display a grossly slowed response time in a relatively simple movement behavior, as revealed by the roll-over assay, indicating sluggish integration of sensory input and sequential motor output. Obviously, there are many possible causes of such a behavioral defect. In contrast, *dfmr1* null mutants perform this task as well as wildtype. This is somewhat surprising given that *dfmr1* mutants are more obvious impaired than *dmGluRA* mutants in many published cellular assays of synaptic structuring and function (Zhang et al., 2001; Bogdanik et al., 2004; Xu et al., 2004). The most important finding here, however, is that the *dmGluRA* defect can be rescued entirely simply by removing dFMRP in double null mutants (Figure 4.2). This is a rather remarkable finding as it shows that the behavioral impairment caused by the absence of mGluR signaling can be entirely compensated for by the co-absence of FMRP function. Although the nature of the dysfunction is unknown, this interaction shows that FMRP must act to enable a mechanism that is over active in the absence of mGluR signaling; a mechanism important for facilitating coordinated movement behavior. These results provide *in vivo* genetic evidence for a functional connection between dFMRP and DmGluRA in the sensory and

motor response loop.

One obvious place for dFMRP-DmGluRA pathway regulation is the NMJ synapse. Both *dfmr1* and *dmGluRA* single null mutants display striking defects in NMJ synaptic properties (Zhang et al. 2001; Bogdanik et al. 2004). Null *dfmr1* mutants display elevated synaptic branch number, increased synaptic terminal area and supernumerary synaptic boutons (Figures 4.3 and 4.4). Blocking mGluR signaling by genetically removing DmGluRA or treating animals with the mGluR antagonist MPEP rescues the branch number defects, but has no significant effect on synaptic area defect. Moreover, although the *dmGluRA* single null mutant displays the opposing phenotype of decreased synaptic bouton number, both double null mutants and MPEP-treated *dfmr1* animals actually display a more severe increase in synaptic bouton number. This complex interaction clearly supports a relationship between dFMRP function and DmGluRA signaling in the regulation of presynaptic architecture, but suggests that this relationship is not a simple direct upstream-downstream signaling cascade. Rather, dFMRP function is likely controlled by several converging intercellular signaling pathways, of which DmGluRA-mediated glutamatergic synaptic signaling is only one. Some of the synaptic structuring mechanisms may involve overlapping dFMRP and DmGluRA functions, while others likely involve quite independent pathways that can converge at multiple levels.

A similar conclusion derives from our ultrastructural studies of presynaptic

differentiation. dFMRP clearly plays critical roles in the regulation of synaptic vesicle pools; *dfmr1* null mutants display elevated overall synaptic vesicle density, an increased pool of clustered vesicles at active sites and an elevated number of docked vesicles at the presynaptic membrane (Figure 4.5). These defects provide a mechanistic explanation for the elevated presynaptic glutamate release that we previously characterized at this synapse (Zhang et al. 2001). In addition, many presynaptic protein transcripts have been identified as putative direct targets of FMRP binding, including MUNC-13, NAP-22, SEC-7 and RAB-5 (Brown et al. 2001; Miyashiro et al. 2003). Several of these encoded proteins are known to play important roles in vesicle cycling and trafficking, consistent with the presynaptic vesicle defects reported here in *dfmr1* mutants. In contrast, DmGluRA plays no detectable function in the modulation of any of these vesicle pools (Figure 4.5). In mammalian system, although Group II/III mGluR signaling has been implicated in vesicular endocytosis and exocytosis cycling in the presynaptic terminal, there is similarly no evidence that loss of mGluR signaling results in defects in presynaptic vesicle pools (Hay et al., 2001; Pamidimukkala and Hay, 2001; Zakharenko et al., 2002). The most important finding here, however, is that the *dfmr1* defects can be rescued simply by blocking DmGluRA signaling in double null mutants (Figure 4.5). Removing DmGluRA function significantly rescues the defects in both the total synaptic vesicle pool and clustered vesicle pool. These findings reinforce the conclusion that dFMRP and DmGluRA functions must intersect in the regulation

of presynaptic properties, in both structuring and functional manifestations.

Fragile X Syndrome is a mental retardation disorder, and therefore it is obviously critical to move into the brain and assay similar functions in neuronal circuits relevant to learning and memory. In *Drosophila*, the relevant brain region is the Mushroom Body, a well-characterized center of learning and memory consolidation (Heisenberg 1998; Heisenberg 2003). We have shown previously that all classes of MB neurons display a cell-autonomous requirement of dFMRP in mediating correct axonal patterning (Pan et al., 2004). In the absence of dFMRP, these learning circuit neurons display improper axonal growth and branching, and strong defects in presynaptic connectivity (Figure 4.6). Similarly, mammalian FMRP is localized in the axon process and growth cone in mouse hippocampal neurons (Antar, Afroz et al. 2004; Antar, Li et al. 2006) and loss of FMRP results in excess axonal filopodia and altered motility of the axonal growth cone (Antar et al., 2006). Moreover, recent studies in mouse brain hippocampal slices mosaic for FMRP expression have revealed that presynaptic axons lacking FMRP form fewer functional presynaptic terminals than control axons (Hanson and Madison, 2007). Thus, mammalian FMRP and dFMRP clearly play conserved roles is establishing correct presynaptic connectivity in the brain.

We do not have similar knowledge of the roles of DmGluRA signaling in the brain. Technical limitations with the MARCM clonal technique mean that comparable studies are not possible for *dmGluRA* null MB neurons, so we do not

know whether there are *dmGluRA* single mutant defects in related presynaptic mechanisms. Moreover, the MARCM technique does not allow us to pursue the same powerful double mutant analyses we performed at the NMJ. Therefore, we are limited to blocking DmGluRA signaling by treating MARCM clonal animals with the mGluR antagonist MPEP, in order to pharmacologically block mGluR signaling. The most important finding here, however, is that the *dfmr1* defects can be rescued simply by blocking mGluR signaling (Figure 4.6). MPEP treatment significantly rescues both the increased axon branching and presynaptic axon overgrowth that would otherwise occur in *dfmr1* null mutant neurons. This single cell level finding is consistent with a previous report that treating *dfmr1* null animals with MPEP rescues the gross anatomical defect of MB axonal lobe fusion (McBride et al. 2005). This MPEP-treatment rescue shows that an overlapping mechanism exists between mGluR signaling and FMRP function in regulating neuronal circuit architecture in central nervous system. Thus, the results in both the peripheral and central presynaptic processes consistently support a mechanistic interaction between mGluR and FMRP in controlling presynaptic structure and differentiation.

Acknowledgements

We are most grateful to the Fragile X Foundation for the generous gift of MPEP. We thank the Iowa Developmental Studies Hybridoma Bank for providing

critical antibodies, and the Bloomington *Drosophila* Stock Center for providing essential stocks. This work was supported by NIH grant GM54544 to K.B.

Experimental Procedures

Drosophila Genetics

All *Drosophila* stocks were maintained at 25°C on standard food under standard conditions. The P-element imprecise excision $dmGluRA^{112b}$ null mutant was used as the *dmGluRA* single mutant, and $dmGluRA^{2b}$ (hereafter called 2b), a p-element precise excision line from the same screen, was used as its genetic background control (Bogdanik, Mohrmann et al. 2004). The w^{1118}; $dfmr1^{50M}$ and w^{1118}; $dfmr1^{3}$ null mutant strains were used as two independent *dfmr1* single mutants, with w^{1118} as the genetic background control (Zhang, Bailey et al. 2001; Dockendorff, Su et al. 2002). For all assays involving *dmGluRA* and *dfmr1* mutants, both *dfmr1* alleles were back-crossed into the 2b genetic background, to generate a common background for all single and double mutants. Several multiply mutant strains were generated for this study: 1) the $dfmr1^{50M}$; $dmGluRA^{112b}$ and $dfmr1^{3}$; $dmGluRA^{112b}$ double null mutants, and 2) the $dfmr1^{50M}$; 2b and $dfmr1^{3}$; 2b genetic background control combinations. For drug treatment studies, MPEP, a generous gift from Fragile X Foundation, wass dissolved in ddH_2O, and added to standard fly food to final concentration 86μM as previously

reported (McBride et al. 2005).

Immunocytochemistry

Wandering 3rd instar larvae were dissected in standard saline, followed by 4% paraformaldehyde fixation for 30 mins (for staining dFMRP, HRP and DLG) or Bouin's Fixative for 30 mins (for staining DmGluRA). The monoclonal mouse antibody against dFMRP (6A15; Sigma) was used at 1:1000. The monoclonal mouse antibody against DLG (4F3; used at 1:500) was obtained from the Developmental Studies Hybridoma Bank (University of Iowa). The Texas Red-conjugated anti-Horseradish Peroxidase (HRP; used at 1:200) was from Jackson. All primary antibodies were visualized using fluorescent dye-conjugated secondary antibodies, including Alexa Fluor 488 goat anti-mouse IgG (1:200; Molecular Probes) and cy3-conjugated goat anti-mouse IgG (1:200; Jackson). All fluorescent images were collected using a Zeiss LSM 510 meta laser scanning confocal microscope and Zeiss image-collection software. All image processing was done with Adobe Photoshop 7.0.

Immuno-Electron Microscopy

Wandering 3rd instar larvae were processed by adapting published methods (McDonald, 1999; Edelmann, 2002; Spehner et al., 2002). Dissected larvae were fixed for 1 hr in 4% paraformaldehyde plus 0.5% glutaraldehyde, rinsed in PBS for

6 mins, and passed through an ethanol series (50%, 70%, 100%; 20 mins each). 1:1 propylene oxide: araldite was used as a transition media to 100% araldite. Tissue was placed in a flat embedding mold and cured overnight in a 60^{o}C oven. Gold thin sections were obtained from Leica UCT Ultracut microtome, using 200-mesh nickel grids on which to collect sections. Grids were blocked for 15 mins with 1% BSA in DPBS, and incubated overnight at 4^{o}C in either DmGluRA or dFMRP primary antibody. Grids were washed for 1 hr in DPBS with Tween-20, and for 15 mins in TRIS buffer with 0.05% Tween-20, blocked for 15 mins with 1% BSA in TRIS buffer, and incubated for 1 hr at room temperature in secondary antibody conjugated to 10 or 25nm gold particles (1/50 dilution). Grids were washed for 15 mins in TRIS buffer + 0.05%, washed again for 15 mins in dH_2O, and blotted dry. Sections were stained with uranyl acetate and lead citrate, and imaged as for TEM.

Behavior Assay

Animals were cultured at 25^{0}C in regular food to the wandering 3rd instar larval stage. All assays were done at room temperature (RT). Before every assay, larvae and test agar plates were placed at RT for 2 hrs to acclimatize. For the assay, an individual animal was placed on the agar plate, and allowed to move freely for 2 mins. Using a soft brush, the test animal was then rolled over to a completely inverted position, as defined by the ventral midline. The time that the

animal spent to totally right itself was recorded. Three assays were done for each animal, and then averaged to produce one data point. Statistical analysis was done using GraphPad InStat 3 software. Significance levels in figures were represented as $0.001<P<0.05$(*); $0.0001<P<0.001$(**); $P<0.0001$(***). All error bars represent Standard Error of Mean (SEM), appropriate for comparison of the mean of means distribution.

NMJ structure quantification

All images used in NMJ structure quantification were 3D-projections from complete Z-stacks through the entire NMJ. The lateral, longitudinal muscle 4 in abdominal segment A3 was used for all quantification. Data from the two-paired hemisegments were averaged for each animal, to produce each single data point. Synaptic boutons were defined according to HRP (presynaptic) and DLG (postsynaptic) staining. Branches originating directly from the nerve entry point were defined as primary braches, and each higher order branch was counted only when two or more boutons could be observed in a subsequent branch fork. For total synaptic area, LSM 5 Confocal Image Examiner software was used in the "histogram" display mode. Synaptic regions were user-defined with the closed free shape curve drawing tools, defined by the boundary of DLG staining. The software output reports the area for each region automatically. Statistical analysis was done using GraphPad InStat 3 software. Significance levels in figures were

represented as 0.001<P<0.05(*); 0.0001<P<0.001(**); P<0.0001(***). All error bars represent SEM, for comparison of the mean of means distribution.

Ultrastructural Analysis

Wandering 3rd instar larvae were dissected, fixed, sectioned and visualized in parallel using standard TEM techniques, as reported previously (Featherstone et al., 2001; Haas et al., 2007). Staged animals were dissected in 1XPBS and subsequently fixed with 2.0% glutaraldehyde in 0.05M PBS for 15 mins; replaced with fresh 2.0% glutaraldehyde for 1 hr. Preparations were washed three times in PBS, transferred to 1% OsO_4 in dH_2O for 2 hrs, and then washed three times in dH_2O. Preparations were stained *en bloc* in 1% aqueous uranyl acetate for 1 hr, washed three times in dH_2O, dehydrated in an EtoH series (30-100%), passed through propylene oxide, transferred to a 1:1 araldite: propylene oxide mixture, and embedded in araldite embedding media. Ultra-thin serial sections (50-60nm) were made on a Leica UCT Ultracut microtome and transferred to formvar-coated grids. Grids were examined and images collected on a Phillips CM10 TEM equipped with an AMT 2 mega pixel camera. NMJs were sectioned, and profiles for each synaptic bouton were quantified in sections containing only a single prominent electron-dense active zone (AZ) and T-bar structure. Synaptic vesicles in the “clustered” pool were defined as those within 250 nm of an AZ. Docked vesicle were defined as those <0.5 vesicles diameter (<20 nm) from the

electron-dense plasma membrane at the AZ. Measurements and quantifications were made using Image J 1.32j free software from NIH. Each profile was scored for bouton/mitochondria area, and the number of docked, clustered vesicles and total vesicle density (corrected for mitochondria area). Mean quantified parameters were statistically compared using the Mann-Whitney test, and presentation images were processed in Adobe Photoshop.

Mushroom Body MARCM analysis

The Mosaic Analysis of Repressible Cell Marker (MARCM) clonal technique was employed as first described in Lee and Luo (1999). Single neuron MARCM clones were made in the brain Mushroom Body, within the population of γ neurons. Staged embryos were collected within a 4 hrs window and cultured at 25^{o}C. Mature embryos at 20 hrs were heat-shocked at 37^{o}C for 1 hr to induce recombination and clone formation. Animals were then cultured to maturity at 25^{o}C. Adult brains were dissected out within 1 day following eclosion. Brains were dissected in 1XPBS, fixed in 4% paraformaldehyde for 30 mins and processed with immuno-staining. MB axon lobe was labeled by mouse anti-*Drosophila* Fasciclin II 1D4 (1:20, Developmental Studies Hybridoma Bank, University of Iowa), and the MARCM clone was labeled by rat anti-mouse CD8 (1:100, Caltag). Primary antibodies were visualized using Cy3-conjugated goat anti-mouse IgG (1:100, Jackson), and FITC-conjugated goat anti-rat IgG (1:100, Jackson). For

γ-neuron axonal quantification, the primary axon branch was identified first as the single projection joined γ-lobe, and all other axon processes extended from this main trunk were counted as branches. The length of each branch was measured based on 3D-projections from complete Z-stacks from confocal microscopy. All branch lengths of single axon branches were added together to obtain the total cumulative axon length. Statistical analysis was done using GraphPad InStat 3 software. Significance levels in figures were represented as $0.001<P<0.05$(*); $0.0001<P<0.001$(**); $P<0.0001$(***). All error bars represent SEM, for comparison of the mean of means distribution.

CHAPTER V

SUMMARY AND FUTURE DIRECTIONS

In this thesis, I described my work of using *Drosophila* model to study cellular and molecular mechanisms of Fragile X Syndrome.

First, using MARCM technique, I assayed single cell architecture of Mushroom Body neurons in the intact *Drosophila* brain. In *dfmr1* null mutant neurons, cell bodies extend supernumerary projections, and both dendrites and axon display overgrowth and overbranching compared to wild type. Consistently, over-expression of dFMRP in MB neurons results in simpler structure, including more clean cell bodies, undergrowth and underbranching in dendrites and axons. Ultrastructure analysis shows enlarged synaptic bouton size, and abnormal vesicle accumulation in *dfmr1* synaptic boutons, which indicate altered synaptogenesis and arrested synaptic function. These results are consistent with former reports about neuronal structure defects in peripheral nerve system in *dfmr1* mutants. Taking all central and peripheral data together, we can conclude *Drosophila* FMRP is a global negative regulator of neuronal architecture (Figure 5.1).

Second, using tissue staining with specific antibodies and fluorescence intensity quantification, I investigated the regulatory function of dFMRP on the

Figure 5.1 dFMRP is a global negative regulator of neuronal architecture

In motor neurons, *dfmr1* mutant NMJ synapses are overgrown and overbranched, while over-expression of dFMRP results in undergrowth and underbranching. In sensory neurons, *dfmr1* null dendrites display terminal-overelaborated, while over-expression causees opposite phenotypes. In central nervous system, *dfmr1* mutant cell bodies extend more excess projections, and both *dfmr1* null dendrites and axon display overgrowth and overbraching phenotypes, while over-expression dFMRP simplifies the neuronal architecture. This figure is cited from Zhang and Broadie, *Trends in Genetics*, 2005.

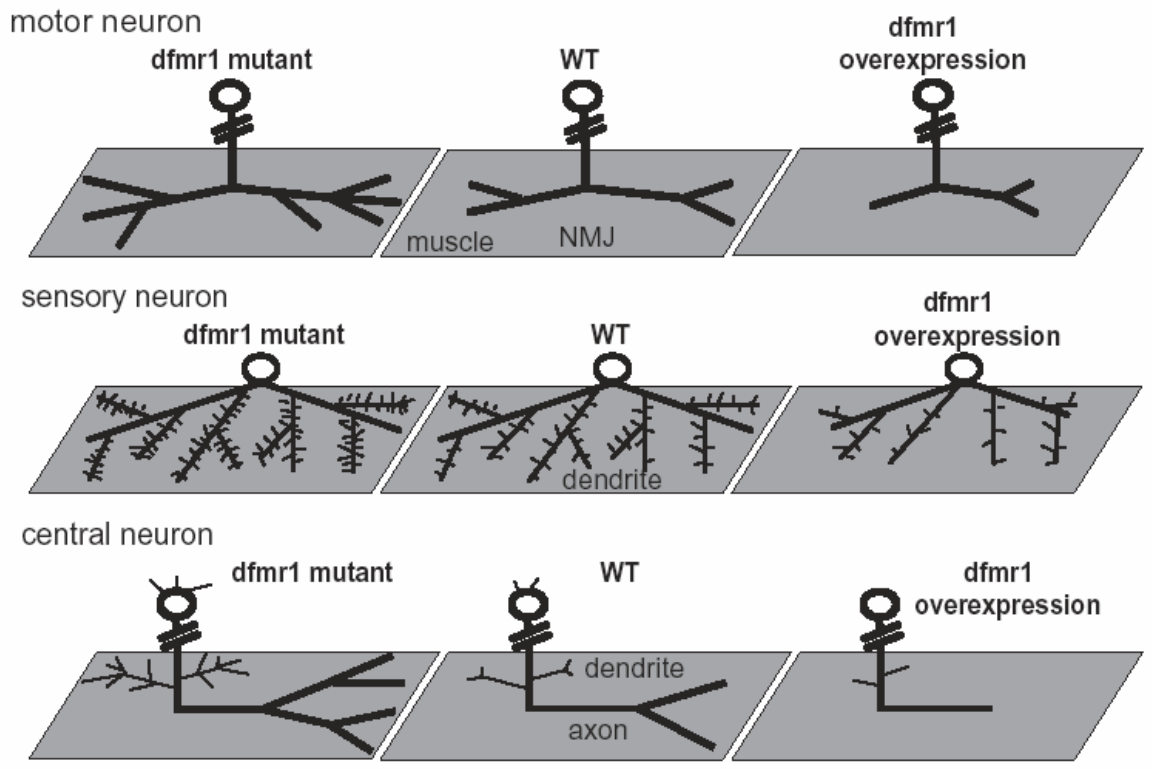
motor neuron
dfmr1 mutant
WT
dfmr1
overexpression
muscle
NMJ
sensory neuron
dfmr1 mutant
WT
dfmr1
overexpression
dendrite
central neuron
dfmr1 mutant
WT
dfmr1
overexpression
dendrite
axon

Ionotropic glutamate receptors (iGluR) at the *Drosophila* NMJ synapses, and the hypothesized relationship between dFMRP function and metabotropic glutamate receptor signaling. I found that dFMRP regulates two iGluR classes in opposite directions. The A-class receptor population is increased, while B-class is decreased in *dfmr1* mutants, consequently resulting in strong increase of A- to B-class receptor ratio. Over-expression dFMRP targeted to either pre- or post-synaptic terminals indicate that the regulatory function of dFMRP on iGluRs is postsynaptic. In contrast, DmGluRA negatively regulates both iGluR classes in common. Both A- and B- iGluR classes are increased in *dmGluRA* mutants. Over-expression assays indicate that DmGluRA functions in both pre- and post-synaptic terminals. Postsynaptic over-expression of DmGluRA displayed opposite changes of the iGluR population compared to *dfmr1* null, which suggested an overlap between dFMRP function and DmGluRA signaling in the postsynaptic compartment. Targeted rescue of dFMRP expression in the presynaptic neuron didn't rescue iGluR expression level changes, which further demonstrated that dFMRP acts in the postsynaptic terminals to regulate iGluR expression. Double mutants of *dfmr1* and *dmGluRA* always displayed an additive effect of the two single mutants, which suggests independent, convergent pathways between dFMRP and DmGluRA regulation. Taken together, both dFMRP and DmGluRA regulate synaptic expression level of ionotropic glutamate receptors at *Drosophila* NMJ. While dFMRP functions in a class-specific way and in postsynaptic

terminals, DmGluRA signal regulates total iGluR level and functions in both pre- and post- synaptic terminals. There is overlap between dFMRP function and DmGluRA signal at postsynaptic side, however independent pathways of these two proteins also exist (Figure 3.9 B).

In the third part of this thesis, I further examined mechanistic relationships between dFMRP and the sole *Drosophila* mGluR (DmGluRA) by assaying protein expression, behavior and neuron structure in brain and NMJ; in single mutants, double mutants and with an mGluR antagonist. At the protein level, dFMRP is upregulated in *dmGluRA* mutants, and DmGluRA upregulated in *dfmr1* mutants, demonstrating mutual negative feedback. Null *dmGluRA* mutants display defects in coordinated movement behavior, which are rescued by removing dFMRP expression. Null *dfmr1* mutants display increased NMJ presynaptic structural complexity and elevated presynaptic vesicle pools, which are rescued by blocking mGluR signaling. Null *dfmr1* brain neurons similarly display increased presynaptic architectural complexity, which is rescued by blocking mGluR signaling. These data show that DmGluRA and dFMRP convergently regulate presynaptic properties.

Taken together, my work has clarified the cellular function of dFMRP on neuronal architecture, uncovered new molecular mechanisms showing that dFMRP regulates class-specific ionotropic glutamate receptor levels in synaptic terminals, and elucidated the mechanistic relationship between dFMRP function

and DmGluRA signaling.

Functional relationship between dFMRP and DmGluRA

Although behavioral and neuron morphological assays suggest that both overlapping and independent mechanisms exist between dFMRP and DmGluRA, more experiments should be done to further dissect this connection.

Ultrastructure analysis showed increased presynaptic vesicle density in *dfmr1* mutant synaptic boutons in both CNS and NMJ synapses (Chapter II and IV), which suggests defective synatogenesis and/or plasticity. At NMJ, this vesicle density increase can be rescued by deleting DmGluRA signaling. In addition, both *dfmr1* and *dmGluRA* mutants display increased synaptic plasticity at NMJ. At *dfmr1* null NMJ, evoked EJC is increased, and both amplitude and frequency of spontaneous release are enhanced (Zhang et al., 2001). In contrast, *dmGluRA* mutants display normally basal synaptic transmission, but synaptic facilitation during short-term stimulus is significantly increased (Bogdanik et al., 2004). It would be interesting to know the performance of *dfmr1; dmGluRA* double mutants in functional assays. Moreover, the connections among these results, which would be generated from neuronal architecture assay, electron microscopy, and electrophysiological examinations, may provide a deeper view of the functions of dFMRP and DmGluRA.

Potential downstream pathways of dFMRP in postsynaptic terminals

In chapter III of this thesis, I showed that dFMRP regulated ionotropic glutamate receptors in a class-specific mechanism. Regulating GluR class composition in the postsynaptic domain is an important mechanism for controlling neurotransmission strength and synaptic plasticity properties. The subunit composition of mammalian NMDA and AMPA receptors are both known to be regulated in this fashion (Sheng et al., 1994; Washburn et al., 1997). Similarly at the *Drosophila* NMJ, the independent regulation of GluR classes is critical, since each receptor class has distinct functional properties (DiAntonio, 2006). The molecular mechanisms for controlling each GluR therefore must be distinct. dFMRP, like its mammalian counterparts, is an RNA-binding protein and a regulator of protein synthesis. However, there is no evidence to show that any subunit of ionotropic GluRs is a direct target of FMRP. So dFMRP likely regulates iGluR synaptic expression levels by regulating the translation of important factors upstream of iGluR localization. Presumably, these translation regulatory mechanisms underlie the differential, and opposing, regulation of A- and B-class GluRs by dFMRP (Figure 5.2).

At the *Drosophila* NMJ, distinct mechanisms regulating specific iGluR classes have been identified. For example, the A-class GluR specificity is negatively regulated by the *Drosophila* protein kinase A (PKA) phosphorylation, modulated by α-protein kinase C (α-PKC). This specificity is important because

the A-class receptor mediates retrograde signaling and displays larger, slower-decaying transmission events with a smaller single channel conductance (Petersen et al., 1997; Davis et al., 1998; DiAntonio et al., 1999; Ruiz-Canada et al., 2004; Chen et al., 2005). Moreover, the *Drosophila* the Rho-type GEF, dPix (Werner and Manseau, 1997; Hakeda-Suzuki et al., 2002), its interacting *Drosophila* p-21 activated kinase (dPak), a serine threonine kinase activated by GTPases Rac and Cdc42 (Harden et al., 1996; Newsome et al., 2000; Mentzel and Raabe, 2005), and a dPak binding partner, the adaptor Dreadlocks (Dock; Nck homolog) (Rao and Zipursky, 1998; Buday et al., 2002; Ang et al., 2003; Rao, 2005), are all required to facilitate synaptic expression of A-class GluRs, but GluRIIB is reportedly not affected in mutants of this pathway (Parnas et al., 2001; Albin and Davis, 2004). Trafficking mechanisms likely involve GluR tethering to the cytoskeleton. The actin-interacting Coracle (mammalian brain 4.1 protein) binds only GluRIIA to specifically regulate its abundance, with no role in B-class GluR tethering (Chen et al., 2005). Interestingly, one recent report showed PAK directly interacts with FMRP in mouse brain, and inhibition of PAK activity can rescue abnormal dendritic spine morphology and some behavioral defects in *fmr1* knockout mice (Hayashi et al., 2007). Therefore, it will be interesting to examine the relationship between dPix-dPak pathway and dFMRP function, as well as interaction between PAK and dFMRP. These work should answer the question of which down-stream mechanism dFMRP regulates A-class iGluR expression.

Figure 5.2 Distinct mechanisms regulating A- and B- class iGluRs

A-class GluRs are negatively regulated by PKA phosphorylation, and modulated by α-PKC. dPix and dPAK interact with each other and both regulate synaptic expression of A-class iGluRs. Another factor in this pathway is Dock, a binding partnet of PAK. DLG is a PDZ-domain scaffolding protein involved in the specific localization of B-class GluRs. CamKII plays a role to regulate DLG activity.

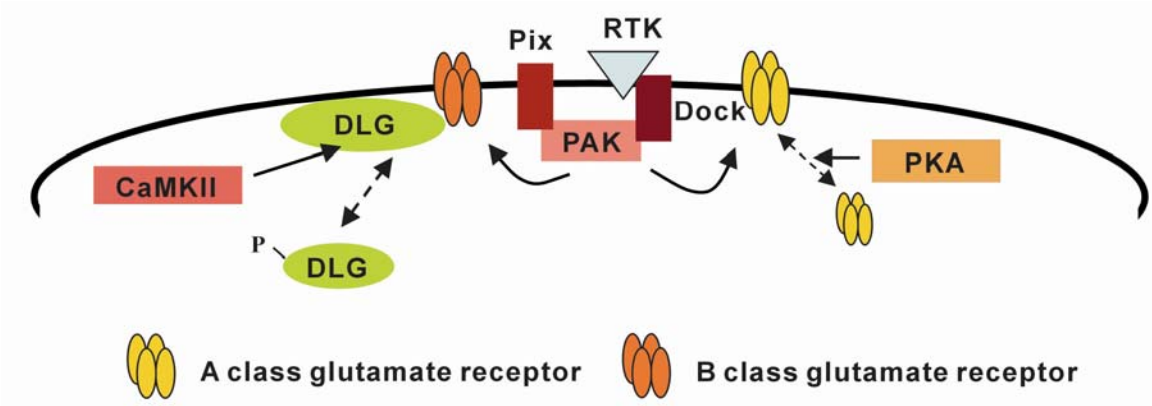
Pix
RTK
Dock
PAK
DLG
CaMKII
PKA
P
DLG
A class glutamate receptor
B class glutamate receptor

There are also some specific mechanisms known to be involved in B-class iGluRs synaptic localization. For example, the PDZ-domain scaffold Discs Large (DLG), a mammalian postsynaptic synaptic density protein 95 (PSD-95) homologue, is involved in the localization of many synaptic proteins (Lahey et al., 1994; Budnik et al., 1996; Guan et al., 1996; Tejedor et al., 1997; Thomas et al., 1997; Thomas et al., 2000; Mathew et al., 2002; Roche et al., 2002), and plays a specific role in B-class iGluR regulation: GluRIIB abundance correlates with DLG level (Chen et al., 2005), but GluRIIA localization is unaffected in *dlg* mutants. In addition, the synaptic translation of PSD-95 is regulated by both mGluR signaling and FMRP in mouse hippocampus (Todd et al., 2003; Ferrari et al., 2007). PSD-95 mRNA is also identified as a direct target of FMRP, and FMRP may regulate the stability of PSD-95 mRNA (Zalfa et al., 2007). Another potential candidate is Ca^{2+}/calmodulin-dependent protein kinase II (CamKII), which plays a role in regulation of DLG activity (Beumer et al., 2002). Mammalian α-CamKII subunit mRNA has been identified as a direct target of FMRP; and FMRP regulates the translation of α-CamKII by interaction with the small dendritic non-translatable RNA BC1 (Zalfa et al., 2003). Thus, more work examining the relationship between dFMRP function and CamKII-DLG pathway is also a potentially important direction.

Pre- and Post- synaptic regulation by dFMRP

FMRP is mostly localized in neuronal soma, with a much lower expression level in neuronal processes and synapses. As an RNA-binding protein and translational regulator, mammalian FMRP displays affinity to about 4% of total brain mRNA (Brown et al., 1998; Brown et al., 2001). Microarray analysis has identified hundreds of potential direct mRNA targets of FMRP binding and translational regulation, which suggested a global function of FMRP (Brown et al., 2001). Although several interactive factors and direct downstream targets of FMRP have been identified in past few years (Bagni and Greenough, 2005; Zhang and Broadie, 2005), these represent but still a drop in the bucket compared to the long list of potential candidates. It is reasonable to predict more interactive factors and more mRNA targets will be found, which will provide us a broader view of FMRP functions. Even if we only consider the already established co-worker proteins and mRNA targets, the diversity suggests that FMRP is involved in multiple pathways, in which the mGluR hypothesis expostulate the most attractive and the most studied one, but not the only one.

The mGluR theory is about postsynaptic cooperation between FMRP and mGluR in regulating ionotropic GluR levels to alter the synaptic plasticity (Bear et al., 2004). The abnormal dedritic spines in cortex and decreased specific LTD in hippocampus both suggested a strong postsynaptic function of FMRP (Bear et al., 2004). In the chapter III of this thesis, I found that dFMRP regulates iGluR level in

the NMJ synapses by a similar postsynaptic mechanism. Both FMRP and *FMR1* mRNA are localized in dendritic processes and dendritic spines, and this localization responds to mGluR activation (Antar et al., 2004; Antar et al., 2005). So, the postsynaptic mechanism of FMRP is clearly supported.

However, if we extend our scope outside postsynaptic terminals, there is also growing evidence for presynaptic pathways regulated by FMRP function. Identification of FMRP mRNA targets has mostly suggested presynaptic functions. The most notable target group is cytoskeleton control pathways. A key function of FMRP/dFMRP appears to be regulating microtubule and actin filament dynamics via regulating expression of key cytoskeleton-binding proteins, such as Futsch/MAP1b (Zhang et al., 2001; Lee et al., 2003; Schenck et al., 2003; Lu et al., 2004; Antar et al., 2006), Arc/Arg3.1 (Zalfa et al., 2003), Ca^{2+}/calmodulin-dependent protein kinase II (Zalfa et al., 2003) and the small GTPase Rac1 (Lee et al., 2003). An interesting interactive factor of FMRP, CYFIP/Sra-1, also plays a role in regulating cytoskeleton (Schenck et al., 2003). In the nervous system, dFMRP acts as a negative translational regulator of Futsch, the *Drosophila* homologue of MAP1B (Zhang et al., 2001). In *fmr1* knockout mouse hippocampus, MAP1B is upregulated and microtubule stability is enhanced (Lu et al., 2004). These results predict that the neuronal microtubule cytoskeleton should be hyperstabilized in *fmr1* mutants. Hyperstabilization of microtubules is known to result in the formation of supernumerary processes, excess branching and

overgrowth (Gordon-Weeks and Fischer, 2000; Buck and Zheng, 2002; Dehmelt et al., 2003): strikingly reminiscent of all of the documented *dfmr1* mutant phenotypes. Alteration of cytoskeleton dynamics/stability would provide a likely direct explanation for defects in neuronal architecture in *fmr1* mutants.

In chapter IV of this thesis, I found blocking mGluR activity by deleting mGluR expression or receptor antagonist treatment can only rescue part of neuron morphological defects. Increased bouton number and increased total synaptic area can be rescued by blocking mGluR signaling, which suggests that the cooperation between dFMRP and DmGluRA is not the only affected pathway in *dfmr1* mutants. However, in our former work, we showed *dfmr1*; *futsch* double mutation can rescue all morphological defects of *dfmr1* single null at NMJ (Zhang et al., 2001). Thus, clarifying regulatory function of FMRP on cytoskeleton dynamics/stability would be the attractive directions in future work. While several cytoskeleton associated proteins have been identified as direct targets or co-worker proteins of FMRP, direct evidence proving FMRP regulates cytoskeleton dynamic or stability is still limited. More work, for example, on live imaging of microtubule and actin remodeling in *fmr1* mutant neurons, especially in vivo examination, should provide a deeper understanding of FMRP function on cytoskeleton regulation and neuronal elaboration.

FMRP is also detected in axon processes and growth cone in cultured neurons of mouse hippocampus (Antar et al., 2004; Antar et al., 2006). Lots of

presynaptic proteins have been identified as direct targets of FMRP, including MUNC-13, NAP-22, SEC-7 and RAB-5 (Brown et al., 2001; Miyashiro et al., 2003). MAP1B, as the best proven mRNA target of FMRP, is also localized in axon and growth cone of same culture, with similar localization of FMRP (Antar et al., 2006). Hyperabundance of filopodia is found in *fmr1* knockout neurons (Antar et al., 2006). These data suggested a presynaptic mechanism of FMRP to control axon growth and synaptic elaboration. In *Drosophila* central neurons, I similarly found increased presynaptic bouton size and enhanced synaptic vesicle density, which suggests defects in synaptogenesis and synaptic plasticity (Pan et al., 2004). In the NMJ synapses, both spontaneous release quantal size and quantal frequency are increased (Zhang et al., 2001). While changed quantal size always represents a postsynaptic alternation, the quantal frequency is usually due to the presynaptic changes. These functional data suggests both pre- and postsynaptic mechanisms of dFMRP function. Our finding that dFMRP specifically regulates different iGluR classes in postsynaptic terminals at NMJ might be one explanation of increased quantal size. Loss of dFMRP results in significant increased A-class with decreased B-class iGluRs, which mimic the over-expression of GluRIIA subunits (DiAntonio et al., 1999). This A-class over- expression situation results in significant increased quantal size. However, presynaptic mechanisms of dFMRP are still waiting for elucidation. One potential mechanism is FMRP regulates synaptic vesicle release or cycling. It will be interesting to know whether

endocytosis or exocytosis level is changed in *fmr1* mutants. If this is demonstrated, the next question would be which proteins are regulated by FMRP in presynaptic terminals, and which pathways are FMRP involved in to regulate neuronal transmission from presynaptic side.

Since FMRP is an mRNA-binding protein, which does not have solo direct target, I believed that more and more detailed mechanisms about FMRP functions will be found, which can elucidate the Fragile X Mental Retardation disease situation and broaden our view of how our nervous system make its function.

REFERENCES

Adinolfi, S., Bagni, C., Castiglione Morelli, M. A., Fraternali, F., Musco, G., and Pastore, A. (1999a). Novel RNA-binding motif: the KH module. Biopolymers *51*, 153-164.

Adinolfi, S., Bagni, C., Musco, G., Gibson, T., Mazzarella, L., and Pastore, A. (1999b). Dissecting FMR1, the protein responsible for fragile X syndrome, in its structural and functional domains. Rna *5*, 1248-1258.

Adinolfi, S., Ramos, A., Martin, S. R., Dal Piaz, F., Pucci, P., Bardoni, B., Mandel, J. L., and Pastore, A. (2003). The N-terminus of the fragile X mental retardation protein contains a novel domain involved in dimerization and RNA binding. Biochemistry *42*, 10437-10444.

Albin SD, Davis GW (2004) Coordinating structural and functional synapse development: postsynaptic p21-activated kinase independently specifies glutamate receptor abundance and postsynaptic morphology. J Neurosci 24:6871-6879.

Allingham-Hawkins, D. J., Babul-Hirji, R., Chitayat, D., Holden, J. J., Yang, K. T., Lee, C., Hudson, R., Gorwill, H., Nolin, S. L., Glicksman, A.*, et al.* (1999). Fragile X premutation is a significant risk factor for premature ovarian failure: the International Collaborative POF in Fragile X study--preliminary data. Am J Med Genet *83*, 322-325.

Ang LH, Kim J, Stepensky V, Hing H (2003) Dock and Pak regulate olfactory axon pathfinding in Drosophila. Development 130:1307-1316.

Antar, L. N., Afroz, R., Dictenberg, J. B., Carroll, R. C., and Bassell, G. J. (2004). Metabotropic glutamate receptor activation regulates fragile x mental retardation protein and FMR1 mRNA localization differentially in dendrites and at synapses. J Neurosci *24*, 2648-2655.

Antar, L. N., Dictenberg, J. B., Plociniak, M., Afroz, R., and Bassell, G. J. (2005). Localization of FMRP-associated mRNA granules and requirement of microtubules for activity-dependent trafficking in hippocampal neurons. Genes Brain Behav *4*, 350-359.

Antar, L. N., Li, C., Zhang, H., Carroll, R. C., and Bassell, G. J. (2006). Local

functions for FMRP in axon growth cone motility and activity-dependent regulation of filopodia and spine synapses. Mol Cell Neurosci *32*, 37-48.

Aschrafi, A., Cunningham, B. A., Edelman, G. M., and Vanderklish, P. W. (2005). The fragile X mental retardation protein and group I metabotropic glutamate receptors regulate levels of mRNA granules in brain. Proc Natl Acad Sci U S A *102*, 2180-2185.

Ashley, C. T., Jr., Wilkinson, K. D., Reines, D., and Warren, S. T. (1993a). FMR1 protein: conserved RNP family domains and selective RNA binding. Science *262*, 563-566.

Ashley, C. T., Sutcliffe, J. S., Kunst, C. B., Leiner, H. A., Eichler, E. E., Nelson, D. L., and Warren, S. T. (1993b). Human and murine FMR-1: alternative splicing and translational initiation downstream of the CGG-repeat. Nat Genet *4*, 244-251.

Aravamudan, B., Fergestad, T., Davis, W. S., Rodesch, C. K., and Broadie, K. (1999). Drosophila UNC-13 is essential for synaptic transmission. Nat Neurosci *2*, 965-971.

Bagni C, Greenough WT (2005) From mRNP trafficking to spine dysmorphogenesis: the roots of fragile X syndrome. Nat Rev Neurosci 6:376-387.

Bakker, C. E. e. a. (1994). Fmr1 knockout mice: a model to study fragile X mental retardation. The Dutch-Belgian Fragile X Consortium. Cell *78*, 23-33.

Bardoni B, Schenck A, Mandel JL (1999) A novel RNA-binding nuclear protein that interacts with the fragile X mental retardation (FMR1) protein. Hum Mol Genet 8:2557-2566.

Bardoni B, Willemsen R, Weiler IJ, Schenck A, Severijnen LA, Hindelang C, Lalli E, Mandel JL (2003a) NUFIP1 (nuclear FMRP interacting protein 1) is a nucleocytoplasmic shuttling protein associated with active synaptoneurosomes. Exp Cell Res 289:95-107.

Bardoni B, Castets M, Huot ME, Schenck A, Adinolfi S, Corbin F, Pastore A, Khandjian EW, Mandel JL (2003b) 82-FIP, a novel FMRP (fragile X mental retardation protein) interacting protein, shows a cell cycle-dependent intracellular localization. Hum Mol Genet 12:1689-1698.

Barth, M., Hirsch, H. V., Meinertzhagen, I. A., and Heisenberg, M. (1997).

Experience-dependent developmental plasticity in the optic lobe of Drosophila melanogaster. J Neurosci *17*, 1493-1504.

Bear, M. F., Huber, K. M., and Warren, S. T. (2004). The mGluR theory of fragile X mental retardation. Trends Neurosci *27*, 370-377.

Beumer K, Matthies HJ, Bradshaw A, Broadie K (2002) Integrins regulate DLG/FAS2 via a CaM kinase II-dependent pathway to mediate synapse elaboration and stabilization during postembryonic development. Development 129:3381-3391.

Bodily, K. D., C. M. Morrison, et al. (2001). "A novel member of the Ig superfamily, turtle, is a CNS-specific protein required for coordinated motor control." J Neurosci **21**(9): 3113-25.

Bogdanik L, Mohrmann R, Ramaekers A, Bockaert J, Grau Y, Broadie K, Parmentier ML (2004) The Drosophila metabotropic glutamate receptor DmGluRA regulates activity-dependent synaptic facilitation and fine synaptic morphology. J Neurosci 24:9105-9116.

Brand, A. H., and Perrimon, N. (1993). Targeted gene expression as a means of altering cell fates and generating dominant phenotypes. Development *118*, 401-415.

Brennan FX, Albeck DS, Paylor R (2006) Fmr1 knockout mice are impaired in a leverpress escape/avoidance task. Genes Brain Behav 5:467-471.

Broadie, K. S. (1996). Regulation of the synaptic vesicle cycle in Drosophila. Biochem Soc Trans *24*, 639-645.

Broadie, K. S., and Richmond, J. E. (2002). Establishing and sculpting the synapse in Drosophila and C. elegans. Curr Opin Neurobiol *12*, 491-498.

Brown, V., Jin, P., Ceman, S., Darnell, J. C., O'Donnell, W. T., Tenenbaum, S. A., Jin, X., Feng, Y., Wilkinson, K. D., Keene, J. D.*, et al.* (2001). Microarray identification of FMRP-associated brain mRNAs and altered mRNA translational profiles in fragile X syndrome. Cell *107*, 477-487.

Brown, V., Small, K., Lakkis, L., Feng, Y., Gunter, C., Wilkinson, K. D., and Warren, S. T. (1998). Purified recombinant Fmrp exhibits selective RNA binding as an intrinsic property of the fragile X mental retardation protein. J Biol Chem *273*,

15521-15527.

Buck KB, Zheng JQ (2002) Growth cone turning induced by direct local modification of microtubule dynamics. J Neurosci 22:9358-9367.

Buday L, Wunderlich L, Tamas P (2002) The Nck family of adapter proteins: regulators of actin cytoskeleton. Cell Signal 14:723-731.

Budnik V, Koh YH, Guan B, Hartmann B, Hough C, Woods D, Gorczyca M (1996) Regulation of synapse structure and function by the Drosophila tumor suppressor gene dlg. Neuron 17:627-640.

Carroll, R. C., Lissin, D. V., von Zastrow, M., Nicoll, R. A., and Malenka, R. C. (1999). Rapid redistribution of glutamate receptors contributes to long-term depression in hippocampal cultures. Nat Neurosci *2*, 454-460.

Caudy, A. A., Myers, M., Hannon, G. J., and Hammond, S. M. (2002). Fragile X-related protein and VIG associate with the RNA interference machinery. Genes Dev *16*, 2491-2496.

Cauli O, Llansola M, Rodrigo R, El Mlili N, Errami M, Felipo V (2005) Altered modulation of motor activity by group I metabotropic glutamate receptors in the nucleus accumbens in hyperammonemic rats. Metab Brain Dis 20:347-358.

Ceman S, Brown V, Warren ST (1999) Isolation of an FMRP-associated messenger ribonucleoprotein particle and identification of nucleolin and the fragile X-related proteins as components of the complex. Mol Cell Biol 19:7925-7932.

Chelly, J., Khelfaoui, M., Francis, F., Cherif, B., and Bienvenu, T. (2006). Genetics and pathophysiology of mental retardation. Eur J Hum Genet *14*, 701-713.

Chen K, Featherstone DE (2005) Discs-large (DLG) is clustered by presynaptic innervation and regulates postsynaptic glutamate receptor subunit composition in Drosophila. BMC Biol 3:1.

Chen, L., and Toth, M. (2001). Fragile X mice develop sensory hyperreactivity to auditory stimuli. Neuroscience *103*, 1043-1050.

Chiurazzi, P., Pomponi, M. G., Willemsen, R., Oostra, B. A., and Neri, G. (1998). In vitro reactivation of the FMR1 gene involved in fragile X syndrome. Hum Mol Genet *7*, 109-113.

Comery, T. A., Harris, J. B., Willems, P. J., Oostra, B. A., Irwin, S. A., Weiler, I. J., and Greenough, W. T. (1997). Abnormal dendritic spines in fragile X knockout mice: maturation and pruning deficits. Proc Natl Acad Sci U S A *94*, 5401-5404.

Connolly, J. B., Roberts, I. J., Armstrong, J. D., Kaiser, K., Forte, M., Tully, T., and O'Kane, C. J. (1996). Associative learning disrupted by impaired Gs signaling in Drosophila mushroom bodies. Science *274*, 2104-2107.

Costa, A., Wang, Y., Dockendorff, T. C., Erdjument-Bromage, H., Tempst, P., Schedl, P., and Jongens, T. A. (2005). The Drosophila fragile X protein functions as a negative regulator in the orb autoregulatory pathway. Dev Cell *8*, 331-342.

Couteaux R, Pecot-Dechavassine M (1970) [Synaptic vesicles and pouches at the level of "active zones" of the neuromuscular junction]. C R Acad Sci Hebd Seances Acad Sci D 271:2346-2349.

Crittenden, J. R., Skoulakis, E. M., Han, K. A., Kalderon, D., and Davis, R. L. (1998). Tripartite mushroom body architecture revealed by antigenic markers. Learn Mem *5*, 38-51.

Darnell, J. C., Jensen, K. B., Jin, P., Brown, V., Warren, S. T., and Darnell, R. B. (2001). Fragile X mental retardation protein targets G quartet mRNAs important for neuronal function. Cell *107*, 489-499.

Davis GW, DiAntonio A, Petersen SA, Goodman CS (1998) Postsynaptic PKA controls quantal size and reveals a retrograde signal that regulates presynaptic transmitter release in Drosophila. Neuron 20:305-315.

Davis, R. L. (1993). Mushroom bodies and Drosophila learning. Neuron *11*, 1-14.

Davis, R. L., and Han, K. A. (1996). Neuroanatomy: mushrooming mushroom bodies. Curr Biol *6*, 146-148.

de Belle, J. S., and Heisenberg, M. (1994). Associative odor learning in Drosophila abolished by chemical ablation of mushroom bodies. Science *263*, 692-695.

De Boulle, K., Verkerk, A. J., Reyniers, E., Vits, L., Hendrickx, J., Van Roy, B., Van den Bos, F., de Graaff, E., Oostra, B. A., and Willems, P. J. (1993). A point mutation in the FMR-1 gene associated with fragile X mental retardation. Nat

Genet *3*, 31-35.

Dehmelt L, Smart FM, Ozer RS, Halpain S (2003) The role of microtubule-associated protein 2c in the reorganization of microtubules and lamellipodia during neurite initiation. J Neurosci 23:9479-9490.

Devys, D., Lutz, Y., Rouyer, N., Bellocq, J. P., and Mandel, J. L. (1993). The FMR-1 protein is cytoplasmic, most abundant in neurons and appears normal in carriers of a fragile X premutation. Nat Genet *4*, 335-340.

D'Hooge, R., Nagels, G., Franck, F., Bakker, C. E., Reyniers, E., Storm, K., Kooy, R. F., Oostra, B. A., Willems, P. J., and De Deyn, P. P. (1997). Mildly impaired water maze performance in male Fmr1 knockout mice. Neuroscience *76*, 367-376.

DiAntonio A, Petersen SA, Heckmann M, Goodman CS (1999) Glutamate receptor expression regulates quantal size and quantal content at the Drosophila neuromuscular junction. J Neurosci 19:3023-3032.

Dobkin, C., Rabe, A., Dumas, R., El Idrissi, A., Haubenstock, H., and Brown, W. T. (2000). Fmr1 knockout mouse has a distinctive strain-specific learning impairment. Neuroscience *100*, 423-429.

Dockendorff, T. C., Su, H. S., McBride, S. M., Yang, Z., Choi, C. H., Siwicki, K. K., Sehgal, A., and Jongens, T. A. (2002). Drosophila lacking dfmr1 activity show defects in circadian output and fail to maintain courtship interest. Neuron *34*, 973-984.

Eberhart, D. E., Malter, H. E., Feng, Y., and Warren, S. T. (1996). The fragile X mental retardation protein is a ribonucleoprotein containing both nuclear localization and nuclear export signals. Hum Mol Genet *5*, 1083-1091.

Edelmann L (2002) Freeze-dried and resin-embedded biological material is well suited for ultrastructure research. J Microsc 207:5-26.

Featherstone, D. E., Davis, W. S., Dubreuil, R. R., and Broadie, K. (2001). Drosophila alpha- and beta-spectrin mutations disrupt presynaptic neurotransmitter release. J Neurosci *21*, 4215-4224.

Featherstone DE, Rushton E, Broadie K (2002) Developmental regulation of glutamate receptor field size by nonvesicular glutamate release. Nat Neurosci

5:141-146.

Featherstone DE, Rushton E, Rohrbough J, Liebl F, Karr J, Sheng Q, Rodesch CK, Broadie K (2005) An essential Drosophila glutamate receptor subunit that functions in both central neuropil and neuromuscular junction. J Neurosci 25:3199-3208.

Feng, Y., Gutekunst, C. A., Eberhart, D. E., Yi, H., Warren, S. T., and Hersch, S. M. (1997). Fragile X mental retardation protein: nucleocytoplasmic shuttling and association with somatodendritic ribosomes. J Neurosci *17*, 1539-1547.

Ferrari F, Mercaldo V, Piccoli G, Sala C, Cannata S, Achsel T, Bagni C (2007) The fragile X mental retardation protein-RNP granules show an mGluR-dependent localization in the post-synaptic spines. Mol Cell Neurosci 34(3): 343-54.

Fiala, J. C., Spacek, J., and Harris, K. M. (2002). Dendritic spine pathology: cause or consequence of neurological disorders? Brain Res Brain Res Rev *39*, 29-54.

Fischer, J. A., Giniger, E., Maniatis, T., and Ptashne, M. (1988). GAL4 activates transcription in Drosophila. Nature *332*, 853-856.

Fong DK, Rao A, Crump FT, Craig AM (2002) Rapid synaptic remodeling by protein kinase C: reciprocal translocation of NMDA receptors and calcium/calmodulin-dependent kinase II. J Neurosci 22:2153-2164.

Fu, Y. H., Kuhl, D. P., Pizzuti, A., Pieretti, M., Sutcliffe, J. S., Richards, S., Verkerk, A. J., Holden, J. J., Fenwick, R. G., Jr., Warren, S. T., and et al. (1991). Variation of the CGG repeat at the fragile X site results in genetic instability: resolution of the Sherman paradox. Cell *67*, 1047-1058.

Galvez, R., Gopal, A. R., and Greenough, W. T. (2003). Somatosensory cortical barrel dendritic abnormalities in a mouse model of the fragile X mental retardation syndrome. Brain Res *971*, 83-89.

Garber K, Smith KT, Reines D, Warren ST (2006) Transcription, translation and fragile X syndrome. Curr Opin Genet Dev 16:270-275.

Gedeon, A. K., Baker, E., Robinson, H., Partington, M. W., Gross, B., Manca, A., Korn, B., Poustka, A., Yu, S., Sutherland, G. R., and et al. (1992). Fragile X syndrome without CCG amplification has an FMR1 deletion. Nat Genet *1*, 341-344.

Ghisolfi, L., Joseph, G., Amalric, F., and Erard, M. (1992). The glycine-rich domain of nucleolin has an unusual supersecondary structure responsible for its RNA-helix-destabilizing properties. J Biol Chem *267*, 2955-2959.

Godfraind, J. M., Reyniers, E., De Boulle, K., D'Hooge, R., De Deyn, P. P., Bakker, C. E., Oostra, B. A., Kooy, R. F., and Willems, P. J. (1996). Long-term potentiation in the hippocampus of fragile X knockout mice. Am J Med Genet *64*, 246-251.

Gordon-Weeks PR, Fischer I (2000) MAP1B expression and microtubule stability in growing and regenerating axons. Microsc Res Tech 48:63-74.

Greenough, W. T., Klintsova, A. Y., Irwin, S. A., Galvez, R., Bates, K. E., and Weiler, I. J. (2001). Synaptic regulation of protein synthesis and the fragile X protein. Proc Natl Acad Sci U S A *98*, 7101-7106.

Grossman, A. W., G. M. Aldridge, et al. (2006). "Local protein synthesis and spine morphogenesis: Fragile X syndrome and beyond." J Neurosci **26**(27): 7151-5.

Guan B, Hartmann B, Kho YH, Gorczyca M, Budnik V (1996) The Drosophila tumor suppressor gene, dlg, is involved in structural plasticity at a glutamatergic synapse. Curr Biol 6:695-706.

Haas KF, Woodruff Iii E, Broadie K (2007) Proteasome function is required to maintain muscle cellular architecture. Biol Cell, 99(11): 615-26.

Hagerman, R. J., and Hagerman, P. J. (2002). The fragile X premutation: into the phenotypic fold. Curr Opin Genet Dev *12*, 278-283.

Hagerman, R. J., Leehey, M., Heinrichs, W., Tassone, F., Wilson, R., Hills, J., Grigsby, J., Gage, B., and Hagerman, P. J. (2001). Intention tremor, parkinsonism, and generalized brain atrophy in male carriers of fragile X. Neurology *57*, 127-130.

Hakeda-Suzuki S, Ng J, Tzu J, Dietzl G, Sun Y, Harms M, Nardine T, Luo L, Dickson BJ (2002) Rac function and regulation during Drosophila development. Nature 416:438-442.

Hanson JE, Madison DV (2007) Presynaptic FMR1 genotype influences the degree of synaptic connectivity in a mosaic mouse model of fragile X syndrome. J Neurosci 27:4014-4018.

Harden N, Lee J, Loh HY, Ong YM, Tan I, Leung T, Manser E, Lim L (1996) A Drosophila homolog of the Rac- and Cdc42-activated serine/threonine kinase PAK is a potential focal adhesion and focal complex protein that colocalizes with dynamic actin structures. Mol Cell Biol 16:1896-1908.

Hay M, Hoang CJ, Pamidimukkala J (2001) Cellular mechanisms regulating synaptic vesicle exocytosis and endocytosis in aortic baroreceptor neurons. Ann N Y Acad Sci 940:119-131.

Hayashi ML, Rao BS, Seo JS, Choi HS, Dolan BM, Choi SY, Chattarji S, Tonegawa S (2007) Inhibition of p21-activated kinase rescues symptoms of fragile X syndrome in mice. Proc Natl Acad Sci U S A 104:11489-11494.

Heisenberg, M. (1998). What do the mushroom bodies do for the insect brain? an introduction. Learn Mem *5*, 1-10.

Heisenberg, M. (2003). Mushroom body memoir: from maps to models. Nat Rev Neurosci *4*, 266-275.

Heitz, D., Rousseau, F., Devys, D., Saccone, S., Abderrahim, H., Le Paslier, D., Cohen, D., Vincent, A., Toniolo, D., Della Valle, G., and et al. (1991). Isolation of sequences that span the fragile X and identification of a fragile X-related CpG island. Science *251*, 1236-1239.

Hinds, H. L., Ashley, C. T., Sutcliffe, J. S., Nelson, D. L., Warren, S. T., Housman, D. E., and Schalling, M. (1993). Tissue specific expression of FMR-1 provides evidence for a functional role in fragile X syndrome. Nat Genet *3*, 36-43.

Hinton, V. J., Brown, W. T., Wisniewski, K., and Rudelli, R. D. (1991). Analysis of neocortex in three males with the fragile X syndrome. Am J Med Genet *41*, 289-294.

Hou, L., Antion, M. D., Hu, D., Spencer, C. M., Paylor, R., and Klann, E. (2006). Dynamic translational and proteasomal regulation of fragile X mental retardation protein controls mGluR-dependent long-term depression. Neuron *51*, 441-454.

Huber, K. M., Gallagher, S. M., Warren, S. T., and Bear, M. F. (2002). Altered synaptic plasticity in a mouse model of fragile X mental retardation. Proc Natl Acad Sci U S A *99*, 7746-7750.

Huber, K. M., Kayser, M. S., and Bear, M. F. (2000). Role for rapid dendritic protein synthesis in hippocampal mGluR-dependent long-term depression. Science *288*, 1254-1257.

Huber, K. M., Roder, J. C., and Bear, M. F. (2001). Chemical induction of mGluR5- and protein synthesis--dependent long-term depression in hippocampal area CA1. J Neurophysiol *86*, 321-325.

Inoue, S., Shimoda, M., Nishinokubi, I., Siomi, M. C., Okamura, M., Nakamura, A., Kobayashi, S., Ishida, N., and Siomi, H. (2002). A role for the Drosophila fragile X-related gene in circadian output. Curr Biol *12*, 1331-1335.

Irwin, S. A., Galvez, R., and Greenough, W. T. (2000). Dendritic spine structural anomalies in fragile-X mental retardation syndrome. Cereb Cortex *10*, 1038-1044.

Irwin, S. A., Idupulapati, M., Gilbert, M. E., Harris, J. B., Chakravarti, A. B., Rogers, E. J., Crisostomo, R. A., Larsen, B. P., Mehta, A., Alcantara, C. J.*, et al.* (2002). Dendritic spine and dendritic field characteristics of layer V pyramidal neurons in the visual cortex of fragile-X knockout mice. Am J Med Genet *111*, 140-146.

Irwin, S. A., Patel, B., Idupulapati, M., Harris, J. B., Crisostomo, R. A., Larsen, B. P., Kooy, F., Willems, P. J., Cras, P., Kozlowski, P. B.*, et al.* (2001). Abnormal dendritic spine characteristics in the temporal and visual cortices of patients with fragile-X syndrome: a quantitative examination. Am J Med Genet *98*, 161-167.

Ishizuka, A., Siomi, M. C., and Siomi, H. (2002). A Drosophila fragile X protein interacts with components of RNAi and ribosomal proteins. Genes Dev *16*, 2497-2508.

Jin P, Warren ST (2000) Understanding the molecular basis of fragile X syndrome. Hum Mol Genet 9:901-908.

Jin, P., Zarnescu, D. C., Ceman, S., Nakamoto, M., Mowrey, J., Jongens, T. A., Nelson, D. L., Moses, K., and Warren, S. T. (2004). Biochemical and genetic interaction between the fragile X mental retardation protein and the microRNA pathway. Nat Neurosci *7*, 113-117.

Katz F, Moats W, Jan YN (1988) A carbohydrate epitope expressed uniquely on the cell surface of Drosophila neurons is altered in the mutant nac (neurally altered carbohydrate). Embo J 7:3471-3477.

Kiledjian, M., and Dreyfuss, G. (1992). Primary structure and binding activity of the hnRNP U protein: binding RNA through RGG box. Embo J *11*, 2655-2664.

Kittel RJ, Wichmann C, Rasse TM, Fouquet W, Schmidt M, Schmid A, Wagh DA, Pawlu C, Kellner RR, Willig KI, Hell SW, Buchner E, Heckmann M, Sigrist SJ (2006) Bruchpilot promotes active zone assembly, Ca2+ channel clustering, and vesicle release. Science 312:1051-1054.

Koekkoek, S. K., Yamaguchi, K., Milojkovic, B. A., Dortland, B. R., Ruigrok, T. J., Maex, R., De Graaf, W., Smit, A. E., VanderWerf, F., Bakker, C. E.*, et al.* (2005). Deletion of FMR1 in Purkinje cells enhances parallel fiber LTD, enlarges spines, and attenuates cerebellar eyelid conditioning in Fragile X syndrome. Neuron *47*, 339-352.

Kooy, R. F. (2003). Of mice and the fragile X syndrome. Trends Genet *19*, 148-154.

Kooy, R. F., D'Hooge, R., Reyniers, E., Bakker, C. E., Nagels, G., De Boulle, K., Storm, K., Clincke, G., De Deyn, P. P., Oostra, B. A., and Willems, P. J. (1996). Transgenic mouse model for the fragile X syndrome. Am J Med Genet *64*, 241-245.

Laggerbauer, B., Ostareck, D., Keidel, E. M., Ostareck-Lederer, A., and Fischer, U. (2001). Evidence that fragile X mental retardation protein is a negative regulator of translation. Hum Mol Genet *10*, 329-338.

Lahey T, Gorczyca M, Jia XX, Budnik V (1994) The Drosophila tumor suppressor gene dlg is required for normal synaptic bouton structure. Neuron 13:823-835.

Larson, J., Jessen, R. E., Kim, D., Fine, A. K., and du Hoffmann, J. (2005). Age-dependent and selective impairment of long-term potentiation in the anterior piriform cortex of mice lacking the fragile X mental retardation protein. J Neurosci *25*, 9460-9469.

Laval, S. H., Blair, H. J., Hirst, M. C., Davies, K. E., and Boyd, Y. (1992). Mapping of FMR1, the gene implicated in fragile X-linked mental retardation, on the mouse X chromosome. Genomics *12*, 818-821.

Lee, A., Li, W., Xu, K., Bogert, B. A., Su, K., and Gao, F. B. (2003). Control of dendritic development by the Drosophila fragile X-related gene involves the small GTPase Rac1. Development *130*, 5543-5552.

Lee, T., Lee, A., and Luo, L. (1999). Development of the Drosophila mushroom bodies: sequential generation of three distinct types of neurons from a neuroblast. Development *126*, 4065-4076.

Lee, T., and Luo, L. (1999). Mosaic analysis with a repressible cell marker for studies of gene function in neuronal morphogenesis. Neuron *22*, 451-461.

Leonard, H., and Wen, X. (2002). The epidemiology of mental retardation: challenges and opportunities in the new millennium. Ment Retard Dev Disabil Res Rev *8*, 117-134.

Li, J., Pelletier, M. R., Perez Velazquez, J. L., and Carlen, P. L. (2002). Reduced cortical synaptic plasticity and GluR1 expression associated with fragile X mental retardation protein deficiency. Mol Cell Neurosci *19*, 138-151.

Li, Z., Zhang, Y., Ku, L., Wilkinson, K. D., Warren, S. T., and Feng, Y. (2001). The fragile X mental retardation protein inhibits translation via interacting with mRNA. Nucleic Acids Res *29*, 2276-2283.

Liebl FL, Chen K, Karr J, Sheng Q, Featherstone DE (2005) Increased synaptic microtubules and altered synapse development in Drosophila sec8 mutants. BMC Biol 3:27.

Ling SC, Fahrner PS, Greenough WT, Gelfand VI (2004) Transport of Drosophila fragile X mental retardation protein-containing ribonucleoprotein granules by kinesin-1 and cytoplasmic dynein. Proc Natl Acad Sci U S A 101:17428-17433.

Lu, R., Wang, H., Liang, Z., Ku, L., O'Donnell W, T., Li, W., Warren, S. T., and Feng, Y. (2004). The fragile X protein controls microtubule-associated protein 1B translation and microtubule stability in brain neuron development. Proc Natl Acad Sci U S A *101*, 15201-15206.

Malter, H. E., Iber, J. C., Willemsen, R., de Graaff, E., Tarleton, J. C., Leisti, J., Warren, S. T., and Oostra, B. A. (1997). Characterization of the full fragile X syndrome mutation in fetal gametes. Nat Genet *15*, 165-169.

Markham JA, Beckel-Mitchener AC, Estrada CM, Greenough WT (2006)Corticosterone response to acute stress in a mouse model of Fragile X syndrome. Psychoneuroendocrinology 31:781-785.

Marrus SB, Portman SL, Allen MJ, Moffat KG, DiAntonio A (2004) Differential localization of glutamate receptor subunits at the Drosophila neuromuscular junction. J Neurosci 24:1406-1415.

Mathew D, Gramates LS, Packard M, Thomas U, Bilder D, Perrimon N, Gorczyca M, Budnik V (2002) Recruitment of scribble to the synaptic scaffolding complex requires GUK-holder, a novel DLG binding protein. Curr Biol 12:531-539.

McBride, S. M., Giuliani, G., Choi, C., Krause, P., Correale, D., Watson, K., Baker, G., and Siwicki, K. K. (1999). Mushroom body ablation impairs short-term memory and long-term memory of courtship conditioning in Drosophila melanogaster. Neuron *24*, 967-977.

McBride, S. M., Choi, C. H., Wang, Y., Liebelt, D., Braunstein, E., Ferreiro, D., Sehgal, A., Siwicki, K. K., Dockendorff, T. C., Nguyen, H. T.*, et al.* (2005). Pharmacological rescue of synaptic plasticity, courtship behavior, and mushroom body defects in a Drosophila model of fragile X syndrome. Neuron *45*, 753-764.

McDonald K (1999) High-pressure freezing for preservation of high resolution fine structure and antigenicity for immunolabeling. Methods Mol Biol 117:77-97.

Mentzel B, Raabe T (2005) Phylogenetic and structural analysis of the Drosophila melanogaster p21-activated kinase DmPAK3. Gene 349:25-33.

Michel CI, Kraft R, Restifo LL (2004) Defective neuronal development in the mushroom bodies of Drosophila fragile X mental retardation 1 mutants. J Neurosci 24:5798-5809.

Mineur YS, Huynh LX, Crusio WE (2006) Social behavior deficits in the Fmr1 mutant mouse. Behav Brain Res 168:172-175.

Mineur, Y. S., Sluyter, F., de Wit, S., Oostra, B. A., and Crusio, W. E. (2002). Behavioral and neuroanatomical characterization of the Fmr1 knockout mouse. Hippocampus *12*, 39-46.

Mitri C, Parmentier ML, Pin JP, Bockaert J, Grau Y (2004) Divergent evolution in metabotropic glutamate receptors. A new receptor activated by an endogenous ligand different from glutamate in insects. J Biol Chem 279:9313-9320.

Miyashiro, K. Y., Beckel-Mitchener, A., Purk, T. P., Becker, K. G., Barret, T., Liu, L., Carbonetto, S., Weiler, I. J., Greenough, W. T., and Eberwine, J. (2003). RNA

cargoes associating with FMRP reveal deficits in cellular functioning in Fmr1 null mice. Neuron *37*, 417-431.

Morales, J., Hiesinger, P. R., Schroeder, A. J., Kume, K., Verstreken, P., Jackson, F. R., Nelson, D. L., and Hassan, B. A. (2002). Drosophila fragile X protein, DFXR, regulates neuronal morphology and function in the brain. Neuron *34*, 961-972.

Muddashetty, R. S., Kelic, S., Gross, C., Xu, M., and Bassell, G. J. (2007). Dysregulated metabotropic glutamate receptor-dependent translation of AMPA receptor and postsynaptic density-95 mRNAs at synapses in a mouse model of fragile X syndrome. J Neurosci *27*, 5338-5348.

Musumeci, S. A., Bosco, P., Calabrese, G., Bakker, C., De Sarro, G. B., Elia, M., Ferri, R., and Oostra, B. A. (2000). Audiogenic seizures susceptibility in transgenic mice with fragile X syndrome. Epilepsia *41*, 19-23.

Newsome TP, Schmidt S, Dietzl G, Keleman K, Asling B, Debant A, Dickson BJ (2000) Trio combines with dock to regulate Pak activity during photoreceptor axon pathfinding in Drosophila. Cell 101:283-294.

Nimchinsky, E. A., Oberlander, A. M., and Svoboda, K. (2001). Abnormal development of dendritic spines in FMR1 knock-out mice. J Neurosci *21*, 5139-5146.

Nistri A, Ostroumov K, Sharifullina E, Taccola G (2006) Tuning and playing a motor rhythm: how metabotropic glutamate receptors orchestrate generation of motor patterns in the mammalian central nervous system. J Physiol 572:323-334.

Nosyreva, E. D., and Huber, K. M. (2005). Developmental switch in synaptic mechanisms of hippocampal metabotropic glutamate receptor-dependent long-term depression. J Neurosci *25*, 2992-3001.

Nosyreva, E. D., and Huber, K. M. (2006). Metabotropic receptor-dependent long-term depression persists in the absence of protein synthesis in the mouse model of fragile X syndrome. J Neurophysiol *95*, 3291-3295.

O'Donnell, W. T., and Warren, S. T. (2002). A decade of molecular studies of fragile X syndrome. Annu Rev Neurosci *25*, 315-338.

Pamidimukkala J, Hay M (2001) Frequency dependence of endocytosis in aortic baroreceptor neurons and role of group III mGluRs. Am J Physiol Heart Circ

Physiol 281:H387-395.

Pan, L, Broadie, K, (2007) Drosophila fragile X mental retardation protein and metabotropic glutamate receptor A convergently regulate the synaptic ratio of ionotropic glutamate receptor subclasses. J Neurosci 27(45): 12378-12389.

Pan, L., Zhang, Y. Q., Woodruff, E., and Broadie, K. (2004). The Drosophila fragile X gene negatively regulates neuronal elaboration and synaptic differentiation. Curr Biol *14*, 1863-1870.

Paradis S, Sweeney ST, Davis GW (2001) Homeostatic control of presynaptic release is triggered by postsynaptic membrane depolarization. Neuron 30:737-749.

Parmentier ML, Pin JP, Bockaert J, Grau Y (1996) Cloning and functional expression of a Drosophila metabotropic glutamate receptor expressed in the embryonic CNS. J Neurosci 16:6687-6694.

Parnas D, Haghighi AP, Fetter RD, Kim SW, Goodman CS (2001) Regulation of postsynaptic structure and protein localization by the Rho-type guanine nucleotide exchange factor dPix. Neuron 32:415-424.

Petersen SA, Fetter RD, Noordermeer JN, Goodman CS, DiAntonio A (1997) Genetic analysis of glutamate receptors in Drosophila reveals a retrograde signal regulating presynaptic transmitter release. Neuron 19:1237-1248.

Pfeiffer, B. E., and Huber, K. M. (2006). Current advances in local protein synthesis and synaptic plasticity. J Neurosci *26*, 7147-7150.

Pieretti, M., Zhang, F. P., Fu, Y. H., Warren, S. T., Oostra, B. A., Caskey, C. T., and Nelson, D. L. (1991). Absence of expression of the FMR-1 gene in fragile X syndrome. Cell *66*, 817-822.

Proops, R., and Webb, T. (1981). The 'fragile' X chromosome in the Martin-Bell-Renpenning syndrome and in males with other forms of familial mental retardation. J Med Genet *18*, 366-373.

Purpura, D. P. (1974). Dendritic spine "dysgenesis" and mental retardation. Science *186*, 1126-1128.

Qin G, Schwarz T, Kittel RJ, Schmid A, Rasse TM, Kappei D, Ponimaskin E,

Heckmann M, Sigrist SJ (2005a) Four different subunits are essential for expressing the synaptic glutamate receptor at neuromuscular junctions of Drosophila. J Neurosci 25:3209-3218.

Qin M, Kang J, Burlin TV, Jiang C, Smith CB (2005b) Postadolescent changes in regional cerebral protein synthesis: an in vivo study in the FMR1 null mouse. J Neurosci 25:5087-5095.

Ramaekers, A., M. L. Parmentier, et al. (2001). "Distribution of metabotropic glutamate receptor DmGlu-A in Drosophila melanogaster central nervous system." J Comp Neurol **438**(2): 213-25.

Ramos, A., Hollingworth, D., Adinolfi, S., Castets, M., Kelly, G., Frenkiel, T. A., Bardoni, B., and Pastore, A. (2006). The structure of the N-terminal domain of the fragile X mental retardation protein: a platform for protein-protein interaction. Structure *14*, 21-31.

Rao Y (2005) Dissecting Nck/Dock Signaling Pathways in Drosophila Visual System. Int J Biol Sci 1:80-86.

Rao Y, Zipursky SL (1998) Domain requirements for the Dock adapter protein in growth- cone signaling. Proc Natl Acad Sci U S A 95:2077-2082.

Reddy, K. S. (2005). Cytogenetic abnormalities and fragile-X syndrome in Autism Spectrum Disorder. BMC Med Genet *6*, 3.

Reeve, S. P., Bassetto, L., Genova, G. K., Kleyner, Y., Leyssen, M., Jackson, F. R., and Hassan, B. A. (2005). The Drosophila fragile X mental retardation protein controls actin dynamics by directly regulating profilin in the brain. Curr Biol *15*, 1156-1163.

Renden, R., Berwin, B., Davis, W., Ann, K., Chin, C. T., Kreber, R., Ganetzky, B., Martin, T. F., and Broadie, K. (2001). Drosophila CAPS is an essential gene that regulates dense-core vesicle release and synaptic vesicle fusion. Neuron *31*, 421-437.

Reyniers, E., Martin, J. J., Cras, P., Van Marck, E., Handig, I., Jorens, H. Z., Oostra, B. A., Kooy, R. F., and Willems, P. J. (1999). Postmortem examination of two fragile X brothers with an FMR1 full mutation. Am J Med Genet *84*, 245-249.

Roche JP, Packard MC, Moeckel-Cole S, Budnik V (2002) Regulation of synaptic

plasticity and synaptic vesicle dynamics by the PDZ protein Scribble. J Neurosci 22:6471-6479.

Rogers, S. J., Wehner, D. E., and Hagerman, R. (2001). The behavioral phenotype in fragile X: symptoms of autism in very young children with fragile X syndrome, idiopathic autism, and other developmental disorders. J Dev Behav Pediatr *22*, 409-417.

Ropers, H. H. (2006). X-linked mental retardation: many genes for a complex disorder. Curr Opin Genet Dev *16*, 260-269.

Ropers, H. H., and Hamel, B. C. (2005). X-linked mental retardation. Nat Rev Genet *6*, 46-57.

Rudelli, R. D., Brown, W. T., Wisniewski, K., Jenkins, E. C., Laure-Kamionowska, M., Connell, F., and Wisniewski, H. M. (1985). Adult fragile X syndrome. Clinico-neuropathologic findings. Acta Neuropathol (Berl) *67*, 289-295.

Ruiz-Canada C, Ashley J, Moeckel-Cole S, Drier E, Yin J, Budnik V (2004) New synaptic bouton formation is disrupted by misregulation of microtubule stability in aPKC mutants. Neuron 42:567-580.

Schaeffer, C., Bardoni, B., Mandel, J. L., Ehresmann, B., Ehresmann, C., and Moine, H. (2001). The fragile X mental retardation protein binds specifically to its mRNA via a purine quartet motif. Embo J *20*, 4803-4813.

Schenck, A., Bardoni, B., Langmann, C., Harden, N., Mandel, J. L., and Giangrande, A. (2003). CYFIP/Sra-1 controls neuronal connectivity in Drosophila and links the Rac1 GTPase pathway to the fragile X protein. Neuron *38*, 887-898.

Schuman EM, Dynes JL, Steward O (2006) Synaptic regulation of translation of dendritic mRNAs. J Neurosci 26:7143-7146.

Schuster CM, Ultsch A, Schloss P, Cox JA, Schmitt B, Betz H (1991) Molecular cloning of an invertebrate glutamate receptor subunit expressed in Drosophila muscle. Science 254:112-114.

Sheng M, Cummings J, Roldan LA, Jan YN, Jan LY (1994) Changing subunit composition of heteromeric NMDA receptors during development of rat cortex. Nature 368:144-147.

Sigrist SJ, Thiel PR, Reiff DF, Schuster CM (2002) The postsynaptic glutamate receptor subunit DGluR-IIA mediates long-term plasticity in Drosophila. J Neurosci 22:7362-7372.

Siomi, H., Matunis, M. J., Michael, W. M., and Dreyfuss, G. (1993). The pre-mRNA binding K protein contains a novel evolutionarily conserved motif. Nucleic Acids Res *21*, 1193-1198.

Siomi, M. C., Siomi, H., Sauer, W. H., Srinivasan, S., Nussbaum, R. L., and Dreyfuss, G. (1995). FXR1, an autosomal homolog of the fragile X mental retardation gene. Embo J *14*, 2401-2408.

Siomi, M. C., Zhang, Y., Siomi, H., and Dreyfuss, G. (1996). Specific sequences in the fragile X syndrome protein FMR1 and the FXR proteins mediate their binding to 60S ribosomal subunits and the interactions among them. Mol Cell Biol *16*, 3825-3832.

Snyder, E. M., Philpot, B. D., Huber, K. M., Dong, X., Fallon, J. R., and Bear, M. F. (2001). Internalization of ionotropic glutamate receptors in response to mGluR activation. Nat Neurosci *4*, 1079-1085.

Spehner D, Drillien R, Proamer F, Hanau D, Edelmann L (2002) Embedding in Spurr's resin is a good choice for immunolabelling after freeze drying as shown with chemically unfixed dendritic cells. J Microsc 207:1-4.

Strausfeld, N. J. (1998). "Crustacean-insect relationships: the use of brain characters to derive phylogeny amongst segmented invertebrates." Brain Behav Evol **52**(4-5): 186-206.

Sun B, Salvaterra PM (1995) Characterization of nervana, a Drosophila melanogaster neuron-specific glycoprotein antigen recognized by anti-horseradish peroxidase antibodies. J Neurochem 65:434-443.

Sung, Y. J., Conti, J., Currie, J. R., Brown, W. T., and Denman, R. B. (2000). RNAs that interact with the fragile X syndrome RNA binding protein FMRP. Biochem Biophys Res Commun *275*, 973-980.

Sung, Y. J., Dolzhanskaya, N., Nolin, S. L., Brown, T., Currie, J. R., and Denman, R. B. (2003). The fragile X mental retardation protein FMRP binds elongation factor 1A mRNA and negatively regulates its translation in vivo. J Biol Chem *278*, 15669-15678.

Sutherland, G. R. (1977). Fragile sites on human chromosomes: demonstration of their dependence on the type of tissue culture medium. Science *197*, 265-266.
Terracciano, A., Chiurazzi, P., and Neri, G. (2005). Fragile X syndrome. Am J Med Genet C Semin Med Genet *137*, 32-37.

Tejedor FJ, Bokhari A, Rogero O, Gorczyca M, Zhang J, Kim E, Sheng M, Budnik V (1997) Essential role for dlg in synaptic clustering of Shaker K+ channels in vivo. J Neurosci 17:152-159.

Thomas U, Kim E, Kuhlendahl S, Koh YH, Gundelfinger ED, Sheng M, Garner CC, Budnik V (1997) Synaptic clustering of the cell adhesion molecule fasciclin II by discs-large and its role in the regulation of presynaptic structure. Neuron 19:787-799.

Thomas U, Ebitsch S, Gorczyca M, Koh YH, Hough CD, Woods D, Gundelfinger ED, Budnik V (2000) Synaptic targeting and localization of discs-large is a stepwise process controlled by different domains of the protein. Curr Biol 10:1108-1117.

Todd, P. K., Mack, K. J., and Malter, J. S. (2003a). The fragile X mental retardation protein is required for type-I metabotropic glutamate receptor-dependent translation of PSD-95. Proc Natl Acad Sci U S A *100*, 14374-14378.

Todd, P. K., Malter, J. S., and Mack, K. J. (2003b). Whisker stimulation-dependent translation of FMRP in the barrel cortex requires activation of type I metabotropic glutamate receptors. Brain Res Mol Brain Res *110*, 267-278.

Turner, G., Webb, T., Wake, S., and Robinson, H. (1996). Prevalence of fragile X syndrome. Am J Med Genet *64*, 196-197.

Vanderklish PW, Edelman GM (2002) Dendritic spines elongate after stimulation of group 1 metabotropic glutamate receptors in cultured hippocampal neurons. Proc Natl Acad Sci U S A 99:1639-1644.

van 't Padje, S., Engels, B., Blonden, L., Severijnen, L. A., Verheijen, F., Oostra, B. A., and Willemsen, R. (2005). Characterisation of Fmrp in zebrafish: evolutionary dynamics of the fmr1 gene. Dev Genes Evol *215*, 198-206.

Verheij, C., Bakker, C. E., de Graaff, E., Keulemans, J., Willemsen, R., Verkerk, A. J., Galjaard, H., Reuser, A. J., Hoogeveen, A. T., and Oostra, B. A. (1993).

Characterization and localization of the FMR-1 gene product associated with fragile X syndrome. Nature *363*, 722-724.

Verkerk, A. J., Pieretti, M., Sutcliffe, J. S., Fu, Y. H., Kuhl, D. P., Pizzuti, A., Reiner, O., Richards, S., Victoria, M. F., Zhang, F. P., and et al. (1991). Identification of a gene (FMR-1) containing a CGG repeat coincident with a breakpoint cluster region exhibiting length variation in fragile X syndrome. Cell *65*, 905-914.

Vezina P, Kim JH (1999) Metabotropic glutamate receptors and the generation of locomotor activity: interactions with midbrain dopamine. Neurosci Biobehav Rev 23:577-589.

Visootsak, J., Warren, S. T., Anido, A., and Graham, J. M., Jr. (2005). Fragile X syndrome: an update and review for the primary pediatrician. Clin Pediatr (Phila) *44*, 371-381.

Wagh DA, Rasse TM, Asan E, Hofbauer A, Schwenkert I, Durrbeck H, Buchner S, Dabauvalle MC, Schmidt M, Qin G, Wichmann C, Kittel R, Sigrist SJ, Buchner E (2006) Bruchpilot, a protein with homology to ELKS/CAST, is required for structural integrity and function of synaptic active zones in Drosophila. Neuron 49:833-844.

Wan, L., Dockendorff, T. C., Jongens, T. A., and Dreyfuss, G. (2000). Characterization of dFMR1, a Drosophila melanogaster homolog of the fragile X mental retardation protein. Mol Cell Biol *20*, 8536-8547.

Wang, H., Ku, L., Osterhout, D. J., Li, W., Ahmadian, A., Liang, Z., and Feng, Y. (2004). Developmentally-programmed FMRP expression in oligodendrocytes: a potential role of FMRP in regulating translation in oligodendroglia progenitors. Hum Mol Genet *13*, 79-89.

Wang X, Sun B, Yasuyama K, Salvaterra PM (1994) Biochemical analysis of proteins recognized by anti-HRP antibodies in Drosophila melanogaster: identification and characterization of neuron specific and male specific glycoproteins. Insect Biochem Mol Biol 24:233-242.

Washburn MS, Numberger M, Zhang S, Dingledine R (1997) Differential dependence on GluR2 expression of three characteristic features of AMPA receptors. J Neurosci 17:9393-9406.

Watts, R. J., Schuldiner, O., Perrino, J., Larsen, C., and Luo, L. (2004). Glia engulf

degenerating axons during developmental axon pruning. Curr Biol *14*, 678-684.

Weiler, I. J., and Greenough, W. T. (1999). Synaptic synthesis of the Fragile X protein: possible involvement in synapse maturation and elimination. Am J Med Genet *83*, 248-252.

Weiler, I. J., Irwin, S. A., Klintsova, A. Y., Spencer, C. M., Brazelton, A. D., Miyashiro, K., Comery, T. A., Patel, B., Eberwine, J., and Greenough, W. T. (1997). Fragile X mental retardation protein is translated near synapses in response to neurotransmitter activation. Proc Natl Acad Sci U S A *94*, 5395-5400.

Weiler, I. J., Spangler, C. C., Klintsova, A. Y., Grossman, A. W., Kim, S. H., Bertaina-Anglade, V., Khaliq, H., de Vries, F. E., Lambers, F. A., Hatia, F*., et al.* (2004). Fragile X mental retardation protein is necessary for neurotransmitter-activated protein translation at synapses. Proc Natl Acad Sci U S A *101*, 17504-17509.

Werner LA, Manseau LJ (1997) A Drosophila gene with predicted rhoGEF, pleckstrin homology and SH3 domains is highly expressed in morphogenic tissues. Gene 187:107-114.

Wierenga CJ, Ibata K, Turrigiano GG (2005) Postsynaptic expression of homeostatic plasticity at neocortical synapses. J Neurosci 25:2895-2905.

Wohrle, D., Kotzot, D., Hirst, M. C., Manca, A., Korn, B., Schmidt, A., Barbi, G., Rott, H. D., Poustka, A., Davies, K. E., and et al. (1992). A microdeletion of less than 250 kb, including the proximal part of the FMR-I gene and the fragile-X site, in a male with the clinical phenotype of fragile-X syndrome. Am J Hum Genet *51*, 299-306.

Xiao, M. Y., Zhou, Q., and Nicoll, R. A. (2001). Metabotropic glutamate receptor activation causes a rapid redistribution of AMPA receptors. Neuropharmacology *41*, 664-671.

Xu, K., Bogert, B. A., Li, W., Su, K., Lee, A., and Gao, F. B. (2004). The fragile X-related gene affects the crawling behavior of Drosophila larvae by regulating the mRNA level of the DEG/ENaC protein pickpocket1. Curr Biol *14*, 1025-1034.

Yan, Q. J., Rammal, M., Tranfaglia, M., and Bauchwitz, R. P. (2005). Suppression of two major Fragile X Syndrome mouse model phenotypes by the mGluR5 antagonist MPEP. Neuropharmacology *49*, 1053-1066.

Xu, T., and Rubin, G. M. (1993). Analysis of genetic mosaics in developing and adult Drosophila tissues. Development *117*, 1223-1237.

Yasuyama, K., Meinertzhagen, I. A., and Schurmann, F. W. (2002). Synaptic organization of the mushroom body calyx in Drosophila melanogaster. J Comp Neurol *445*, 211-226.

Yoshihara M, Littleton JT (2002) Synaptotagmin I functions as a calcium sensor to synchronize neurotransmitter release. Neuron 36:897-908.

Zakharenko SS, Zablow L, Siegelbaum SA (2002) Altered presynaptic vesicle release and cycling during mGluR-dependent LTD. Neuron 35:1099-1110.

Zalfa, F., and Bagni, C. (2004). Molecular insights into mental retardation: multiple functions for the Fragile X mental retardation protein? Curr Issues Mol Biol *6*, 73-88.

Zalfa F, Eleuteri B, Dickson KS, Mercaldo V, De Rubeis S, di Penta A, Tabolacci E, Chiurazzi P, Neri G, Grant SG, Bagni C (2007) A new function for the fragile X mental retardation protein in regulation of PSD-95 mRNA stability. Nat Neurosci 10:578-587.

Zalfa, F., Giorgi, M., Primerano, B., Moro, A., Di Penta, A., Reis, S., Oostra, B., and Bagni, C. (2003). The fragile X syndrome protein FMRP associates with BC1 RNA and regulates the translation of specific mRNAs at synapses. Cell *112*, 317-327.

Zars, T. (2000). Behavioral functions of the insect mushroom bodies. Curr Opin Neurobiol *10*, 790-795.

Zhang, Y., O'Connor, J. P., Siomi, M. C., Srinivasan, S., Dutra, A., Nussbaum, R. L., and Dreyfuss, G. (1995). The fragile X mental retardation syndrome protein interacts with novel homologs FXR1 and FXR2. Embo J *14*, 5358-5366.

Zhang, Y. Q., Bailey, A. M., Matthies, H. J., Renden, R. B., Smith, M. A., Speese, S. D., Rubin, G. M., and Broadie, K. (2001). Drosophila fragile X-related gene regulates the MAP1B homolog Futsch to control synaptic structure and function. Cell *107*, 591-603.

Zhang YQ, Broadie K (2005) Fathoming fragile X in fruit flies. Trends Genet

21:37-45.

Zhang YQ, Friedman DB, Wang Z, Woodruff E, 3rd, Pan L, O'Donnell J, Broadie K (2005) Protein expression profiling of the drosophila fragile X mutant brain reveals up-regulation of monoamine synthesis. Mol Cell Proteomics 4:278-290.

Zhang, Y. Q., Matthies, H. J. G., Mancuso, J., Andrews, H. K., Woodruff, I., Elvin, Friedman, D., and Broadie, K. (2004). The Drosophila fragile X-related gene regulates axoneme differentiation during spermatogenesis. Developmental Biology 270(2), 290-307.

Zhao, M. G., Toyoda, H., Ko, S. W., Ding, H. K., Wu, L. J., and Zhuo, M. (2005). Deficits in trace fear memory and long-term potentiation in a mouse model for fragile X syndrome. J Neurosci *25*, 7385-7392.

Zhu, S., Chiang, A. S., and Lee, T. (2003). Development of the Drosophila mushroom bodies: elaboration, remodeling and spatial organization of dendrites in the calyx. Development *130*, 2603-2610.